NOTICE

The quality of this microform is heavily dependent upon the quality of the original thesis submitted for microfilming. Every effort has been made to ensure the highest quality of reproduction possible.

If pages are missing, contact the university which granted the degree.

Some pages may have indistinct print especially if the original pages were typed with a poor typewriter ribbon or if the university sent us an inferior photocopy.

Previously copyrighted materials (journal articles, published tests, etc.) are not filmed.

Reproduction in full or in part of this microform is governed by the Canadian Copyright Act, R.S.C. 1970, c. C-30.

AVIS

La qualité de cette microforme dépend grandement de la qualité de la thèse soumise au microfilmage. Nous avons tout fait pour assurer une qualité supérieure de reproduction.

S'il manque des pages, veuillez communiquer avec l'université qui a conféré le grade.

La qualité d'impression de certaines pages peut laisser à désirer, surtout si les pages originales ont été dactylographiées à l'aide d'un ruban usé ou si l'université nous a fait parvenir une photocopie de qualité inférieure.

Les documents qui font déjà l'objet d'un droit d'auteur (articles de revue, tests publiés, etc.) ne sont pas microfilmés.

La reproduction, même partielle, de cette microforme est soumise à la Loi canadienne sur le droit d'auteur, SRC 1970, c. C-30.

THE UNIVERSITY OF ALBERTA

SIZE EFFECT ON THE ELECTRICAL RESISTIVITY OF SIMPLE METALS AT LOW TEMPERATURE

BY

© MOUSTAFA ABDEL-KADER MOHAMED

A THESIS

SUBMITTED TO THE FACULTY OF GRADUATE STUDIES AND RESEARCH IN PARTIAL FULFILMENT OF THE REQUIREMENTS FOR THE DEGREE OF DOCTOR OF PHILOSOPHY

IN

PHYSICS

DEPARTMENT OF PHYSICS

EDMONTON, ALBERTA

(FALL, 1988)

ISBN 0-315-45712-0

University of Exeter

DEPARTMENT OF PHYSICS

Stocker Road, Exeter EX4 4QL

Telex: 42894 EXUNIV G
Switchboard: 0392 - 263263

Direct Line 0392 - 26 4103

JRS/MAC

25 May 1988

Mr M A-K Mohamed
Department of Physics
University of Alberta
Edmonton
Alberta
Canada T6G 2J1

Dear Mr Mohamed

Thank you for your letter of the 14 May. On behalf of Mr Gollege and myself I confirm that you are most welcome to reproduce any part, or parts of any of our papers. However you will probably formally need permission from the publishers who hold the Copyright, also.

I would be grateful to receive any preprints relevant to this work.

Yours sincerely

Dr J R Sambles

UNIVERSITY OF BRISTOL

Professor R. G. Chambers, M.A., Ph.D.
Telephone: Bristol 24161 Ext.49

H. H. WILLS PHYSICS LABORATORY
ROYAL FORT
TYNDALL AVENUE
BRISTOL
BS8 1TL

24 May 1988

M A-K Mohamed
Department of Physics
University of Alberta
Edmonton
Alberta
Canada T6G 2J1

Dear Mr Mohamed

Thank you for your letter of 14 May. I am happy to give permission for you to include in your thesis Fig. 4 and Table 1 of Proc. Roy. Soc. A202, 378, 1950.

Yours sincerely

R G Chambers

THE UNIVERSITY OF ALBERTA

RELEASE FORM

NAME OF AUTHOR: Moustafa Abdel-Kader Mohamed

TITLE OF THESIS : " Size Effect on The Electrical Resistivity of Simple Metals at Low Temperature"

DEGREE FOR WHICH THESIS WAS PRESENTED: Ph. D.

YEAR THIS DEGREE GRANTED: 1988

(Signed) Mostafa Abdel-Kader

Permanent Address: #306 Galbraith House

Michener Park 122- 48th Av.

Edmonton, Alberta, CANADA

T6H 5B5

DATE: Sept. 7th 1988

THE UNIVERSITY OF ALBERTA

FACULTY OF GRADUATE STUDIES AND RESEARCH

The undersigned certify that they have read, and recommend to the Faculty of Graduate Studies and Research for acceptance, a thesis entitled " Size Effect on The Electrical Resistivity of Simple Metals at Low Temperature" submitted by Moustafa Abdel-Kader Mohamed in partial fulfilment of the requirements for the degree of Doctor of Philosophy in Physics.

.....

(Supervisor)

.....

.....

.....

.....

Date: July 4th, 1988.

ABSTRACT

The electrical conductivity (σ) has been measured as function of sample diameter at different low temperatures for potassium, sodium and indium. The sam[illegible]drical wires with diameters between 0.33 and 3.20 mm. At liquid he[illegible]perature the [illegible]tivity of thin potassium wires increased as the sample diameter (d) [illegible]eased for d≤ 1.5 mm. On the other hand, it decreased with d for d> 1.5 mm, but at a lower rate. As the temperature was raised, the initial increase of σ with d was observed only at smaller diameter values and disappeared altogether for temperatures ≥ 20 K. For d> 1.5 mm the decrease of σ with d persisted at higher temperatures, but essentially vanished for T ≥ 50 K. The results for sodium wires showed a very similar behavior but the conductivity maximum occurred at d = 0.90 mm at 4.2 K instead of d= 1.5mm for potassium. The decrease of σ with d for d≥ 0.9 mm was measurable for T< 90 K. The results at 4.2 K for small diameter values (d≤ 1.5mm for potassium or d≤ 0.90 mm for sodium) can be explained qualitatively by Sambles *et al* theory in which surface scattering of electrons decreases the conductivity of small diameter specimens. On the other hand the results for larger diameter values could be explained by the existence of a high conductivity surface layer that forms at low temperatures which does not seem to be very plausible. The results for indium are completely different from those for potassium and sodium. The resistivity oscillated as a function of the sample diameter for d< 1.0 mm and the amplitude of oscillation decreased as d increased. When these results were plotted on a "ρ >< 1/d" graph, the data points were found to fall on three straight lines of different

slopes . Linear behavior on this graph is in qualitative agreement with Sambles *et al* theory, but each line corresponds to a different bulk conductivity.

We have also measured the longitudinal magnetoresistance for the above mentioned elements. For potassium and sodium dR/ dH was negative for low fields and small diameters, that is for d≤ 1.15 mm, giving rise to a negative magnetoresistance, but it was positive and constant for high fields and large diameter values. The negative magnetoresistance was found to also depend on the thermal history of the sample, the effect becoming stronger for more annealed samples. This is in a qualitative agreement with Chamber's theory and the more recent one by Golledge *et al.*. The results for indium are again quite different from those for potassium and sodium. The sample resistance increased quite rapidly for H~ 300 to 600 Oe reaching about 800% relative change then it tended to saturate with a shallow positive slope. For some samples the resistance rise showed more than one step before saturation. This large magnetoresistance, the first step of which has been observed previously, was attributed to the bulk behaviour of indium which becomes a compensated metal at H~ 500 Oe.

ACKNOWLEDGEMENTS

First and foremost I would like to thank Prof. S.B. Woods for his systematic guidance during this work. Through his patience and wisdom I have learned how to deal with the difficulties one usually faces in scientific research. In fact he gave me the complete freedom to work on my own, but he was always there to help whenever a problem arose.

Thanks are also due to Mr. T. Valian for his technical help. He donated lots of his time and experience through discussions needed in designing and modifying different instruments necessary for the present measurements.

I like to thank Prof. J.P. Franck, Dr. H. Zaleski, Dr. G. Oomi, Dr. Toyoda and Dr. J. Jung for some useful discussions.

My sincere thanks to the staff of the electronics shop for their help during the process of interfacing and building of the computer system constructed during the course of this work. Also I wish to thank the staff of the machine shop and of the helium liquefier for their continuous help.

I would like to extend a warm thank you to the other people I had the pleasure of interacting with at the university. Through their friendship my stay here was very pleasant. Lest I forget someone, I will mention no names.

Finally, I thank my wife Sharifa for her understanding and patience particularly during the final stages of this thesis.

TABLE OF CONTENTS

TABLE OF CONTENTS

LIST OF TABLES

LIST OF TABLES

LIST OF TABLES

LIST OF TABLES

LIST OF TABLES

LIST OF TABLES

LIST OF TABLES

LIST OF TABLES

LIST OF TABLES

LIST OF TABLES

LIST OF FIGURES

LIST OF FIGURES

LIST OF FIGURES

LIST OF FIGURES

INTRODUCTION

Over the last two decades a considerable amount of interest has been developed in the study of transport properties of normal metals[1,2] at low temperatures,where size effects are sometimes important. Alkali metals have received the largest attention because they are very close to free-electron systems[3]. The first two elements of this group, namely lithium and sodium, undergo a crystal structure change below room temperature which made the third element, potassium, a more attractive candidate for such a study. The experimental results[4-8] showed large deviations from standard theories at low temperature; for example Rowlands, Duvvury and Woods[4] have found the electrical resistivity of potassium of diameter 0.79 mm did not follow the well known T^2-term due to electron-electron scattering for $0.5 \leq T \leq 2$ K but rather they found $\rho(T)=A\,T^{1.5}$. Similar results were also found by Lee et al[6]. Also Yu et al[9] reported $\rho(T)$ measurements for T=0.08 to 1.8K which display a negative $d\rho/dT$ for sufficiently small diameters. In order to explain the experimental results many theoretical ideas came into being ranging from postulated inhomogeneity within the sample[10] to a charge density wave[11,12] which was applied to explain the results of induced torque peaks in potassium spheres by Schaefer et al[13] and Holroyd and Datars[14].

Recently, 1982, Sambles et al[15] have done a theoretical calculation for size effects on the electrical resistivity at low temperature in thin metal wires of circular cross section. In their theory they assumed that the metal concerned is free-electron-like with a spherical Fermi surface, so one would expect it to apply for data on alkali metals. However, as they pointed out, many of the measurements on these metals in the literature have been done for samples encapsulated in constraining capillaries and as such suffer from unknown and variable levels of strain so they ignored these data and compared their calculations with data for aluminum, indium and mercury thin wires and obtained fairly good agreement.

Also in the past few months, Golledge et al[16], using Chambers[17] kinetic formulation have extended scattering theory to explain the longitudinal magnetoresistance of thin wires. In their calculation they used an angularly dependent specularity for scattering at the surface, first introduced by Soffer[18], which yielded results similar to Chambers results for electrons diffusely scattered by the sample surface. Again the theory was designed for a metal with a spherical Fermi surface, an isotropic bulk mean free path and zero bulk magnetoresistance. The first two conditions are very nearly satisfied by alkali metals but the third one is not[16] as will be discussed later. In comparing their theory with experimental results, Golledge et al did not find enough data of longitudinal magnetoresistance for alkali metals other than the work done in 1950 by MacDonald and Sarginson

on two wires of sodium whose diameters were approximately equal to the bulk mean free path.

In the present work we have studied the size effect on the electrical conductivity for free hanging wires of potassium and sodium metals to compare with Sambles et al theory and the longitudinal magnetoresistance to test Chambers theory or the more recent theory of Golledge et al. In addition we did a similar study for indium wires to further test both theories since it was indicated by the authors that it is [illegible] to apply their calculations to indium in spite of the fact that its fermi su[illegible]ot as simple as it was assumed to be in the theory. The results showed some interesting features which will be discussed in chapter 3.This thesis consists of three chapters. In chapter 1, relevant theories regarding size effect on both electrical resistivity and magnetoresistance are discussed in some details. Chapter 2 contains the description of the experimental set up, sample preparations and measurement techniques. In the last chapter, the results are presented and discussed in light of existing theories.

CHAPTER I

THEORY

I.I) Historical Background :

Since the beginning of this century it had been realized that the apparent resistivity of a thin metallic film or wire will increase when one of its dimensions becomes comparable with the bulk electronic mean free path. As early as 1901, Thomson[19] gave the first approximate expression for the increase in resistivity of a thin film followed by another approximation in 1936 by Lovell[20]. The exact solution for a free-electron conductor was given by Fuchs[21] in 1938 for thin film geometry. For wires of circular cross section, Dingle[22] gave a solution in 1950. These last two theories used a single specularity parameter, P, which was assumed to be independent of the angle of incidence of the conduction electron on the sample boundary. This assumption was questioned by Ziman[23] in 1960 who suggested that P should be a function of the angle of incidence, θ, of the electron to the surface normal, having the form

$$P(\theta) = \mathrm{Exp}[-(4\pi h/\lambda_e)^2 \cos^2\theta\ ], \qquad (1.1.1)$$

where λ_e is the electronic wavelength and h is a mean-square surface roughness[23]. This $P(\theta)$ was used by Soffer[18], in 1967, to get a resistivity expression for the thin film geometry which was proven by Samples et al [24] in 1980 and Stesman[25,26] in 1982 and 1983 to give a satisfactory agreement with the experimental results. The interpretation of these results using this theory does not

require the unphysical introduction of temperature dependence for the $\rho_\infty\lambda_\infty$ (ρ_∞, λ_∞ are the bulk resistivity and mean free path respectively) and P values as often required by Fuchs' theory[21]. In 1982, Samples et al[15] developed a model for thin cylindrical wires incorporating the angular-dependent specularity parameter, $P(\theta)$,which we will discuss in more details later in this chapter.

For magnetoresistance, not as many theoretical calculations are available in the literature. This could be because of the difficulty in solving the Boltzmann equation in the presence of magnetic fields. Also according to standard theories it was expected that the longitudinal magnetoresistance should be zero for a simple metal with a spherical fermi surface[17,27]. In 1950, Chambers[17] gave a theory to explain the effect of sample size on the resistance of a wire in a parallel magnetic field. He considered a cylindrical wire geometry and showed that for low fields the apparent resistance of a sample decreases with increasing field giving rise to a negative magnetoresistance. In 1972 Way and Kao[28] extended Chambers' theory to the thin film geometry and found similar results apart from an initial rise in the film resistivity. In 1986, Preist and Samples[29] developed Way and Kao's calculations using Soffer's surface scattering model, i.e., using an angularly dependent specularity. In 1987 Golledge et al[16] did calculations for the longitudinal magnetoresistance of a thin wire using Chambers'[17] kinetic formulation considering both angularly dependent and constant specularities. The results of their calculations are quite similar to those obtained by Chambers

confirming the low-field negative magnetoresistance behavior without a resistance maximum as for the case of the thin foils geometry[28]. From this, they concluded that wires of rectangular cross-section cannot be approximated to cylindrical wires.

In this chapter we are going to discuss Sambles et al[15] theory followed by a discussion of Chambers[17] theory and the more recent theory of Golledge et al[16] but before that, it may be important to discuss briefly the Boltzmann equation which plays the role of a central base for the theoretical calculation of most of the transport properties.

I.2) The Boltzmann Transport Equation and Relaxation-Time Approximation:

In the absence of magnetic fields and temperature gradients, the Boltzmann transport equation describing the steady-state distribution of electrons in phase space, under an externally applied electric field E, has the form:

$$- (e/\hbar)E. \nabla_k N(k,r) = - (\partial N(k,r)/ \partial t)_{scattering} , \qquad (1.2.1)$$

where e is the electronic charge, $\hbar$ is Planck's constant divided by 2π, and $- (\partial N(k,r)/ \partial t)_{scattering}$ is the rate of change of the electronic distribution function N(k,r) due to scattering by phonons, impurities, and other electrons. N(k.r) measures the number of electrons at position r in the state described by the wave vector k. In bulk material, N(k,r) is taken to be just N(k), independent of position within the lattice[30].

To solve equation (1.2.1), one must know the form of $(\partial N(k,r)/ \partial t)_{scattering}$. A particularly simple form results under the following assumptions:

i) The electronic energy surfaces in k-space are spherical.

ii) The electron scattering is completely elastic, i.e. the electron's energy is conserved.

iii) The probability for scattering from state k to state k' depends only upon the angle between k and k' (isotropic scattering).

In this case one can write[23] :

$$(\partial N(k)/\partial t)_{scattering} = (N(k)-N_0)/\tau(\varepsilon), \tag{1.2.2}$$

where N_0 is the equilibrium distribution function in the absence of an applied electric field and $\tau(\varepsilon)$ is the "isotropic relaxation time" given by :

$$1/\tau(\varepsilon) = \int (1-\cos\theta)\, Q(k,\theta)\, d\Omega, \tag{1.2.3}$$

where $Q(k,\theta)\, d\Omega$ is the probability that an electron in state k will be scattered through an angle θ into the solid angle $d\Omega$.

By solving equations (1.2.1) and (1.2.2) for N(k), the current density "J" can be determined from the equation

$$J = \int e\, v_k\, N(k)\, dk, \tag{1.2.4}$$

where v_k is the velocity of an electron in state k. Then the electrical resistivity can be calculated by using the relation

$$\rho = E / J \tag{1.2.5}$$

By doing that one can write[30] :

$$\rho = 4\pi^3 \hbar / [e^2\, \tau(\varepsilon_f) \int v_k\, dS], \tag{1.2.6}$$

where ε_f is the Fermi energy, dS is a differential area on the Fermi surface and $\tau(\varepsilon_f) \equiv \tau(\kappa_f)$ is the isotropic relaxation time evaluated at ε_f..

For a free-electron gas, $v = \hbar k/m$ and $\int k\, dS = 4\pi^3 n$, where m is the electron mass and n is the number of conduction electrons per unit volume. With this information one can write equation (1.2.6) for a simple metal as :

$$\rho(T) = m/ne^2\, \tau(\varepsilon_f) \tag{1.2.7}$$

If we assume that there exist separate and independent isotropic relaxation times $\tau_0(\varepsilon)$ and $\tau(\varepsilon)$ for the scattering of conduction electrons by static lattice defects and by other mechanisms respectively, then equation (1.2.7) takes the form :

$$\rho(c,T) = (m/ne^2)[(1/\tau_0(\varepsilon)) + (1/\tau(\varepsilon))] \qquad (1.2.8)$$

which is a form of the well-known "Matthiessen's Rule".

I.3) Sambles et al Theory[15] :

Let $N_0(r,v)$ denote the number of electrons per unit volume of ordinary space and per unit volume of velocity space. In general, this distribution function depends on the position, given by the vector r, and velocity given by vector v. When an electric field is applied to the system, $N_0(r,v)$ changes to $N(r,v)$ and one may write the Boltzmann equation as[22] :

$$v\,[\partial N(r,v)/\partial r] + (\partial v/\partial t)[\partial N(r,v)/\partial v] = -[N(r,v) - N_0(r,v)]/\tau, \qquad (1.3.1)$$

where τ is the relaxation time. Now, assuming that the electric field E is applied along the wire in the z-direction, this will imply that $(\partial v/\partial t)$ is zero in x- and y-directions but $(\partial v/\partial t)_z = eE/m$ in z-direction, where e is the electronic charge and m is the electron mass. When stationary state conditions have been established, the distribution function $N \equiv N(x,y,z;\, v_x, v_y, v_z)$ will not vary along the wire in the z-direction, so equation (1.3.1) becomes :

$$v_x\,(\partial N/\partial x) + v_y\,(\partial N/\partial y) - (eE/m)(\partial N_0/\partial v_z) = -(N - N_0)/\tau \qquad (1.3.2)$$

For reasonably small electric fields one can write $N - N_0 = n(x, y;\, v_x, v_y, v_z)$ and equation (1.3.2) will read :

$$v_x\,(\partial n/\partial x) + v_y\,(\partial n/\partial y) + n/\tau = (eE/m)(\partial N_0/\partial v_z) \qquad (1.3.3)$$

Since we are considering a wire of circular cross-section, it might be useful to transfer equation (1.3.3) into cylindrical coordinates which gives[22]:

$$v_r\,(\partial n/\partial r) + (v_\theta^2/r)(\partial n/\partial v_r) - (v_\theta v_r/r)(\partial n/\partial v_\theta) + n/\tau = (eE/m)(\partial N_0/\partial v_z), \qquad (1.3.4)$$

where now $n \equiv n(r,\theta;\ v_r,\ v_\theta,\ v_z)$ and the term of $(\partial n/\partial\theta)$ is zero due to the cylindrical symmetry of the wire. The general solution of (1.3.4) was given by Dingle[22] as :

$$n = (eE\tau/m)(\partial N_0/\partial v_z)\,[1 - f(rv_\theta,\ v_r^2 + v_\theta^2, v_z)\,\mathrm{Exp}\{-r\,v_r/\tau\,(v_r^2 + v_\theta^2)\}], \tag{1.3.5}$$

where f is an arbitrary function of the variables rv_θ, $v_r^2 + v_\theta^2, v_z$ and is an even function of radial velocity. The boundary condition at the wire surface will determine the function f as follows :

A) Diffuse Scattering :

When the conduction electrons are diffusely scattered by the sample surface, the returning electrons must have equal probability of being directed in each inwardly directed unit solid angle. Thus $n(-|v_r|,\ v_\theta,\ v_z,\ r=a)$ must possess no directional properties, where a is the wire radius.Since $(\partial N_0/\partial v_z)$ is certainly directional, therefore from (1.3.5) it follows that :

$$1 - f(rv_\theta,\ v_r^2 + v_\theta^2, v_z)\,\mathrm{Exp}\{-a\,v_r/\tau\,(v_r^2 + v_\theta^2)\} = 0$$

Therefore :

$$f(\alpha,\ \beta,\ \gamma) = \mathrm{Exp}\{-(a^2\beta - \alpha^2)^{0.5}/\tau\beta\}, \tag{1.3.(}$$

where $\alpha = rv_\theta$, $\beta = v_r^2 + v_\theta^2$ and $\gamma = v_z$.

B) Partially Diffuse Scattering :

If we assume that the probability of an electron to be specularly scattered at the surface is $P \neq 0$, then we can write :

$$N(-v_r, v_\theta, v_z, r=a) = P\, N(v_r, v_\theta, v_z, r=a) + g\,, \qquad (1.3.7)$$

where g is the distribution function for the diffusely scattered electrons. Writing $N = N_0 + n$, then (1.3.7) can be written as :

$$\begin{aligned} g &= (1 - P)N_0 + n(-v_r, v_\theta, v_z, r=a) - P\, n(v_r, v_\theta, v_z\, r=a) \\ &= (1 - P)N_0 + (eE\tau/m)(\partial N_0/\partial v_z)\,\{1 - P - f(av_\theta, v_r^2 + v_\theta^2, v_z) \\ &\qquad [\mathrm{Exp}(a\, v_r/\tau\,(v_r^2 + v_\theta^2) - P\,\mathrm{Exp}(-a\, v_r/\tau\,(v_r^2 + v_\theta^2))]\}, \end{aligned} \qquad (1.3.8)$$

by using (1.3.5). Since g must have no direction dependence, but $\partial N_0/\partial v_z$ does ,this means that the quantity in the brackets in front of $\partial N_0/\partial v_z$ must vanish i.e. :

$$\begin{aligned} (1 - P)\, f^{-1}(\alpha,\beta,\gamma) &= \mathrm{Exp}\{(a^2\beta - \alpha^2)^{0.5}/\tau\beta\} - \\ &\qquad P\,\mathrm{Exp}\{-(a^2\beta - \alpha^2)^{0.5}/\tau\beta\}, \end{aligned} \qquad (1.3.9)$$

where α , β and γ are as defined before.

C) Angular-Dependent Specularity :

Now if we allow the specularity parameter to be angularly dependent as suggested by Ziman [23], equation (1.3.1), then the boundary condition at the wire surface will be [18] :

$$n(-v_r, v_\theta, v_z, r=a) = P(\theta)\, n(v_r, v_\theta, v_z, r=a), \qquad (1.3.10)$$

where :

$$P(\theta) = \mathrm{Exp}[-(4\pi h/\lambda_e)^2 \cos^2\theta] = \mathrm{Exp}[-(4\pi H)^2 \cos^2\theta],$$

where $H = h/\lambda_e$ and $\cos^2\theta = v_r^2/(v_r^2 + v_\theta^2 + v_z^2)$.

From (1.3.10) and (1.3.5) one can write the boundary conditions as :

$$0 = (eE\tau/m)(\partial N_0/\partial v_z)\{1 - P - f(av_\theta, v_r^2 + v_\theta^2, v_z)\,[\mathrm{Exp}(a\, v_r/\tau\,(v_r^2+v_\theta^2)) - P\,\mathrm{Exp}(-a\, v_r/\tau\,(v_r^2+v_\theta^2))]\}. \qquad (1.3.11)$$

Therefore,

$$(1-P)\, f^{-1}(\alpha,\beta,\gamma) = \mathrm{Exp}\{(a^2\beta - \alpha^2)^{0.5}/\tau\beta\} - P\,\mathrm{Exp}\{-(a^2\beta - \alpha^2)^{0.5}/\tau\beta\} \qquad (1.3.12)$$

which is similar to equation (1.3.9), but now :

$$P = \mathrm{Exp}[-(4\pi H)^2 v_r^2/(v_r^2+v_\theta^2+v_z^2)],$$

and since :

$$v_r^2/(v_r^2+v_\theta^2+v_z^2) = [a^2(v_r^2+v_\theta^2) - (a\, v_\theta)^2]/a^2(v_r^2+v_\theta^2+v_z^2)$$

therefore P can be written as :

$$P = \mathrm{Exp}[-(4\pi H)^2 (a^2\beta - \alpha^2)/a^2(\beta+\gamma^2)].$$

From (1.3.5) and (1.3.12), one can write :

$$n = (eE\tau/m)(\partial N_0/\partial v_z)\Big[1 - [(1-P)\,\mathrm{Exp}[-\{r\,v_r + (a^2(v_r^2 + v_\theta^2) - r^2 v_\theta^2)^{0.5}\}]/ \tau(v_r^2 + v_\theta^2)]/[1 - P\,\mathrm{Exp}[-2(a^2(v_r^2 + v_\theta^2) - r^2 v_\theta^2)^{0.5}]/\tau(v_r^2 + v_\theta^2)]\Big]. \tag{1.3.13}$$

Now, introducing the velocity spherical coordinate system:

$v_r = v \sin\theta \sin\phi$, $v_\theta = v \sin\theta \cos\phi$, $v_z = v \cos\theta$ with $0<\theta<\pi$ and $0<\phi<2\pi$.

Equation (1.3.13) can be written as[22] :

$$n = (eE\tau/m)(\partial N_0/\partial v_z)\Big[1 - (1-P)\,\Sigma_{v=0}^{\infty} P^v\,\mathrm{Exp}[-\{r \sin\phi + (2v+1)(a^2 - r^2\cos^2\phi)^{0.5}\}/\tau v \sin\theta]\Big]. \tag{1.3.14}$$

The current density J(r) at a radial distance r from the central axis of the wire can be written as :

$$J(r) = e \int v_z\, n(v, r)\, d^3v\,, \tag{1.3.15}$$

where d^3v is the element of volume in velocity space : $d^3v = v^2 \sin\theta\, d\theta\, d\phi$.

Using (1.3.14) in (1.3.15), therefore[22] :

$$J(r) = (e^2E\tau/m) \int_0^{\infty} v^3(\partial N_0/\partial v)\, dv \int_0^{\pi} d\theta \cos^2\theta \sin\theta \int_0^{2\pi} d\phi \Big[1 - (1-P)\,\Sigma_{v=0}^{\infty} P^v\,\mathrm{Exp}[-\{r \sin\phi + (2v+1)(a^2 - r^2\cos^2\phi)^{0.5}\}/\tau v \sin\theta]\Big]. \tag{1.3.16}$$

In order to have the limits of the three integrations in (1.3.16) independent, we have to assume that $N_0(v)$ is isotropic[22] in velocity space, i.e. <u>that the Fermi surface is spherical</u>. Now, by recalling that :

$$J_0 = (4\pi/3)(e^2E\tau/m) \int_0^{\infty} v^3(\partial N_0/\partial v)\, dv$$

then (1.3.16) can be rewritten as :

$$J(r)/J_0 = (3/4\pi)\int_0^{\pi} d\theta \cos^2\theta \sin\theta \int_0^{2\pi} d\phi \left[1 - (1-P)\Sigma_{v=0}^{\infty} P^v \right.$$
$$\left. \mathrm{Exp}[-\{r \sin\phi + (2v+1)(a^2 - r^2\cos^2\phi)^{0.5}\}/\lambda \sin\theta] \right], \qquad (1.3.17)$$

where $\lambda = \tau v_f$ and v_f is the Fermi velocity. In actual experimental data one usually measures the ratio of the apparent overall conductivity σ/σ_0 defined as :

$$\sigma/\sigma_0 = \int_0^a J(r)\, r\, dr \,/\, \int_0^a J_0\, r\, dr = (2/a^2)\int_0^a (J(r)/J_0)\, r\, dr\,, \qquad (1.3.18)$$

where a is the sample radius. Now by using $x = r\cos\phi$ and $y = r\sin\phi$ and substituting (1.3.17) in (1.3.18), one can get[15] :

$$\rho_\infty/\rho = \sigma/\sigma_0 = 1 - (12/\pi\kappa)\int_0^{\pi/2} d\theta \cos^2\theta \sin^2\theta \int_0^{\pi/2} \sin\phi\, d\phi \left[(1-P) \right.$$
$$\left. \{1 - \mathrm{Exp}[-\kappa\sin\phi/\sin\theta]\}/\{1 - P\,\mathrm{Exp}[-\kappa\sin\phi/\sin\theta]\} \right], \qquad (1.3.19)$$

where $\kappa = 2a/\lambda_\infty$, λ_∞ is the bulk mean free path and P is given by :

$$P(\theta) = \mathrm{Exp}[-(4\pi H)^2 \sin^2\theta \sin^2\phi].$$

The right-hand-side of equation (1.3.19) has been calculated numerically by Sambles et al[15] for various values of surface roughness parameter, H, and different values of κ. Their results are summarized in table (1.3.1) and Fig.(1.3.1). Besides the numerical table and graphical representation of the final calculations, Sambles et al deduced the following approximate analytical formulae:

i) $\rho = \rho_\infty + \alpha(\rho_\infty \lambda_\infty / 2a)$, (1.3.20)

where α is a constant $\cong 0.75$ at high κ for diffuse scattering, $H \rightarrow \infty$ or $P \rightarrow 0$.

ii) $\rho = \rho_\infty [1 + \alpha(\lambda_\infty / 2a)^{2/3}]$, (1.3.21)

for fairly smooth surfaces, $P \neq 0$, and $\lambda_\infty > 2a$.

	κ												
H	0.01	0.02	0.03	0.04	0.06	0.08	0.1	0.2	0.3	0.4	0.6	0.8	1.0
0.05	4.332	3.098	2.588	2.297	1.968	1.782	1.659	1.379	1.269	1.209	1.145	1.111	1.090
0.1	9.126	6.197	4.990	4.300	3.517	3.069	2.773	2.079	1.794	1.633	1.454	1.354	1.290
0.15	14.47	9.604	7.606	6.469	5.178	4.442	3.956	2.814	2.343	2.076	1.775	1.606	1.497
0.2	20.02	13.07	10.23	8.615	6.791	5.754	5.071	3.475	2.822	2.452	2.038	1.806	1.657
0.25	25.52	16.41	12.71	10.62	8.259	7.514	6.050	4.021	3.200	2.739	2.229	1.947	1.767
0.3	30.08	19.54	14.98	12.42	9.547	7.931	6.876	4.453	3.487	2.951	2.363	2.042	1.840
0.4	40.48	25.00	18.84	15.40	11.60	9.489	8.125	5.054	3.865	3.219	2.524	2.153	1.922
0.5	48.77	29.43	21.84	17.66	13.09	10.58	8.973	5.424	4.085	3.368	2.608	2.209	1.963
0.6	55.75	32.97	24.17	19.37	14.17	11.35	9.558	5.661	4.218	3.455	2.656	2.240	1.985
0.8	66.48	38.10	27.41	21.67	15.56	12.31	10.27	5.927	4.362	3.547	2.704	2.270	2.006
1.0	74.06	41.48	29.45	23.08	16.38	12.85	10.66	6.061	4.430	3.589	2.725	2.284	2.016

Table(1.3.1) : (ρ/ρ_∞) for different H and κ values, after sambles et al [15].

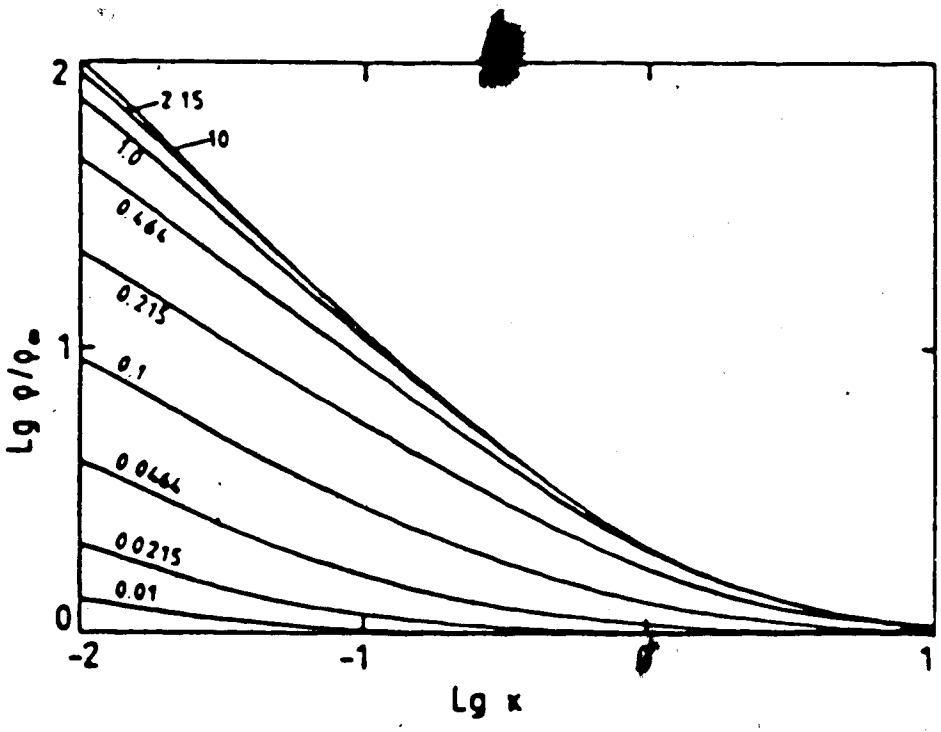

Fig.(1.3.1) : Lg (ρ/ρ_∞) as Function of Lgκ, after Sample et al [15].

I.4) Chambers and Golledge et al Theory[16, 17] :

In this theory, Chambers[17] showed that an exact solution of the thin conductor problem can be obtained simply by kinetic theory arguments without solving the Boltzmann equation. Following the same arguments, lets consider an arbitrary point a in the sample and consider an electron passing through it towards the wire surface where it will collide at point b, see Fig.(1.4.1). By definition of λ, the bulk mean free path, the probability that an electron will travel a distance greater than x is $e^{-x/\lambda}$ for x< the distance ab and that the electrons which arrive at b will certainly collide there. Now, the mean distance travelled by an electron without collision after passing through a can be written as[17] :

$$\lambda_1 = \lambda(1 - e^{-ab/\lambda}). \tag{1.4.1}$$

For an electric field $E \neq 0$ in the z-direction, the conduction electrons will gain a mean drift velocity :

$$\Delta v_z = (eE/ mv) \lambda(1 - e^{-ab/\lambda}).$$

$$= (eE\tau/ m) (1 - e^{-ab/\lambda}), \tag{1.4 2}$$

where $\tau = \lambda/ v$, and v is the electron speed. The change in the number of electrons travelling in the direction ba due to E can be written as :

$$n(ba) = (\partial N_0/\partial v_z) \delta v_z$$

$$= (eE\tau /m) (\partial N_0/\partial v_z) (1 - e^{-ab/\lambda}), \tag{1.4.3}$$

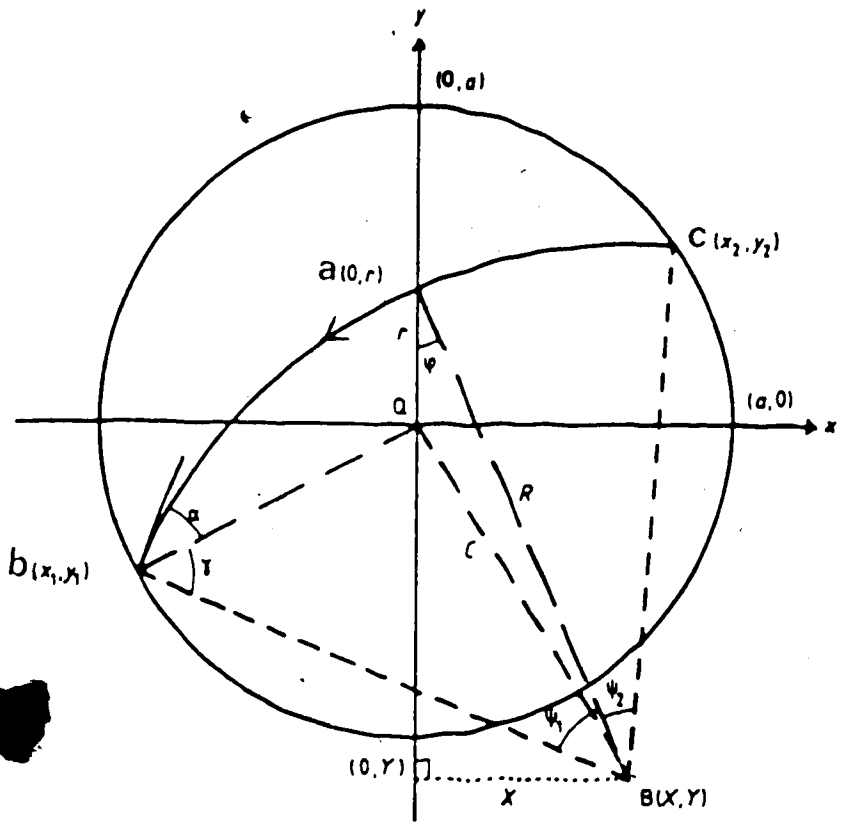

Fig.(1.4.1): Cross section normal to the wire axis showing a projection of an electron trajectory onto the x-y plane, after Golledge et al (16).

where N_0 is the equilibrium density of states with E=0. Using the cylindrical coordinates in velocity space, we can write the total drift current at a as :

$$J(a) = \int_0^{\infty} v^2\, dv \int_0^{2\pi} d\phi \int_0^{\pi} d\theta \sin\theta\, e\, v_z\, n(ba).$$

$$= (e^2 E\tau/m) \int_0^{\infty} v^2\, dv \int_0^{2\pi} d\phi \int_0^{\pi} d\theta \sin\theta\, v_z\, (\partial N_0/\partial v_z)\, (1 - e^{-ab/\lambda})$$

$$= (e^2 E\tau/m) \int_0^{\infty} v^3\, (\partial N_0/\partial v_z)\, dv \int_0^{2\pi} d\phi \int_0^{\pi} d\theta \sin\theta \cos^2\theta\, (1 - e^{-ab/\lambda}), \qquad (1.4.4)$$

where we assumed that $N_0(v)$ is isotropic in velocity space, i.e. <u>the Fermi surface is spherical.</u> The distance ab in equation (1.4.4) is to be expressed in terms of θ and ϕ. The conductivity of a thin cylindrical wire can be calculated by integrating (1.4.4) over the cross-sectional area S[17] :

$$\sigma = (e^2\tau/mS) \int_0^{\infty} v^3\, (\partial N_0/\partial v)\, dv \int_s dS \int_0^{2\pi} d\phi \int_0^{\pi} d\theta \sin\theta \cos^2\theta\, (1 - e^{-ab/\lambda}).$$

Since the bulk conductivity σ_0 is given by :

$$\sigma_0 = (4\pi/3)(e^2\tau/m) \int_0^{\infty} v^3\, (\partial N_0/\partial v)\, dv\,,$$

therefore :

$$\sigma/\sigma_0 = (3/4\pi S) \int_s dS \int_0^{2\pi} d\phi \int_0^{\pi} d\theta \sin\theta \cos^2\theta\, (1 - e^{-ab/\lambda}).$$

$$= 1 - (3/4\pi S) \int_s dS \int_0^{2\pi} d\phi \int_0^{\pi} d\theta \sin\theta \cos^2\theta\, e^{-ab/\lambda}. \qquad (1.4.5)$$

Now, if we apply a longitudinal magnetic field ($H_z // E$) the Lorentz force, given by : $F = e(E + v \times H_z / c)$, will split up into two independent components eE along the z-axis and $e(v \times H_z / c)$ which is always in the (x,y) plane. The magnetic field in this case will act as a modifier to the electronic trajectories.

Electrons travelling at an angle θ to the z-axis will move in helical paths which will have circular projections of radius :

$$r = (mvc/ eH) \sin\theta = r_0 \sin\theta. \qquad (1.4.6)$$

If the projection of ab on the (x,y) plane traverses an angle ψ around that circle, then this projection is $\psi r_0 \sin\theta$, and the distance ab is ψr_0. Using this in equation (1.4.3), one can write :

$$n = (eE\tau/m)(\partial N_0/\partial v_z)(1 - e^{-\psi r_0/\lambda})$$

$$= (eE\tau/m)(\partial N_0/\partial v_z)(1 - e^{-\psi/\eta}), \qquad (1.4.7)$$

where $\eta = \lambda/r_0$. Using the same arguments as before, equation (1.4.5) will take the following form :

$$\sigma/\sigma_0 = 1 - (3/4\pi S)\int_s dS \int_0^{2\pi} d\phi \int_0^{\pi} d\theta \sin\theta \cos^2\theta \; e^{-\psi/\eta}, \qquad (1.4.8)$$

where $\psi = \psi(x,y,\theta,\phi)$.

The evaluation of equation (1.4.8) has been done by Chambers[17] who got an analytical solution only for large fields, i. e. large η, but otherwise he used numerical or graphical methods. In general one should use the last two methods as Chambers noticed. Also he found that it is almost impossible to devise a simple and accurate formula valid in the important region of $\eta\kappa \sim 1$. The results of the numerical calculations done by Chambers[17] are summarized in table (1.4.1) and Fig.(1.4.1).

REFERENCES

1. Falkovsky, L. A., Adv. Phys. (1983), 32,753.
2. Bergmann, A., Kaveh, M. and Wiser, N., J. Phys. F., (1982), 12, 3009.
3. Van Vocht, R. J. M., Van Kempen, H. and Wyder, P., Contemp. Phys. (1985) 853.
4. Rowlands, J. A., Duvvury, C. and Woods, S. B., Phys. Rev. Lett. (1978), 40, 1201.
5. Cook, J. C., Can. J. Phys. (1979), 57, 1216.
6. Lee, C. W., Haerle, M. L., Heinen, V., Bass, J., Prott, W. P., Rowlands, J. A. and Schroeder, P. A. , Phys. Rev. B, (1982), 25, 1411.
7. Amararaschara, C. D. and Keesom, P. N, Phys. Rev. B, (1982) , 26, 2720.
8. Haerle, M. L.; Prott, W. P. and Schroeder, P. A., J. Phys. F., (1983), 13, L243.
9. Yu, Z. Z., Haerle, M., Zwart, J. W., Bass, J., Prott, W. P. and Schroeder, P. A., Phys. Rev. Lett. (1984), 52, 368.
10. Fletcher, R., Phys. Rev. Lett., (1980), 45, 287.
11. Overhauser, A. W; Adv. Phys., (1978), 27, 343.
12. Xiaodong Zhu and Overhauser, A. W., Phys. Rev. B., (1984), 30, 622.
13. Schaefer, J. A and Marcus, J. A., Phys. Rev. Lett. (1971), 27, 935.
14. Holroyed, F. W. and Datars, W. R., Cand. J. Phys. (1975), 53, 2517.

15. Sambles, J. R., Elsom, K. C. and Preist, T. W., J. Phys. F., (1982), 12, 1169.

16. Golledge, J. P., Preist, T. W. and Sambles, J. R., J. Phys. F., (1987), 17, 1411.

17. Chambers, R. G., Proc. R. Soc., (1950), A202, 378.

18. Soffer, S. B., J. Appl. Phys., (1967), 38, 1710.

19.Thomson, J.J. Proc. Camb. Phil. Soc. (1901),11,120.

20. Lovell,A. C. B. Proc. Roy. Soc. (1936), A157, 311.

21. Fuchs, K., Proc. Camb. Phil. Soc. (1938),34,120.

22. Dingle, R. B., Proc. Roy. Soc. (1950), A201, 545.

23. Ziman, J. M.," Electron and Phonons ", London: Oxford University Press (1960).

24. Sambles, J. R. and Elsom, K. C. ,J. Phys.(1980), F10, 1487.

25. Stesmans, A., Solid State Comm. (1982), 44, 727.

26. Stesmans, A., Phys. Rev.(1983), B27,1348.

27. Pippard, A. B., in The Physics of Metals by Ziman, J. M., Cambridge University Press (1969), p164.

28. Way, Y. S. and Kao, Y. H., Phys. Rev. (1972), B5, 2039.

29. Preist, T. W. and Sambles, J. R., J. phys.(1986), F16, 2119.

30. De Bass, J., Adv. in Phys. (1972),21,431.

31. Olsen, J.L., Helv. Phys. Acta., (1958), 31, 713.

32. Luthi, B. and Wyder, D., Helv. Phys. Acta., (1960), 33, 667.

33. Blatt, F. J. and Satz, H. G., Helv. Phys. Acta., (1960), 33, 1007.

34. White,G.K. and Woods, S.B., Can. J. Phys.(1955), 33, 58.

35. White, G.K., "Experimental Techniques in Low Temperature Physics" ,Oxford (1959).

36. Adler, J., "The Thermoelectric Power of Sodium", M.Sc. Thesis, University of Alberta, (1960).

37. Rogers,J. S., "The Lorentz Number of Aluminum", M.Sc. Thesis, University of Alberta, (1962).

38.Seth, R.S.,"Deviations From Matthiessen's Rule in Aluminum-Magnesium Alloys ", M.Sc. Thesis, University of Alberta, (1967).

39.Seth, R.S.,"Electrical Resistivities of Dilute Alloys and Deviations From Matthiessen's Rule ", Ph.D. Thesis, University of Alberta, (1969).

40. Ali, N., "Transport Properties of Rare Earth Hexaborides and Alloys", Ph.D. Thesis, University of Alberta, (1984).

41. Cimberle, M.R., Bbel,G., and Rizzuto, C., Adv. in Phys. (1974),23,639.

42. Wiser, N., Can. J. Phys.(1982), 60, 693.

43. Gruneisen, E., Ann. Phys.(1933), 16, 530.

44. Danino, M., Kaveh, M. and Wiser, N., Physica B(1981), 108,907.

45. Danino, M., Kaveh, M. and Wiser, N., J. Phys.F. (1981), 11,2563.

46. Chi, T.C., J. Phys. Chem. Ref. Data (1979), 8, 339.

47. Corruccini, R.J. and Gniewek,J.,"Thermal Expansion of Technical Solids at Low Temperature", N.B.S. Monograph (1961), 29.

48. Van Kempen, H., Lan, J. S., Ribat, J. H. and Wyder, P. Phys. Rev. lett., (1976), 37, 1574.

49. Gugan, D., Proc. R. Soc., (1971), A325, 223.

50. Barrett, C. S., Acta. Cryst. Camb. (1956), 9, 671.

51. Dugdale, J. S. and Gugan, D., Proc. Roy. Soc. (1960), A254, 184.

52. Dugdale, J. S. and Gugan, D., Cryogenics (1960), 2, 103.

53. Oomi, G., Mohamed, M. A-K. and Woods, S. B., Sol. State Comm.(1987), 62, 141.

54. Kittel, C., "Introduction To Solid State Physics" , Fifth Edition, Wiley, New York (1976), P 154.

55. Van Der Mass, J. and Huguenin, R., Proc. LT-18 , Kyoto, (1987).

56. Sambles, J. R. and Elsom, K. C., J. Phys. F.(1985), 15, 161.

57. Lee, P. A. and Ramakrishnan, T. V., Rev. Mod. Phys. (1985), 57, 287.

58. Debashish, C., Comm. Sol. ST. Phys. (1986), 12, 69.

59.Finlayson, D.M., " Localization And Interaction In Disordered Metals and Doped Semiconductors", Proceeding of The Thirty First Scottish Universities Summer School, Edinburgh University Press (1986).

60. Rzchowski, M. S., Rigby, K. W. and Fairbank, W. M., Proc. LT-18, Kyoto (1987), p. 651.

61. Witteborn, F.C. and Fairbank, W.M., Phys. Rev. Lett.(1967), 19, 1049.

62. Witteborn, F.C. and Fairbank, W.M., Nature (1968), 220, 436.

63. Lockhart, J.M., Witteborn, F.C. and Fairbank, W.M., Phys. Rev. Lett.(1977), 38, 1220.

64. White, G. K. and Woods, S. B., Phil. Mag.(1956),1, 846.

65. Hurd, C.M., " The Hall Effect In Metals And Alloys", Plenum Press, New York- London (1972).

66. Garland, J.C.,Phys.Rev.(1969), 185, 1009.

67. Azbel, M.Ya., Soviet Phys. JETP (1963), 17, 667.

68. Azbel, M.Ya., Soviet Phys. JETP (1963), 17, 851.

69. Azbel, M.Ya.and Peschanskii, Soviet Phys. JETP (1966), 22, 399.

70. Lifshits, I.M., Azbel, M.Ya. and Kaganov, M.I., " Electron Theory Of Metals", Consultants Bureau, New York (1973), P 191.

71. Justi,E., Ann. Physik (1948), 3, 183.

72. Babiskin, J. and Siebenmann, P.G., Phys. Kondens. Materie (1969), 9,113.

73. Babiskin, J. and Siebenmann, P.G., Phys. Rev.(1957), 107, 1249.

74. Penz, P.A. and Bowers, R., Phys. Rev. (1968), 172, 991.

APPENDIX (1)

Simple Circuit to Enable The Cumputer to Switch The Sample Current Automatically

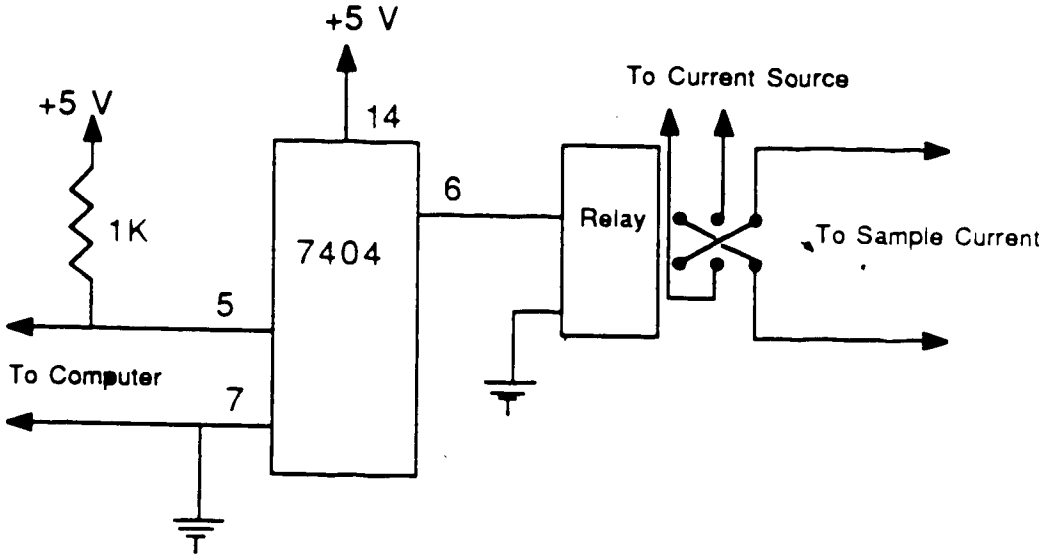

Fig.(A1.1)

APPENDIX(2)

SWITCHING CIRCUIT

1) FIG.(A2.1) : The main interface circuit with the "IEEE 488" bus.

2) FIG.(A2.2) : The latching circuit to activate the selected channel , circuit " A ".

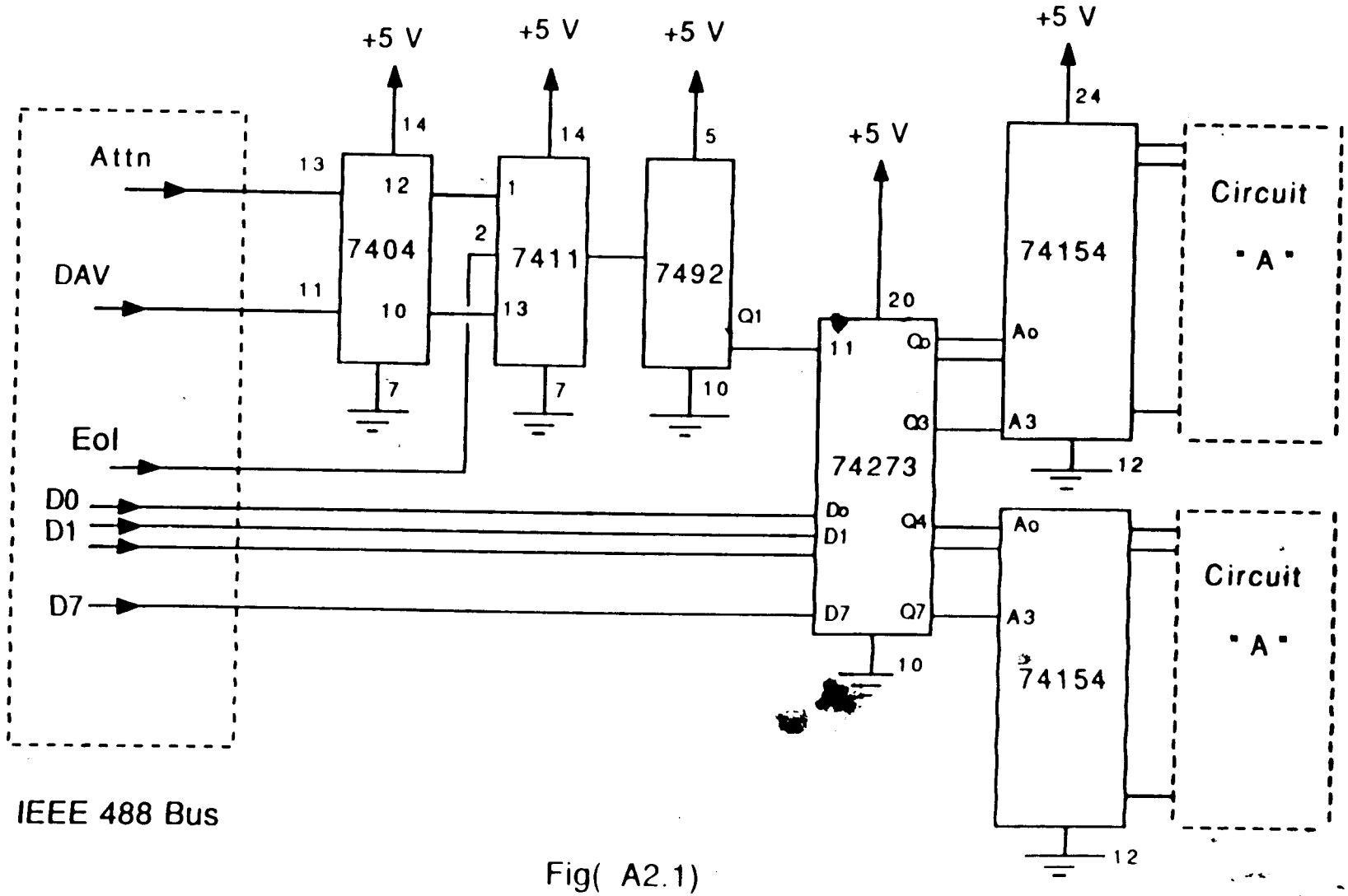
+5 V
+5 V
+5 V
+5 V
+5 V
Attn
DAV
EoI
D0
D1
D7
IEEE 488 Bus
7404
7411
7492
74273
74154
74154
Circuit "A"
Circuit "A"
Q1
Q0
Q3
Q4
Q7
A0
A3
A0
A3

Fig(A2.1)

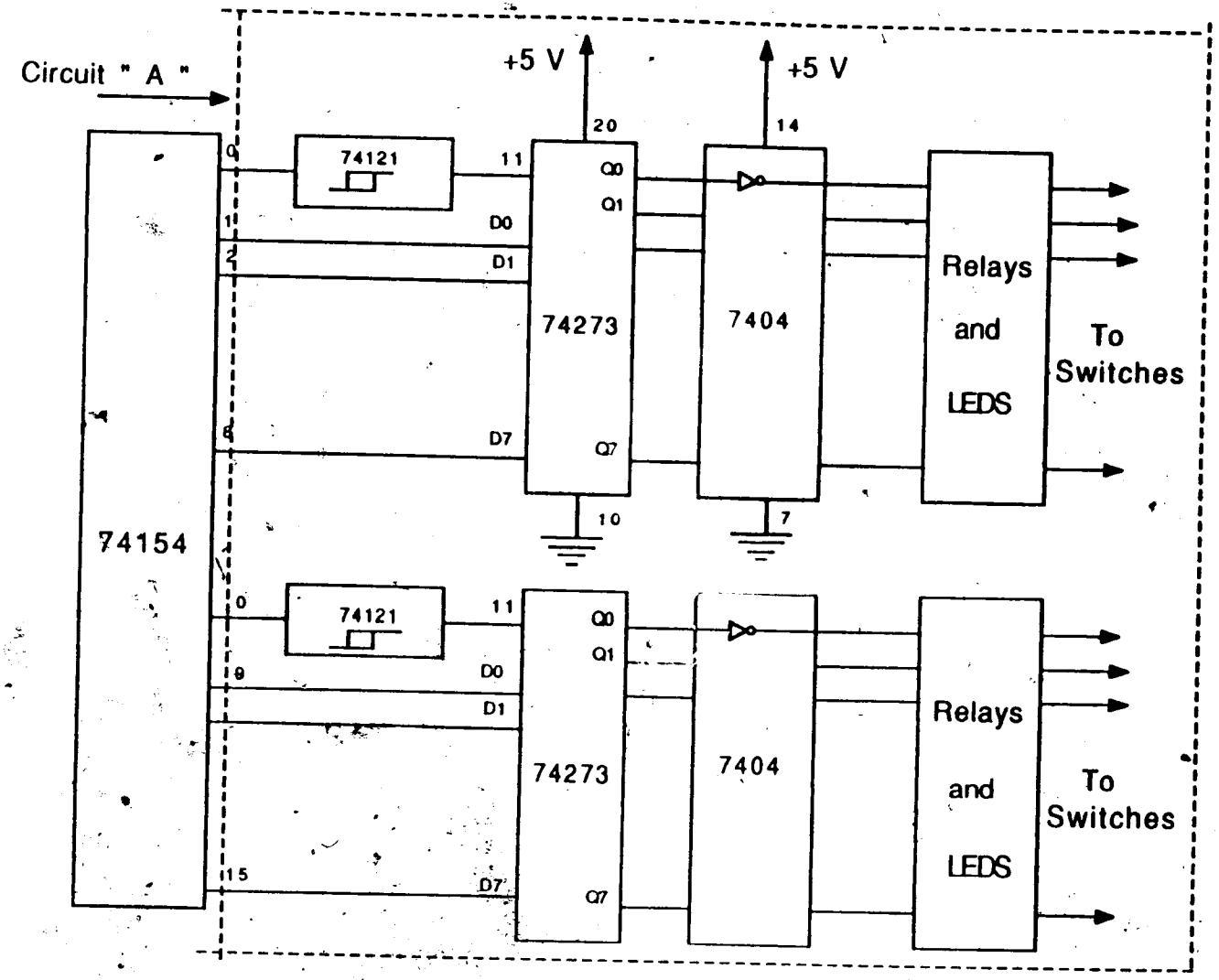
Circuit " A "
74154
74121
74121
+5 V
+5 V
20
14
11
D0
D1
D7
Q0
Q1
Q7
74273
74273
7404
7404
10
7
Relays
and
LEDS
Relays
and
LEDS
To
Switches
To
Switches

Fig.(A2.2)

APPENDIX(3)

" LISTING OF THE COMPUTER PROGRAM WRITTEN AND USED DURING THIS WORK"

```
10 DEF SEG = 0

20 CSEG = (256 * PEEK(&H3C7))+PEEK(&H3C6)
30 DEF SEG
40 INIT% = &H51F :WRSTR% =INIT% + 18:RDSTR% = WRSTR% + 18:R
      DFILE% = RDSTR% + 18
50 WRFILE% = RDFILE% + 18:ADC% =WRFILE% + 18:GRET% = ADC% +
      18:SDL% =GRET% +18
60 LLO% = SDL% + 18:ABORT% = LLO% + 18:PPOLL% = ABORT% + 18
      :PPD% = PPOLL% + 18
70 PPU% = PPD% + 18:RBST% = PPU% + 18:SDR% = RBST% + 18:SPO
      LL% = SDR% + 18
80 PPEN% = SPOLL% + 18:ADTL% = PPEN% + 18:ADTR% = ADTL% + 18
90 TRANSFER% = ADTR% + 18:PCNT% = TRANSFER% + 18:RCNT% = PC
      NT% + 18
100 SDC% = RCNT% + 18:RDSTRS% = SDC% + 18:SETTO% = RDSTRS% +18
120 PRINT "*****************************************************"
130 PRINT"*THIS PROGRAM IS WRITTEN BY MOUSTAFA  A-K. MOHAMED
    UNDER THE  *"
```

```
140 PRINT "* SUPERVISION OF PROFF.: S.B. WOODS . THE MAIN
      FUNCTION OF THE*"

150 PRINT "* PROGRAM IS TO COLLECT DATA AUTOMATICALLY OF
      THE ELECTRICAL     *"

160 PRINT "* RESISTIVITY MEASUREMENTS .IT CAN BE USED ALSO FOR
      DIFFERENT *"
170 PRINT "* EXPERIMENTS BY DOING THE NESSARY MODIFICATIONS
      FOLLOWING THE*"
180 PRINT "* SAME SYNTAX OF CALLING THE REQUIRED SUBROUTINES
            PRESS "F5" WHEN READY... GOOD LUCK! *"
190 PRINT "*********************************************************"
200 STOP
210 DMA% = 3
220 INTR% = 2
230 TCIMODE% = 1
240 MY.ADDR% =1
250 BD.ADDR% = &H31
260 ER% = 0
270 DEF SEG = CSEG
280CALL INIT% (DMA%,INTR%,TCIMODE%,MY.ADDR%,BD.ADDR%,ER%)
290 DEF SEG: IF ER% <> 0 THEN PRINT "ERROR = "ER% : STOP
300  ER%= 0
310 LAD%(0)=5
320 LAD%(1)=199
```

```
330 DEF SEG = CSEG
340 CALL SDC% (LAD%(0),ER%)
350 DEF SEG: IF ER% <> 0 THEN PRINT "ERROR = "ER% : STOP
360 ER%=0
370 ARRAY%(0)=5
380 ARRAY%(1)=199
390 DEF SEG = CSEG
400 CALL SDR%(ARRAY%(0),ER%)
410 DEF SEG: IF ER% <> 0 THEN PRINT "ERROR = "ER% : STOP
420 I=7 :GOSUB 1890
430 COUNT%= 18
440 DEF SEG = CSEG
450 CALL SETTO%(COUNT%)
460 DEF SEG: IF ER% <> 0 THEN PRINT "ERROR = "ER% : STOP
470 TERM%=2 :EOS%=10 :ER%=0
480 LAD%(0)=9
490 LAD%(1)=199
500 FILESP$ ="VOLTMC.BAS:A"
510 DEF SEG =CSEG
520 CALL WRFILE%(EOS%,Q)M%,LAD%(0),FILESP$,ER%)
530 DEF SEG: IF ER% <> 0 THEN PRINT "ERROR = "ER% : STOP
540 ER% = 0
550 LAD%(0)=7
560 LAD%(1)=199
570 DEF SEG = CSEG
580 CALL SDC% (LAD%(0),ER%)
```

```
590 DEF SEG: IF ER% <> 0 THEN PRINT "ERROR = "ER% : STOP
600 ER%=0
610 ARRAY%(0)=7
620 ARRAY%(1)=199
630 DEF SEG = CSEG
640 CALL SDR%(ARRAY%(0),ER%)
650  DEF SEG: IF ER% <> 0 THEN PRINT "ERROR = "ER%
660 COUNT%=18
670 DEF SEG =CSEG
680 CALL SETTO%(COUNT%)
690 DEF SEG: IF ER% <> 0 THEN PRINT "ERROR = "ER% : STOP
700 ER%=0
710 DEF SEG =CSEG
720 CALL GRET%(LAD%(0),ER%)
730 DEF SEG: IF ER% <> 0 THEN PRINT "ERROR = "ER% : STOP
740 I=9 :GOSUB 1670
750 INPUT"TYPE THE SAMPLE CURRENT IN MILLIAMBERS";IC
760 INPUT"TYPE THE RESISTIVITY FACTOR (A/L) IN Cm";F
770 DIM X(100),XY(5000)
780 FOR L=1 TO 4900
790 I=7 :GOSUB 1780
800 'XY(L)=XY
810 IF XY>1000 THEN GOTO 1230
820 R =XY :GOSUB 2480
830 XY(L)= T
840 DT=0.2 : IF T<150 THEN DT=0.1
```

```
850 IF ABS(XY(1)-XY(L))>DT THEN GOTO 1270
860 NEXT L
870 A=5:FILE$="B:KP(T).337":GOSUB 900
880 A=9:FILE$="B:KP(T).2MM":GOSUB 900
890 GOTO 1220
900 FOR K=0 TO 1
910 MOTOR K
920 FOR J=1 TO 6
930  I=A:GOSUB 1780
940 NEXT J
950 X(K)=XY
960 ER% = 0
970 STRNUM% =1
980 TAD%(0)= A
990 TAD%(1)=199
1000 DAT.STR$=SPACE$(55)
1010 DEF SEG =CSEG
1020 CALL RDSTR%(EOS%,TERM%,TAD%(0),DAT.STR$,STRNUM%,ER%)
1030 DEF SEG: IF ER% <> 0 THEN PRINT "ERROR = "ER% ,TAD%(0): STOP
1040 Y(K)=VAL(MID$(DAT.STR$,5,16))
1050 NEXT K
1060 X=(ABS(X(0))+ABS(X(1)))/2
1070 Y=(ABS(Y(0))+ABS(Y(1)))/2
1080 R=Y  :GOSUB 2480
1090 R1=(X/(IC*.001))*F
1100 COUNT=COUNT+1
```

```
1110 PRINT TIME$;" *  ";Y;T," * " ;R1;" *  " ; COUNT ; "*";FILE$
1120 OPEN FILE$ FOR APPEND AS #2
1130 WRITE #2,TIME$ ,Y,T, R1
1140 CLOSE #2
1150 RETURN
1160 TERM%=2 :EOS%=10 :ER%=0
1170  LAD%(0)=I
1180 LAD%(1)=199
1190 FILESP$ ="VOLTMC.BAS:A"
1200 DEF SEG =CSEG
1210 CALL WRFILE%(EOS%,TERM%,LAD%(0),FILESP$,ER%)
1220 DEF SEG: IF ER% <> 0 THEN PRINT "ERROR = "ER% : STOP
1230 RETURN
1240 ER% = 0 :AE=AE+1
1250 STRNUM% =1
1260 TAD%(0)=I :TAD%(1)=199
1270 DAT.STR$=SPACE$(55)
1280 DEF SEG =CSEG
1290 CALLRDSTR%(EOS%,TERM%,TAD%(0),DAT.STR$,STRNUM%,ER%)
1300 IF AE>8 THEN GOTO 1865
1310 DEF SEG: IF ER% <> 0 THEN PRINT "ERROR = "ER% ,I:  GOTO1240
1320 XY= VAL(MID$(DAT.STR$,5,16))
1330 RETURN
1340 ER%=0
1350 ARRAY%(0)=I
1360 ARRAY%(1)=199
```

```
1370 DEF SEG = CSEG
1380 CALL SDR%(ARRAY%(0),ER%)
1390 DEF SEG: IF ER% <> 0 THEN PRINT "ERROR = "ER%
1400 RETURN
1410 1980 ER% = 0
1420 LAD%(0)=I
1430 LAD%(1)=199
1440 DEF SEG = CSEG
1450 CALL SDC% (LAD%(0),ER%)
1460 DEF SEG: IF ER% <> 0 THEN PRINT "ERROR = "ER%
1470 RETURN
1480 FOR I=1 TO 4
1490 OUT &H310,&H50
1500 OUT &H310,&H50+N
1510 NEXT I
1520 RETURN
1530 TERM%=1 :EOS%=10 :ER%=0
1540 STRNUM%=1
1550 LAD%(0)=15
1560 LAD%(1)=199
1570 DATA.STR$ =CHR$(J)
1580 DEF SEG =CSEG
1590CALLWRSTR% (EOS%,TERM%,LAD%(0),DATA.STR$,STRNUM%,ER%)
1600 DEF SEG: IF ER% <> 0 THEN PRINT "ERROR = " ER%
1610 RETURN
1620 ER%=0
```

```
1630 TERM% = 1  :EOS%=0
1640 STRNUM% =2
1650 TAD%(0)=15:TAD%(1)=199
1660 DAT.STR$=SPACE$(55)
1670 DEF SEG =CSEG
1680 CALL RDSTR%(EOS%,TERM%,TAD%(0),DAT.STR$,STRNUM%, ER%)
1690 DEF SEG: IF ER% <> 0 THEN PRINT "ERROR = "ER% :STOP
1700 OUT &H310,&H5F
1710 ZX(1)= ASC(MID$(DAT.STR$,1,1))
1720 ZX(2)= ASC(MID$(DAT.STR$,2,1)) AND &HF
1730 ZX(3)= INT(ASC(MID$(DAT.STR$,2,1))/16)
1740 Z =((ZX(1)+ZX(2)*256)-2048)*5/2048
1750 PRINT ZX(3),Z
1760 IF ZX(3) <>  J THEN N=N+1 :PRINT "ERR0R";N :GOTO 2290
1770 RETURN
1780 T1= 8.99537658# +2.574883460998535#*R-.1749398708343506#*(R^2)
     +5.273688912391662D-03*(R^3)-1.769589289324358D-04*(R^4)
1790 T2= -2.290635237045535D-08*(R^6)+1.096844420844789D-10* (R^7)
     -2.204603687105955D-13*(R^8)
1800 T= T1+T2
1810 RETURN
1820 R=LOG(R)
1830 T1= 4.17021179199219#-4.70204162597656#*R+3.7307243347168#*
     (R^2)-.453216552734375#*(R^3)+.8855181932449341#*(R^ 4)
     -.1091288924217224#*(R^5)
1840 T2= +.091002702713013D-03*(R^6)-3.292248584330082D-04* (R^7)
```

```
    +5.625037374556996D-06*(R^8)
1850 T= T1+T2
1860 T=EXP(T)
1870 RETURN

1880 T= 5.56674194335938# +.52645206451416#*R+.398388043045998D-02*
        (R^2)-.612974684685469D-04*(R^3)+.273722308629658D-06*(R^4)
1890 IF T<79.1 GOTO 1910
1900 RETURN
1910 T1= 4.30778312683106#+4.45681762695312#*R-07.91708374023 44#
    *(R^2)+37.8391723632813#*(R^3)-12.4631652832031#*(R^4)
    +9.40821838378906#*(R^5)
1920 T2= -0.51036071777344#*(R^6)+.587417602539062#*(R^7)-
    .639608442783355 7#*(R^8)+.047004297375679D-02*(R^9)-1.71985
    1512461901D-03*(R^10)
1930 T=T1+T2
1940 RETURN
```

APPENDIX(4)

DATA TABLES

On the following pages the data are tabulated for the electrical conductivity or R(300)/ R(T) at different temperature values as function of sample diameter and the ratio [R(4.2, H) - R(4.2, 0)] / R(4.2, 0) as function of the external applied magnetic field parallel to the wire axis. A number of samples were prepared at one time, as described in chapter II, and referred to as a set with a set number. For purposes of clarity, the temperature at which the data were collected and the sample set number as well as the annealing time at room temperature are listed for each data table. The results are organized in the following order :

1) H = 0 measurements :

A) For potassium.

B) For sodium.

C) For indium.

2) H ≠ 0 measurements :

A) For potassium.

B) For sodium.

C) For indium.

Table(A4.1)

Sample Resistivity, Conductivity at 4.2 K and RRR, the residual resistance ratio, RRR≡ $[R_{300}/ R_{4.2}]$, as a Function of Diameter For Potassium.

Set #1 :

a) Annealing time = one days at room temperature.

d(mm)	(nano-ohm cm)	$\sigma_{4.2}$(nano-ohm cm)$^{-1}$	RRR
0.33	23.75	0.042	284
0.56	15.53	0.064	436
1.15	5.86	0.170	1152
1.47	4.18	0.239	1616
1.75	5.88	0.170	1148
2.02	4.85	0.206	1396
2.32	6.40	0.156	1060
2.65	7.26	0.137	928
3.00	7.98	0.125	848
3.20	9.09	0.110	744

Table(A4.2)

Sample Resistivity, Conductivity at 4.2 K and RRR, the residual resistance ratio, RRR≡ $[R_{300}/R_{4.2}]$, as a Function of Diameter For Potassium.

1) Set #1:

a) Annealing time = 14 days at room temperature.

d(mm)	$\rho_{4.2}$(nano-ohm cm)	$\sigma_{4.2}$(nano-ohm cm)-1	RRR
0.33	135.13	0.007	50
0.56	10.20	0.0[illegible]	667
1.15	3.91	0.255	1740
1.47	1.60	0.621	4252
1.75	1.81	0.552	3760
2.02	2.08	0.480	3266
2.32	2.39	0.417	2837
2.65	[illegible].59	0.385	2622
3.00	2.65	0.376	2560
3.20	3.02	0.330	2247

Table(A4.3)

Sample Resistivity, Conductivity at 4.2 K and RRR, the residual resistance ratio, RRR≡[R_{300}/ $R_{4.2}$], as a Function of Diameter For Potassium.

1) Set #2 :

a) Annealing time = 30 hours at room temperature.

d(mm)	$\rho_{4.2}$(nano-ohm cm)	$\sigma_{4.2}$(nano-ohm cm)-1	RRR
0.33	22.45	0.044	292
0.56	14.24	0.070	460
1.00	8.17	0.122	804
1.15	5.38	0.186	1220
1.25	5.10	0.196	1288
1.47	4.07	0.246	1616
1.75	5.63	0.177	1168
2.02	4.61	0.217	1424
2.32	6.11	0.164	1076
2.65	7.05	0.137	932
3.00	7.64	0.131	860
3.20	8.79	0.114	748

Table(A4.4)

Sample Resistivity, Conductivity at 4.2 K and RRR, the residual resistance ratio, RRR≡[R_{300}/ $R_{4.2}$], as a Function of Diameter For Potassium.

1) Set #2 :

a) Annealing time = 14 days at room temperature.

d(mm)	$\rho_{4.2}$(nano-ohm cm)	$\sigma_{4.2}$(nano-ohm cm)-1	RRR
0.33	44.70	0.008	152
0.56	13.60	0.073	500
1.00	5.67	0.176	1200
1.15	4.53	0.220	1500
1.25	3.40	0.294	2000
1.47	2.62	0.382	2610
1.75	2.87	0.350	2370
2.02	3.18	0.310	2140
2.32	3.61	0.280	1880
2.65	3.98	0.250	1710
3.00	4.25	0.230	1600
3.20	4.47	0.220	1520

Table(A4.5)

Sample Resistivity, Conductivity at 4.2 K and RRR, the residual resistance ratio, RRR≡[R_{300}/ $R_{4.2}$], as a Function of Diameter For Potassium.

1) Set #3 : The samples were extruded through dies made of a machinable ceramic.

a) Annealing time = 30 hours at room temperature.

d(mm)	$\rho_{4.2}$(nano-ohm cm)	$\sigma_{4.2}$(nano-ohm cm)-1	RRR
0.33	21.01	0.047	312
0.40	15.91	0.063	412
0.52	11.71	0.085	560
0.92	7.10	0.141	924
0.97	7.13	0.140	920
2.02	4.85	0.206	1396
2.75	5.66	0.176	1160

Table(A4.6)

Sample Resistivity, Conductivity at 4.2 K and RRR, the residual resistance ratio, RRR≡[R_{300}/ $R_{4.2}$], as a Function of Diameter For Potassium.

1) Set #3 : The samples were extruded through dies made of a machinable ceramic.

a) Annealing time = 14 days at room temperature.

d(mm)	$\rho_{4.2}$(nano-ohm cm)	$\sigma_{4.2}$(nano-ohm cm)-1	RRR
0.33	40.95	0.014	166
0.40	19.40	0.051	350
0.52	14.80	0.068	460
0.92	5.71	0.175	1190
0.97	5.70	0.176	1195
2.02	3.22	0.310	2110
2.75	4.03	0.248	1690

Table(A4.7)

Sample Resistivity at 10 K and $[R_{300}/R_{10}]$, as a Function of Diameter For Potassium.

1) Set #2 :

Annealing time ≥ one month at room temperature.

d(mm)	ρ_{10}(nano-ohm cm)	$[R_{300}/R_{10}]$
0.33	50.70	134
0.56	8.99	756
1.00	9.29	730
1.15	9.20	740
1.25	9.29	730
1.47	9.60	710
1.75	9.64	705
2.02	9.85	690
2.32	10.30	660
2.65	10.22	665
3.00	10.62	640
3.20	10.80	630

Table(A4.8)

Sample Resistivity at 10 K and $[R_{300}/R_{10}]$, as a Function of Diameter For Potassium.

1) Set #3 :

Annealing time ≥ one month at room temperature.

d(mm)	ρ_{10}(nano-ohm cm)	$[R_{300}/R_{10}]$
0.33	50.00	136
0.40	30.90	220
0.52	16.95	401
0.92	9.20	740
0.97	9.20	740
2.02	10.00	680
2.75	10.25	663

Table(A4.9)

Sample Resistivity at 15 K and $[R_{300}/R_{15}]$, as a Function of Diameter For Potassium.

1) Set #2 :

Annealing time ≥ one month at room temperature.

d(mm)	ρ_{15}(nano-ohm cm)	$[R_{300}/R_{15}]$
0.33	52.90	130.0
0.56	50.00	136.0
1.00	50.30	135.0
1.15	51.13	133.0
1.25	51.09	133.1
1.47	51.32	132.5
1.75	51.90	131.0
2.02	52.51	129.5
2.32	53.13	128.0
2.65	53.33	127.5
3.00	54.34	125.0
3.20	54.34	125.0

Table(A4.10)

Sample Resistivity at 15 K and $[R_{300}/R_{15}]$, as a Function of Diameter For Potassium.

1) Set #3 :

Annealing time ≥ one month at room temperature.

d(mm)	ρ_{15}(nano-ohm cm)	$[R_{300}/R_{15}]$
0.33	52.60	132.0
0.40	49.62	137.0
0.52	49.81	136.5
0.92	50.56	134.5
0.97	50.37	135.0
2.03	52.11	130.5
2.75	53.53	127.0

Table(A4.11)

Sample Resistivity at 20 K and $[R_{300}/R_{20}]$, as a Function of Diameter For Potassium.

1) Set #2 :

Annealing time ≥ one month at room temperature.

d(mm)	ρ_{20}(nano-ohm cm)	$[R_{300}/R_{20}]$
0.33	125.9	54.0
0.56	126.6	53.7
1.00	127.1	53.5
1.15	127.6	53.3
1.25	128.3	53.0
1.47	129.5	52.5
1.75	129.3	52.6
2.02	130.8	52.0
2.32	132.6	51.3
2.65	134.6	50.5
3.00	135.1	50.3
3.20	136.0	50.0

.Table(A4.12)

Sample Resistivity at 20 K and $[R_{300}/R_{20}]$, as a Function of Diameter For Potassium.

1) Set #3 :

Annealing time ≥ one month at room temperature.

d(mm)	ρ_{20}(nano-ohm cm)	$[R_{300}/R_{20}]$
0.33	127.5	53.3
0.40	124.8	54.5
0.52	125.9	54.0
0.92	127.6	53.3
0.97	127.8	53.2
2.02	132.0	51.5
2.75	133.6	50.9

Table(A4.13)

Sample Resistivity at 30 K and $[R_{300}/R_{30}]$, as a Function of Diameter For Potassium.

1) Set #2 :

Annealing time ≥ one month at room temperature.

d(mm)	ρ_{30} (10^{-7} ohm cm)	$[R_{300}/R_{30}]$
0.33	1.91	35.5
0.56	1.93	35.2
1.00	1.95	34.8
1.15	1.97	34.6
1.25	1.98	34.4
1.47	1.99	34.2
1.75	2.00	33.9
2.02	2.02	33.7
2.32	2.05	33.1
2.65	2.06	33.0
3.00	2.08	32.6
3.20	2.10	32.3

Table(A4.14)

Sample Resistivity at 30 K and $[R_{300}/R_{30}]$, as a Function of Diameter For Potassium.

1) Set #3 :

Annealing time ≥ one month at room temperature.

d(mm)	ρ_{30}(10^{-7} ohm cm)	$[R_{300}/R_{30}]$
0.33	1.92	35.4
0.40	1.92	35.4
0.52	1.93	35.3
0.92	1.96	34.7
0.97	1.95	34.8
2.02	2.03	33.5
2.75	2.08	32.7

Table(A4.15)

Sample Resistivity at 40 K and $[R_{300}/R_{40}]$, as a Function of Diameter For Potassium.

1) Set #2 :

Annealing time ≥ one month at room temperature.

d(mm)	ρ_{40} (10^{-7} ohm cm)	$[R_{300}/R_{40}]$
0.33	5.00	13.6
0.56	5.03	13.5
1.00	5.07	13.4
1.15	5.07	13.4
1.25	5.11	13.3
1.47	5.15	13.2
1.75	5.19	13.1
2.02	5.23	13.0
2.32	5.27	12.9
2.65	5.31	12.8
3.00	5.40	12.6
3.20	5.39	12.6

Table(A4.16)

Sample Resistivity at 40 K and $[R_{300}/R_{40}]$, as a Function of Diameter For Potassium.

1) Set #3 :

Annealing time ≥ one month at room temperature.

d(mm)	$\rho_{40}(10^{-7}$ ohm cm)	$[R_{300}/R_{40}]$
0.33	5.03	13.5
0.40	5.03	13.5
0.52	5.03	13.5
0.92	5.07	13.4
0.97	5.07	13.4
2.02	5.27	12.9
2.75	5.31	12.8

Table(A4.17)

Sample Resistivity at 50 K and $[R_{300}/R_{50}]$, as a Function of Diameter For Potassium.

1) Set #2 :

Annealing time ≥ one month at room temperature.

d(mm)	$\rho_{50}(10^{-7}$ ohm cm)	$[R_{300}/R_{50}]$
0.33	6.63	10.25
0.56	6.60	10.30
1.00	6.57	10.35
1.15	6.60	10.30
1.25	6.60	10.30
1.47	6.57	10.35
1.75	6.63	10.25
2.02	6.60	10.30
2.32	6.60	10.30
2.65	6.60	10.30
3.00	6.57	10.35
3.20	6.63	10.25

Table(A4.18)

Sample Resistivity at 50 K and $[R_{300}/R_{50}]$, as a Function of Diameter For Potassium.

1) Set #3.:

Annealing time ≥ one month at room temperature.

d(mm)	$\rho_{50}(10^{-7}$ ohm cm)	$[R_{300}/R_{50}]$
0.33	6.63	10.25
0.40	6.60	10.30
0.52	6.57	10.35
0.92	6.60	10.30
0.97	6.60	10.30
2.02	6.57	10.35
2.75	6.63	10.25

Table(A4.19)

Sample Resistivity at 77 K and $[R_{300}/R_{77}]$, as a Function of Diameter For Potassium.

1) Set #1 :

Annealing time = 14 days at room temperature.

d(mm)	ρ_{77} (10^{-7} ohm cm)	$[R_{300}/R_{77}]$
0.33	12.60	5.40
0.56	12.36	5.50
1.15	12.36	5.50
1.47	12.36	5.50
1.75	12.36	5.50
2.02	12.36	5.50
2.32	12.36	5.50
2.65	12.36	5.50
3.00	12.36	5.50
3.20	12.36	5.50

Table(A4.20)

Sample Resistivity at 77 K and $[R_{300}/R_{77}]$, as a Function of Diameter For Potassium.

1) Set #2 :

Annealing time ≥ one month at room temperature.

d(mm)	ρ_{77} (10^{-7} ohm cm)	$[R_{300}/R_{77}]$
0.33	12.48	5.45
0.56	12.25	5.55
1.00	12.36	5.50
1.15	12.36	5.50
1.25	12.36	5.50
1.47	12.36	5.50
1.75	12.36	5.50
2.02	12.36	5.50
2.32	12.36	5.50
2.65	12.36	5.50
3.00	12.36	5.50
3.20	12.48	5.45

Table(A4.21)

Sample Resistivity at 77 K and $[R_{300}/R_{77}]$, as a Function of Diameter For Potassium.

1) Set #3 :

Annealing time ≥ one month at room temperature.

d(mm)	ρ_{77}(10^{-7} ohm cm)	$[R_{300}/R_{77}]$
0.33	12.36	5.50
0.40	12.25	5.55
0.52	12.36	5.50
0.92	12.48	5.45
0.97	12.36	5.50
2.02	12.25	5.55
2.75	12.36	5.50

Table(A4.22)

Sample Resistivity, Conductivity at 4.2 K and RRR, the residual resistance ratio, RRR≡[R_{300}/ $R_{4.2}$], as a Function of Diameter For Sodium.

1) Set #1 :

a) Annealing time = one days at room temperature.

d(mm)	$\rho_{4.2}$(nano-ohm cm)	$\sigma_{4.2}$(nano-ohm cm)-1	RRR
0.33	74.1	0.013	180
0.36	46.3	0.022	189
0.40	35.6	0.028	216
0.53	25.8	0.039	221
0.78	17.2	0.058	343
1.00	14.8	0.068	401
1.30	14.8	0.066	394
1.47	15.0	0.067	364
2.03	15.8	0.063	372
2.32	16.8	0.059	317
2.65	16.7	0.060	363
3.00	18.2	0.055	319

Table(A4.23)

Sample Resistivity, Conductivity at 4.2 K and RRR, the residual resistance ratio, RRR≡ $[R_{300}/ R_{4.2}]$, as a Function of Diameter For Sodium.

1) Set [illegible]

a) [illegible] = one day at room temperature.

d(mm)	$\rho_{4.2}$(nano-ohm cm)	$\sigma_{4.2}$(nano-ohm cm)-1	RRR
0.33	32.3	0.031	197
0.40	29.3	0.034	217
0.53	26.5	0.038	240
0.65	25.1	0.040	253
0.83	19.5	0.051	326
0.88	19.2	0.052	331
0.90	20.2	0.050	315
0.93	20.0	0.050	317
1.48	21.1	0.048	302
2.03	15.8	0.063	250
3.00	18.2	0.055	205

Table(A4.24)

Sample Resistivity, Conductivity at 4.2 K and RRR, the residual resistance ratio, RRR≡[R_{300}/ $R_{4.2}$], as a Function of Diameter For Sodium.

1) Set #3 :

a) Annealing time = two days at room temperature.

(mm)	$\rho_{4.2}$(nano-ohm cm)	$\sigma_{4.2}$(nano-ohm cm)-1	RRR
0.33	94.8	0.011	65.4
0.36	[illegible].7	0.010	59.2
0.40	77.4	0.013	80.1
0.53	65.3	0.015	94.9
0.60	51.9	0.019	119.3
0.62	38.5	0.026	161.2
0.82	30.8	0.032	201.1
0.92	28.0	0.360	221.3
1.47	30.3	0.033	204.9
2.03	32.4	0.031	191.5
2.32	32.5	0.031	190.8
2.62	40.2	0.025	154.3

Table(A4.25)

Sample Resistivity, Conductivity at 4.2 K and RRR, the residual resistance ratio, RRR≡[R_{300}/ $R_{4.2}$], as a Function of Diameter For Sodium.

1) Set #4 : The samples were extruded through dies made of a machinable ceramic.

a) Annealing time = two days at room temperature.

d(mm)	$\rho_{4.2}$(nano-ohm cm)	$\sigma_{4.2}$(nano-ohm cm)-1	RRR
0.33	101.3	0.010	61.2
0.40	86.9	0.012	71.3
0.52	73.1	0.014	84.8
0.92	28.2	0.036	220.0
0.97	28.2	0.035	21[illegible]7
2.02	35.5	0.028	174.8
2.75	40.9	0.025	151.6

Table(A4.26)

Sample Resistivity, Conductivity at 4.2 K and RRR, the residual resistance ratio, RRR≡[R_{300}/ $R_{4.2}$], as a Function of Diameter For Sodium.

1) Set #3 :

a) Annealing time = 14 days at room temperature.

d(mm)	$\rho_{4.2}$(nano-ohm	$\sigma_{4.2}$(nano-ohm cm)-1	RRR
0.33	36.2	0.028	171.2
0.36	36.3	0.028	170.5
0.40	32.4	0.031	191.3
0.53	29.2	0.034	212.4
0.60	24.9	0.040	248.8
0.62	15.6	0.064	398.6
0.82	12.4	0.081	501.1
0.92	10.1	0.099	612.3
1.47	11.7	0.085	529.5
2.03	11.7	0.085	529.0
2.32	13.5	0.074	459.2
2.62	11.1	0.090	556.3

Table(A4.27)

Sample Resistivity, Conductivity at 4.2 K and RRR, the residual resistance ratio, RRR≡[R_{300}/ $R_{4.2}$], as a Function of Diameter For Sodium.

1) Set #4 : The samples were extruded through dies made of a machinable ceramic.

a) Annealing time = 14 days at room temperature.

d(mm)	$\rho_{4.2}$(nano-ohm cm)	$\sigma_{4.2}$(nano-ohm cm)-1	RRR
0.33	38.[illegible]	0.026	161.6
0.40	36.7	0.027	169.0
0.52	30.9	0.032	200.5
0.92	10.3	0.097	601.3
0.97	10.3	0.097	600.9
2.02	12.4	0.081	498.9
2.75	14.8	0.067	417.8

Table(A4.28)

Sample Resistivity at 10 K and [R_{300}/ R_{10}], as a Function of Diameter For Sodium.

1) Set #3 :

Annealing time ≥ one month at room temperature.

d(mm)	ρ_{10}(nano-ohm cm)	R_{300}/R_{10}
0.33	38.5	161.0
0.36	33.6	184.7
0.40	30.8	201.5
0.53	16.5	374.8
0.60	14.5	427.3
0.62	14.5	428.6
0.82	14.6	425.0
0.92	15.5	400.9
1.47	16.1	384.7
2.03	16.5	375.4
2.32	19.3	321.1
2.62	20.6	300.2

Table(A4.29)

Sample Resistivity at 10 K and [R_{300}/ R_{10}], as a Function of Diameter For Sodium.

1) Set #4 :

Annealing time ≥ one month at room temperature.

d(mm)	ρ_{10}(nano-ohm cm)	R_{300}/R_{10}
0.33	35.4	175.3
0.40	24.8	149.7
0.52	20.7	299.8
0.92	14.6	424.9
0.97	14.6	424.5
2.02	18.3	339.8
2.75	19.1	325.1

Table(A4.

Sample Resistivity at 15 K and [R_{300}/R_{15}], as a Function of Diameter For Sodium.

1) Set #3 :

Annealing time ≥ one month at room temperature.

d(mm)	ρ_{10}(nano-ohm cm)	R_{300}/R_{15}
0.33	42.8	144.8
0.36	41.3	150.2
0.40	35.4	175.3
0.53	20.3	305.0
0.60	21.8	284.7
0.62	20.1	304.8
0.82	21.8	284.5
0.92	21.0	295.1
1.47	24.3	254.9
2.03	25.8	240.0
2.32	27.3	227.4
2.62	29.6	209.8

Table(A4.31)

Sample Resistivity at 15 K and [R_{300}/ R_{15}], as a Function of Diameter For Sodium.

1) Set #4 :

Annealing time ≥ one month at room temperature.

d(mm)	ρ_{15}(nano ohm cm)	R_{300}/R_{15}
0.33	47.5	130.6
0.40	35.4	175.3
0.52	22.4	276.2
0.92	21.7	285.1
0.97	21.8	284.9
2.02	27.4	226.4
2.75	30.9	200.5

Table(A4.32)

Sample Resistivity at 20 K and $[R_{300}/R_{20}]$, as a Function of Diameter For Sodium.

1) Set #3 :

Annealing time ≥ one month at room temperature.

d(mm)	ρ_{20}(nano-ohm cm)	$[R_{300}/R_{20}]$
0.33	66.6	93.1
0.36	62.1	99.8
0.40	41.3	150.2
0.53	42.8	144.9
0.60	43.4	142.7
0.62	41.3	150.0
0.82	42.1	147.3
0.92	41.4	149.8
1.47	45.1	137.4
2.03	46.6	133.1
2.32	42.7	145.1
2.62	47.6	130.2

Table(A4.33)

Sample Resistivity at 20 K and $[R_{300}/R_{20}]$, as a Function of Diameter For Sodium.

1) Set #4 :

Annealing time ≥ one month at room temperature.

d(mm)	ρ_{20}(nano-ohm cm)	$[R_{300}/R_{20}]$
0.33	63.8	97.2
0.40	54.8	113.1
0.52	43.6	142.3
0.92	42.7	145.0
0.97	42.8	144.8
2.02	45.0	137.8
2.75	49.4	125.4

Table(A4.34)

Sample Resistivity at 30 K and $[R_{300}/R_{30}]$, as a Function of Diameter For Sodium.

1) Set #3 :

Annealing time ≥ one month at room temperature.

d(mm)	ρ_{30}(n ohm cm)	$[R_{300}/R_{30}]$
0.33	89.9	68.9
0.36	90.8	68.3
0.40	84.9	73.0
0.53	88.3	70.2
0.60	91.0	68.1
0.62	86.2	71.9
0.82	88.8	69.8
0.92	91.1	68.0
1.47	90.2	68.7
2.03	96.4	64.3
2.32	114.4	54.2
2.62	107.1	57.9

Table(A4.35)

Sample Resistivity at 30 K and $[R_{300}/R_{30}]$, as a Function of Diameter For Sodium.

1) Set #4 :

Annealing time ≥ one month at room temperature.

d(mm)	ρ_{30}(n ohm cm)	$[R_{300}/R_{30}]$
0.33	88.4	70.1
0.40	88.2	70.3
0.52	91.3	67.9
0.92	88.4	70.1
0.97	90.0	68.9
2.02	100.8	61.5
2.75	103.3	60.0

Table(A4.36)

Sample Resistivity at 40 K and $[R_{300}/R_{40}]$, as a Function of Diameter For Sodium.

1) Set #3 :

Annealing time ≥ one month at room temperature.

d(mm)	ρ_{40} (10^{-7} ohm cm)	$[R_{300}/R_{40}]$
0.33	2.78	22.3
0.36	2.64	23.5
0.40	2.64	23.5
0.53	2.82	22.0
0.60	2.81	22.1
0.62	2.69	23.0
0.82	2.76	22.5
0.92	2.82	22.0
1.47	2.94	21.1
2.03	3.18	19.5
2.32	4.00	15.5
2.62	3.54	17.5

Table(A4.37)

Sample Resistivity at 40 K and $[R_{300}/R_{40}]$, as a Function of Diameter For Sodium.

1) Set #4 :

Annealing time ≥ one month at room temperature.

d(mm)	$\rho_{40}(10^{-7}$ ohm cm)	$[R_{300}/R_{40}]$
0.33	2.77	22.4
0.40	2.76	22.5
0.52	2.69	23.0
0.92	2.82	22.0
0.97	2.81	22.1
2.02	2.99	20.7
2.75	3.54	17.5

Table(A4.38)

Sample Resistivity at 50 K and $[R_{300}/R_{50}]$, as a Function of Diameter For Sodium.

1) Set #3 :

Annealing time ≥ one month at room temperature.

d(mm)	ρ_{50}(10^{-7} ohm cm)	$[R_{300}/R_{50}]$
0.33	3.71	16.7
0.36	3.46	17.9
0.40	3.42	18.1
0.53	3.65	17.0
0.60	3.76	16.5
0.62	3.58	17.3
0.82	3.54	17.5
0.92	3.71	16.7
1.47	3.54	17.5
2.03	3.63	17.1
2.32	4.10	15.5
2.62	3.82	16.2

Table(A4.39)

Sample Resistivity at 50 K and $[R_{300}/R_{50}]$, as a Function of Diameter For Sodium.

1) Set #4 :

A[illegible]e month at room temperature.

d(mm)	$\rho_{50}(10^{-7}$ ohm cm)	$[R_{300}/R_{50}]$
0.33	3.65	17.0
0.40	3.63	17.1
0.52	3.54	17.5
0.92	3.69	16.8
0.97	3.69	16.8
2.02	3.80	16.3
2.75	3.80	16.3

Table(A4.40)

Sample Resistivity at 60 K and $[R_{300}/R_{60}]$, as a Function of Diameter For Sodium.

1) Set #3 :

Annealing time ≥ one month at room temperature

d(mm)	ρ_{60} (10^{-7} ohm cm)	$[R_{300}/R_{60}]$
0.33	5.63	11.0
0.36	5.69	10.9
0.40	5.58	11.1
0.53	5.58	11.1
0.60	5.63	11.0
0.62	5.74	10.8
0.82	5.63	11.0
0.92	5.85	10.6
1.47	5.58	11.1
2.03	5.69	10.9
2.32	6.02	10.3
2.62	6.08	10.2

Table(A4.41)

Sample Resistivity at 60 K and $[R_{300}/R_{60}]$, as a Function of Diameter For Sodium.

1) Set #4

Annealing time > one month at room temperature.

d(mm)	ρ_{60}(10^{-7} ohm cm)	$[R_{300}/R_{60}]$
0.33	5.69	10.9
0.40	5.69	10.9
0.52	5.69	10.9
0.92	5.79	10.7
0.97	5.79	10.7
2.02	6.02	10.3
2.75	6.02	10.3

Table(A4.42)

Sample Resistivity at 70 K and $[R_{300}/R_{70}]$, as a Function of Diameter For Sodium.

1) Set #3 :

Annealing time ≥ one month at room temperature.

d(mm)	$\rho_{70}(10^{-7}$ ohm cm)	$[R_{300}/R_{70}]$
0.33	7.75	8.0
0.36	7.47	8.3
0.40	7.56	8.2
0.53	7.56	8.2
0.60	7.85	7.9
0.62	7.65	8.1
0.82	7.56	8.2
0.92	7.95	7.8
1.47	7.47	8.3
2.03	7.85	7.9
2.32	7.65	8.1
2.62	7.85	7.9

Table (A4.43)

Sample Resistivity at 70 K and $[R_{300}/R_{70}]$, as a Function of Diameter For Sodium.

1) Set #4 :

Annealing time ≥ one month at room temperature.

d(mm)	ρ_{70} (10^{-7} ohm cm)	$[R_{300}/R_{70}]$
0.33	7.85	7.9
0.40	7.71	8.0
0.52	7.75	8.0
0.92	7.74	8.0
0.97	7.73	8.0
2.02	7.62	8.1
2.75	7.73	8.0

Table(A4.44)

Sample Resistivity at 77 K and $[R_{300}/R_{77}]$, as a Function of Diameter For Sodium

1) Set #3

Annealing time = 14 days at room temperature

d(mm)	ρ_{77} ($\times 10^{-9}$ ohm cm)	$[R_{300}/R_{77}]$
0.33	9.84	6.30
0.36	10.08	6.15
0.40	9.69	6.40
0.52	9.92	6.25
0.60	10.00	6.20
0.62	9.84	6.30
0.82	9.76	6.35
0.92	9.92	6.25
1.47	10.03	6.18
2.02	10.07	6.15
2.32	10.28	6.03
2.62	10.33	6.00

Table(A4.45)

Sample Resistivity at 77 K and $[R_{300}/R_{77}]$, as a Function of Diameter For Sodium.

1) Set #4 :

Annealing time ≥ one month at room temperature.

d(mm)	ρ_{77}(10^{-7} ohm cm)	$[R_{300}/R_{77}]$
0.33	9.98	6.21
0.40	9.96	6.22
0.52	9.76	6.35
0.92	10.08	6.15
0.97	10.05	6.17
2.02	10.29	6.03
2.75	10.32	6.01

Table(A4,46)

Sample Resistivity at 90 K and $[R_{300}/R_{90}]$, as a Function of Diameter For Sodium.

1) Set #3 :

Annealing time ≥ one month at room temperature.

d(mm)	ρ_{90} (10^{-7} ohm cm)	$[R_{300}/R_{90}]$
0.33	11.70	5.30
0.36	11.81	5.25
0.40	11.69	5.30
0.53	11.92	5.20
0.60	11.59	5.35
0.62	11.80	5.25
0.82	11.93	5.20
0.92	11.82	5.25
1.47	11.60	5.35
2.03	11.93	5.20
2.32	11.48	5.40
2.62	11.91	5.20

Table(A4.47)

Sample Resistivity at 90 K and $[R_{300}/R_{90}]$, as a Function of Diameter For Sodium.

1) Set #4 :

Annealing time ≥ one month at room temperature.

d(mm)	ρ_{90}(10^{-7} ohm cm)	$[R_{300}/R_{90}]$
0.33	11.90	5.20
0.40	11.93	5.20
0.52	11.70	5.30
0.92	11.80	5.25
0.97	11.83	5.25
2.02	11.68	5.30
2.75	11.81	5.25

Table(A4.48)

Sample Resistivity at 4.2 K as a Function of Diameter for Indium.

1) Set #1 :

No annealing effect has been detected.

d(mm)	$\rho_{4.2}$(n ohm cm)
0.25	4.61
0.33	4.86
0.36	1.66
0.40	1.63
0.45	4.15
0.53	0.96
0.61	1.70
0.65	1.01
0.73	3.36
0.82	0.89
0.95	0.84
2.00	0.74
0.75*	2.02
0.56*	1.33
0.63*	1.55

*) These samples were measured indevidually.

Table(A4.49)

Sample Resistivity at 4.2 K as a Function of Diameter for Indium,

(Olsen's[31] results).

d(mm)	$\rho_{4.2}$(n ohm cm)
0.06	3.16
0.08	2.63
0.20	1.07
0.30	1.18
0.31	1.24
0.40	1.36
0.57	0.72
2.54	0.46
2.54	0.50

Table(A4.50)

Sample Relative Resistance Change as a Function of Longitudinal Applied Magnetic Field For Potassium, d= 0.33 mm and T= 4.2 K.

B(KOe)	[R(B)-R(0)]/R(0)	B(KOe)	[R(B)-R(0)]/R(0)
1.03	-0.032	20.60	-0.160
1.94	-0.087	22.50	-0.143
2.36	-0.109	24.40	-0.115
2.82	-0.127	26.30	-0.099
3.28	-0.145	28.20	-0.082
3.75	-0.157	30.00	-0.057
4.22	-0.171		
4.68	-0.181		
5.15	-0.189		
5.62	-0.199		
6.18	-0.206		
6.60	-0.211		
7.03	-0.215		
7.97	-0.227		
8.90	-0.227		
10.40	-0.237		
12.20	-0.235		
14.10	-0.219		
15.90	-0.198		

Table(A4.51)

Sample Relative Resistance Change as a Function of Longitudinal Applied Magnetic Field For Potassium, d= 0.36 mm and T= 4.2 K.

B(KOe)	[R(B)-R(0)]/R(0)	B(KOe)	[R(B)-R(0)]/R(0)
0.33	-0.006	21.57	0.182
0.51	-0.017	24.37	0.219
0.90	-0.042	27.20	0.252
1.20	-0.061	30.02	0.286
1.44	-0.074		
1.89	-0.094		
2.36	-0.108		
2.81	-0.115		
3.29	-0.118		
3.75	-0.118		
4.22	-0.115		
4.69	-0.108		
5.64	-0.098		
7.03	-0.074		
8.50	-0.042		
10.36	-0.006		
12.22	0.028		
14.09	0.064		
16.00	0.098		

Table(A4.52)

Sample Relative Resistance Change as a Function of Longitudinal Applied Magnetic Field For Potassium, d= 0.40 mm and T= 4.2 K.

B(KOe)	[R(B)-R(0)]/R(0)	B(KOe)	[R(B)-R(0)]/R(0)
0.51	-0.006	16.89	0.040
0.90	-0.018	18.81	0.056
1.18	-0.028	21.59	0.081
1.44	-0.037	24.40	0.101
1.72	-0.050	27.18	0.121
2.16	-0.061	30.05	0.140
2.82	-0.072		
3.30	-0.076		
3.54	-0.076		
3.76	-0.076		
4.22	-0.076		
4.69	-0.074		
5.16	-0.073		
5.64	-0.070		
6.56	-0.061		
7.52	-0.054		
9.40	-0.034		
11.25	-0.014		
13.15	0.005		

Table(A4.53)

Sample Relative Resistance Change as a Function of Longitudinal Applied Magnetic Field For Potassium, d= 0.52 mm and T= 4.2 K.

B(KOe)	[R(B)-R(0)]/R(0)	B(KOe)	[R(B)-R(0)]/R(0)
0.48	-0.006	27.19	0.131
1.00	-0.012	30.02	0.149
1.42	-0.013		
1.90	-0.021		
2.36	-0.024		
2.84	-0.028		
3.28	-0.030		
3.92	-0.030		
4.72	-0.028		
5.63	-0.024		
7.51	-0.014		
9.43	-0.002		
11.29	0.010		
13.14	0.027		
15.04	0.044		
16.89	0.055		
18.76	0.072		
22.26	0.097		
24.40	0.112		

Table(A4.54)

Sample Relative Resistance Change as a Function of Longitudinal Applied Magnetic Field For Potassium, d= 0.60 mm and T= 4.2 K.

B(KOe)	[R(B)-R(0)]/R(0)	B(KOe)	[R(B)-R(0)]/R(0)
0.51	-0.004	27.22	0.247
0.94	-0.013	30.02	0.270
1.44	-0.021		
1.89	-0.026		
2.41	-0.029		
2.85	-0.029		
3.30	-0.029		
3.81	-0.026		
4.29	-0.026		
4.75	-0.017		
5.65	-0.008		
7.50	0.016		
9.40	0.040		
11.25	0.070		
13.19	0.098		
15.00	0.118		
16.92	0.143		
18.77	0.161		
21.57	0.195		

Table(A4.55)

Sample Relative Resistance Change as a Function of Longitudinal Applied Magnetic Field For Potassium, d= 1.15 mm and T= 4.2 K.

B(KOe)	[R(B)-R(0)]/R(0)	B(KOe)	[R(B)-R(0)]/R(0)
0.11	0.000		
0.25	0.001		
0.51	0.008		
0.95	0.017		
1.45	0.020		
1.91	0.024		
2.85	0.029		
3.75	0.037		
4.70	0.046		
6.62	0.065		
8.48	0.086		
10.36	0.108		
13.74	0.150		
20.69	0.230		
24.44	0.269		
27.37	0.296		
30.12	0.320		

Table(A4.56)

Sample Relative Resistance Change as a Function of Longitudinal Applied Magnetic Field For Potassium, d= 0.56 mm and T= 4.2 K. Annealing time at room temperature = One day.

B(KOe)	[R(B)-R(0)]/R(0)	B(KOe)	[R(B)-R(0)]/R(0)
0.94	-0.044		
1.88	-0.088		
2.81	-0.106		
3.75	-0.125		
4.68	-0.133		
5.62	-0.141		
7.49	-0.152		
9.38	-0.152		
11.27	-0.148		
13.12	-0.133		
18.00	-0.106		
24.00	-0.056		

Table(A4.57)

Sample Relative Resistance Change as a Function of Longitudinal Applied Magnetic Field For Potassium, d= 0.56 mm and T= 4.2 K. Annealing time at room temperature = 11 days.

B(KOe)	[R(B)-R(0)]/R(0)	B(KOe)	[R(B)-R(0)]/R(0)
0.47	-0.033	18.74	-0.136
0.94	-0.101	20.71	-0.106
1.12	-0.129	22.50	-0.089
1.41	-0.165	24.37	-0.068
1.65	-0.185	26.25	-0.048
1.87	-0.204	28.12	-0.028
2.36	-0.231	29.98	-0.005
2.81	-0.252		
3.29	-0.266		
3.75	-0.275		
4.23	-0.282		
4.68	-0.282		
5.62	-0.282		
7.50	-0.274		
9.37	-0.252		
11.25	-0.225		
13.12	-0.204		
15.06	-0.178		
16.86	-0.159		

Table(A4.58)

Sample Relative Resistance Change as a Function of Longitudinal Applied Magnetic Field For Potassium, d= 0.56 mm and T= 4.2 K.

Annealing time at room temperature = 19 days

B(KOe)	[R(B)-R(0)]/R(0)	B(KOe)	[R(B)-R(0)]/R(0)
0.28	0.012	15.00	0.214
0.48	0.037	16.87	0.187
0.93	-0.124	18.76	0.168
1.42	-0.207	20.62	-0.142
1.87	-0.243	22.50	-0.113
2.35	-0.272	24.37	0.090
2.82	-0.304	26.25	0.068
3.28	-0.312	28.14	0.042
3.75	-0.320	30.00	-0.017
4.22	-0.328		
4.69	-0.328		
5.18	-0.328		
5.63	-0.328		
6.56	-0.328		
7.50	-0.320		
8.45	-0.304		
9.38	-0.304		
11.27	-0.280		

Table(A4.59)

Percentage Resistance Change as a Function of Longitudinal Applied Magnetic Field For Sodium, d= 0.36 mm and T= 4.2 K.

B(KOe)	{[R(B)-R(0)] x 100} /R(0)
4.76	-0.041
7.15	-0.124
9.40	-0.165
12.19	-0.186
14.08	-0.206
16.41	-0.206
18.78	-0.165
21.09	-0.124
23.51	-0.041
25.79	0.000
28.15	0.083

Table(A4.60)

Percentage Resistance Change as a Function of Longitudinal Applied Magnetic Field For Sodium, d= 0.52 mm and T= 4.2 K.

B(KOe)	{[R(B)-R(0)] x 100} /R(0)
0.00	0.000
1.41	0.000
2.37	-0.153
4.69	-0.229
7.03	-0.306
9.42	-0.459
14.14	-0.535
18.74	-0.612
23.49	-0.575
28.13	-0.459

Table(A4.61)

Percentage Resistance Change as a Function of Longitudinal Applied Magnetic Field For Sodium, d= 3.00 mm and T= 4.2 K.

B(KOe)	{[R(B)-R(0)] x 100} /R(0)
0.00	0.000
9.55	1.429
14.09	2.143
18.93	2.857
28.23	3.902

Table(A4.62)

Percentage Resistance Change as a Function of Longitudinal Applied Magnetic Field For Sodium, d= 0.33 mm and T= 4.2 K.

B(KOe)	{[R(B) R(0)] x 100} /R(0)
0.00	0.000
1.58	-0.067
3.82	-0.134
5.65	-0.268
7.53	-0.402
9.40	-0.536
11.25	-0.603
13.14	-0.737
14.99	-0.804
16.89	-0.804
22.56	-0.804
25.32	-0.737
28.15	-0.603

Table(A4.63)

Percentage Resistance Change as a Function of Longitudinal Applied Magnetic Field For Sodium, d= 0.65 mm and T= 4.2 K.

B(KOe)	{[R(B)-R(0)] x 100} /R(0)
0.00	0.000
1.93	-0.271
4.67	-0.542
9.10	-0.620
15.06	-0.542
23.55	-0.271
28.14	-0.136

Table(A4.64)

Percentage Resistance Change as a Function of Longitudinal Applied Magnetic Field For Sodium, d= 3.00 mm and T= 4.2 K.

B(KOe)	{[R(B)-R(0)] x 100} /R(0)
0.00	0.000
6.66	1.364
14.96	2.272
22.1	3.560
28.24	4.545

Table(A4.65)

Sample Resistance as a Function of Longitudinal Applied Magnetic Field For Indium, d= 0.36 mm and T= 4.2 K.

B(KOe)	R(B)[10^{-8} Ohm]	B(KOe)	R(B)[10^{-8} Ohm]
0.0018	860.	0.3569	1420.
0.0487	870.	0.3644	1470.
0.0749	880.	0.3766	1560.
0.0946	890.	0.3860	1620.
0.1124	900.	0.3944	1690.
0.1311	910.	0.4029	1750.
0.1414	920.	0.4085	1790.
0.1602	930.	0.4132	1820.
0.1799	940.	0.4216	1880.
0.2061	970.	0.4357	1940.
0.2258	1000.	0.4413	2010.
0.2436	1030.	0.4497	2070.
0.2670	1080.	0.4628	2190.
0.2876	1130.	0.4694	2260.
0.3017	1180.	0.4797	2420.
0.3270	1280.	0.4863	2530.
0.3382	1330.	0.4975	2810.
0.3476	1370.	0.5059	3120.

Table(A4.65)(Continued)

Sample Resistance as a Function of Longitudinal Applied Magnetic Field For Indium, d= 0.36 mm and T= 4.2 K.

B(KOe)	R(B)[10^{-8} Ohm]	B(KOe)	R(B)[10^{-8} Ohm]
0.5162	3680.	0.9416	6340.
0.5247	4140.	1.4064	6450.
0.5340	4700.	1.8824	6520.
0.5462	5110.	2.3987	6570.
0.5537	5300.	2.8737	6630.
0.5640	5460.	3.7470	6850.
0.5771	5580.	4.6878	7370.
0.5828	5610.	5.1984	7470.
0.5931	5660.	5.6435	7480.
0.6090	5720.	6.5889	7490.
0.6296	5800.	8.4498	7520.
0.6474	5880.	11.2618	7530.
0.6699	5990.	15.0088	7560.
[illegible]	6060.	18.8168	7590.
0.[illegible]	[illegible]0.	22.6688	7620.
0.[illegible]	[illegible].	26.2519	7650.
0.[illegible]	[illegible]0.		
0.800[illegible]	6240.		
0.8451	6280.		

$\kappa \backslash \eta$	0	10^{-1}	1	10^{1}	10^{2}	10	10^{3}	10^{4}	10^{5}
10	0·925	0·933	0·946	0·963	0·979	0·989	0·9948	0·9975	0·9988
5	0·853	0·869	0·893	0·928	0·959	0·979	0·9896	0·9950	0·9977
2	0·678	0·693	0·748	0·826	0·899	0·947	0·9741	0·9876	0·9942
1	0·489	0·504	0·555	0·674	0·805	0·896	0·9484	0·9753	0·9884
0·5	0·318	0·324	0·340	0·440	0·635	0·799	0·8984	0·9509	0·9768
0·2	0·158	—	0·163	0·186	0·295	0·549	0·758	0·8801	0·9425
0·1	0·0873	—	0·0899	0·0960	0·1266	0·272	0·5565	0·7691	0·8872
0·05	0·0464	—	—	0·0482	0·0556	0·0968	0·272	0·5746	0·7821
0·02	0·0192	—	—	—	0·0201	0·0281	0·0612	0·1992	0·5140
0·01	0·00976	—	—	—	—	0·0109	0·0200	0·0598	0·228

Table(1.4.1) : (σ/σ_0) for different values of κ and η, after Chambers[17].

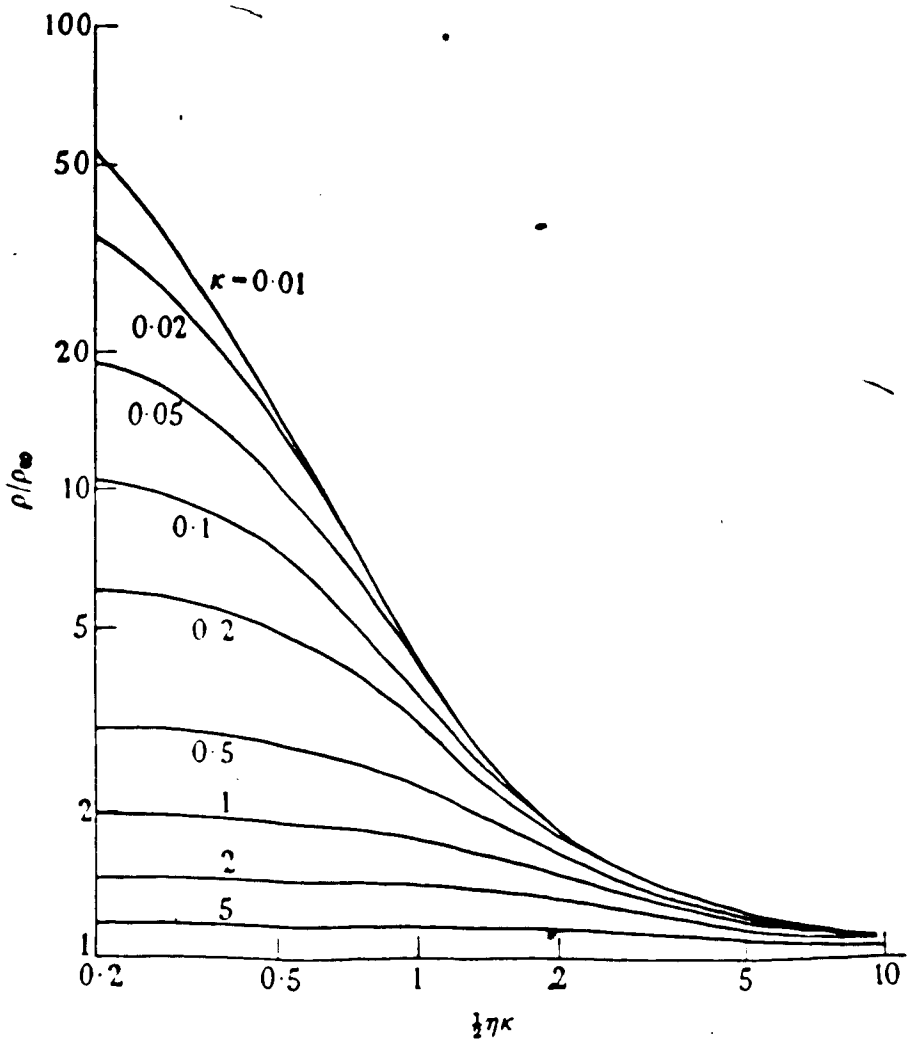

Fig.(1.4.1) : (ρ/ρ_∞) against $(\eta\kappa/2)$ for different κ values, after Chambers[17].

The above discussion was for the diffuse scattering case, i. e., P=0. For $P \neq 0$, equation (1.4.1) has to be replaced by a slightly more complicated one as :

$$\lambda_1 = \lambda[\ 1-(1-P)\, e^{-ab/\lambda}\ ]/[\ 1-P\, e^{-bc/\lambda}\ ], \qquad (1.4.9)$$

where ab and bc are defined by Fig.(1.4.2). In this case equation (1.4.5) will take the form :

$$\sigma/\sigma_0 = 1 - (3/4\pi S) \int_s dS \int_0^{2\pi} d\phi \int_0^{\pi} d\theta\ \sin\theta \cos^2\theta\ [\{(1-P)\, e^{-ab/\lambda}\}/\{1-Pe^{-bc/\lambda}\}]. \qquad (1.4.10)$$

Now, from Fig.(1.4.1), the projections of ab and bc on the (x, y) plane are $\psi_1 R_0 \sin\theta$ and $(\psi_1 + \psi_2) R_0 \sin\theta$ respectively. So the actual distances ab and bc are given by $\psi_1 R_0$ and $(\psi_1 + \psi_2) R_0$ respectively[16]. Replacing P by $P(\theta)$ and substituting for ab and bc, equation (1.4.10) will read[16] :

$$\sigma/\sigma_0 = 1 - (3/2\pi a^2) \int_0^a r dr \int_0^{2\pi} d\phi \int_0^{\pi} d\theta\ \sin\theta \cos^2\theta\ [\{(1-P(\theta))\, e^{-\psi_1/\eta}\}/\{1-P(\theta)\, e^{-(\psi_1+\psi_2)/\eta}\}], \qquad (1.4.11)$$

where η is defined as before. To carry out the integration on the right hand side of equation (1.4.11), one has to express ψ_1 and ψ_2 in terms of R, r, θ and ϕ and perform the integration numerically. Details of such a calculation are described by Golledge et al[16] who did it for P=0 and confirmed the results of Chambers[17]. Also they considered the two cases of $P \equiv P(\theta)$, given by equation (1.1.1), and P

independent of θ, with $0 \leq P \leq 1$, to extend Chambers calculations. To their surprise, Golledge et al[16] found an almost total lack of distinguishability between these two cases for the longitudinal magnetoresistance of a cylindrical wire unlike the situation for all other surface-modified transport properties they considered.

I.5) Other Models :

In 1958, Olsen[31] measured the electrical resistivity of fine indium wires in the temperature range between 1.5 and 4.2 K. He analyzed his data according to the following general expression :

$$\rho(c, T, d) = \rho_0(c) + \rho_i(T,\infty) + \Delta(c, T, d), \qquad (1.5.1)$$

where c is the concentration of physical defects and chemical impurities,d is the sample diameter, $\rho_0(c)$ is the residual resistivity, $\rho_i(T,\infty)$ is the bulk resistivity and $\Delta(c, T, d)$ is a deviation from Matthiessen's Rule (DMR), mentioned before. He found that his results gave size-dependent DMR which were several times larger than those predicted by Dingle[22]. In order to explain that, Olsen pointed out that one has to take into account the effect of small angle scattering of conduction electrons by phonons at low temperatures. Although these processes make a negligible contribution to the resistivity in a bulk metal, they may cause the electrons to strike the surface of thin specimens where diffuse scattering may take place. In this process the phonons will create more temperature dependent resistivity in thin samples than they do in thick ones.

In 1960, Luthi and Wyder[32] made a Monte Carlo calculation of the motion of free-electrons in a fine wire to test Olsen's model. With this technique they were able to reproduce the form of Olsen's experimental results and concluded that this model was correct. Also Blatt and Satz[33] carried out theoretical calculations

based on the same model. For $\lambda_\infty >> a$ they obtained the following expression for the temperature dependent part of the surface scattering contribution to the sample resistivity :

$$\Delta\rho(d,T) \equiv \rho(d,T) - \rho(d,0) - \Delta\rho_\infty(T)$$
$$= \beta\, T^{2/3}\, [\, \Delta\rho_\infty(T)]^{1/3}\, a^{2/3}\,, \qquad (1.5.2)$$

where a=d/2, β is a fitting parameter to be determined from experimental results and $\Delta\rho_\infty(T) \equiv \rho_\infty(T) - \rho_\infty(0)$ is the temperature dependent part of the bulk resistivity. For a given temperature this expression gives the same thickness dependence as equation (1.3.21) obtained by Sambles et al[15].

CHAPTER II

EXPERIMENTAL WORK

2.1) The Cryostat :

To measure the temperature dependence of the samples electrical resistivity we used the cryostat shown in Fig.(2.1.1). This cryostat has been described by White and Woods[34,35] and in more details by Adler[36], Rogers[37] and Seth[38,39]. It was modified and rewired for the purpose of the present work. In this cryostat the specimens and the thermometers were enclosed in a copper vessel C1, 11 in. long and 2.5 in. in diameter. This vessel and the pumping chamber P.C. were entirely surrounded by a shield S kept at the same temperature as the vessel C1. These were mounted by thin-walled stainless steel tubes in a copper vacuum enclosure C2, 17 in. long and 3.5 in. in diameter. This provided thermal isolation of the specimen chamber C1 from the refrigerant bath. Helium exchange gas at a pressure of a few torrs in C1 was used to keep the samples and thermometers at the same temperature. The electrical leads were brought in through the pumping tube P1 and then thermally anchored to the copper post t so as to minimize the heat conduction to the inner chamber. A radiation trap consisting of blackened copper wool between two loose fitting of styrofoam was inserted at A in the pumping tube P1. The specimen chamber was cooled below the temperature of the bath by

pumping through P2 over the refrigerant which could be let into the pumping chamber P.C. through a needle valve V.

For magnetoresistance measurements a simpler cryostat was used which has been described by Ali[40]. A different insert was designed to suit the purpose of the present work, see Fig.(2.1.2). In this cryostat the sample can was in direct contact with the refrigerant liquid. A superconducting solenoid, of 8 in. in length and 2 in. inner diameter, was used to produce magnetic fields up to 30 KG at liquid helium temperature. The sample can was designed to slip-fit into that solenoid to achieve the longitudinal magnetoresistance geometry.

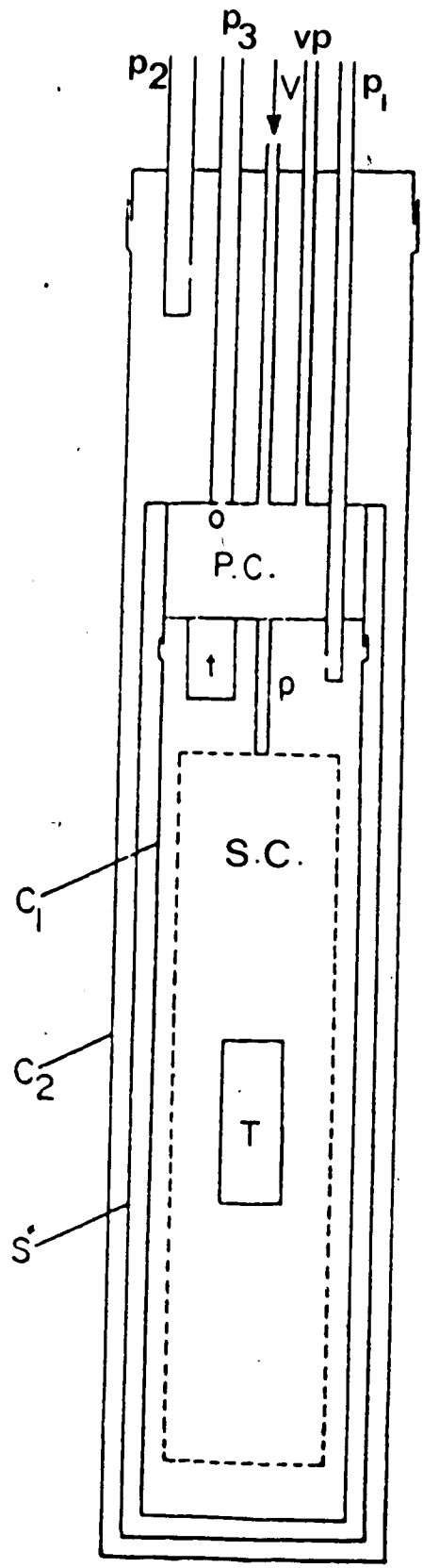

Figure (2.1.1) : The Cryostat Used For The Electrical Resistivity Measurements

P_1, P_2, P_3	Pumping tubes.
V	Needle valve.
v.p.	Vapor pressure line.
o	Orifice.
P.C.	Pumping chamber.
t	Post for thermal anchoring of the leads.
p	Post for mounting the sample can.
C_1, C_2	Inner and outer vessels.
S	Shield.
S.C.	Sample can.
T	Thermometers.

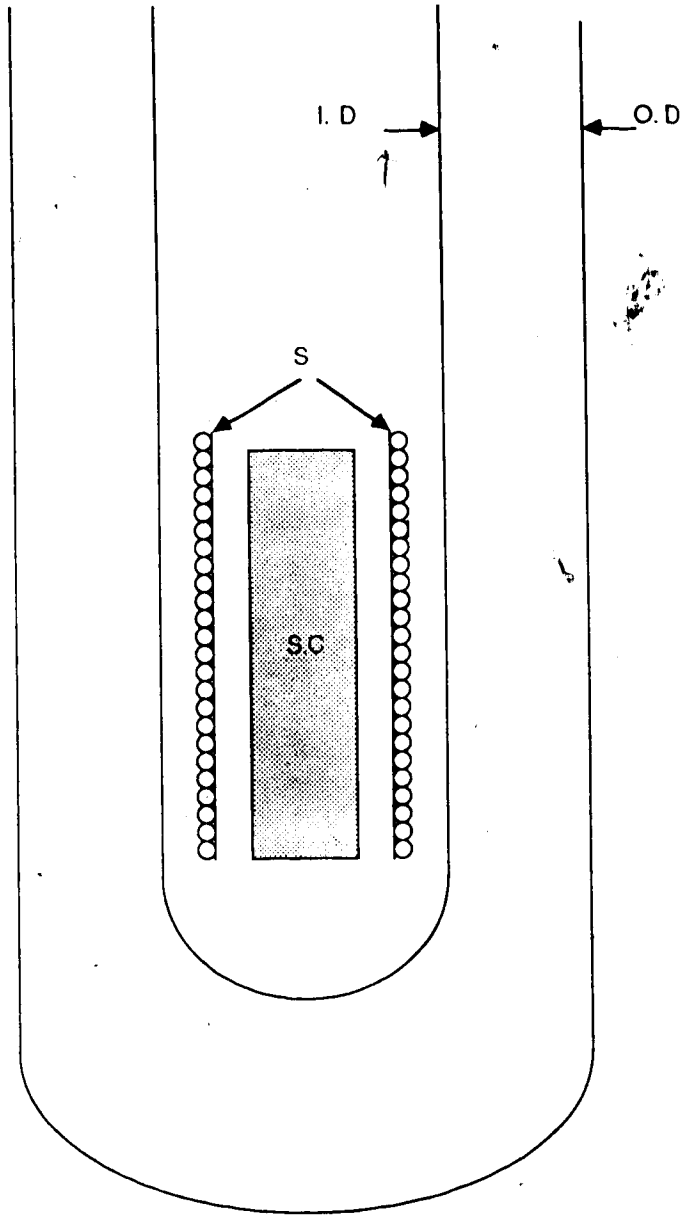

Fig.(2.1.2) : Simple cryostat used for magnetoresistance measurements.

S : is a superconducting solenoid.

I.D., O.D. : inner and outer dewar respectively.

S.C. : Sample can.

2.2) Sample Holders :

In the present work, three similar sample holders have been designed and used, one for each metal to avoid any possible contamination. Fig.(2.2.1) shows a schematic diagram for one of these holders which was made of a teflon cylinder. Twelve grooves, each greater in width than the diameter of the corresponding specimen, were machined lengthwise into the periphery of that cylinder. Copper contacts were pressed into holes near the ends of the grooves to facilitate making four-terminal measurement connections. Holes were drilled in these contacts at right angles to the grooves and copper wires were soldered into them. The specimen holder was mounted on the inside of one end of a brass can sealed with an indium o-ring coated with grease. For potassium and sodium sample holders, the electrical leads were soldered to oxford connectors sealed through the top of the can, but for the indium sample holder these leads were run through a vacuum tube connected to the lid. This tube facilitated pumping air out of the sample can and replacing it by helium exchange gas.

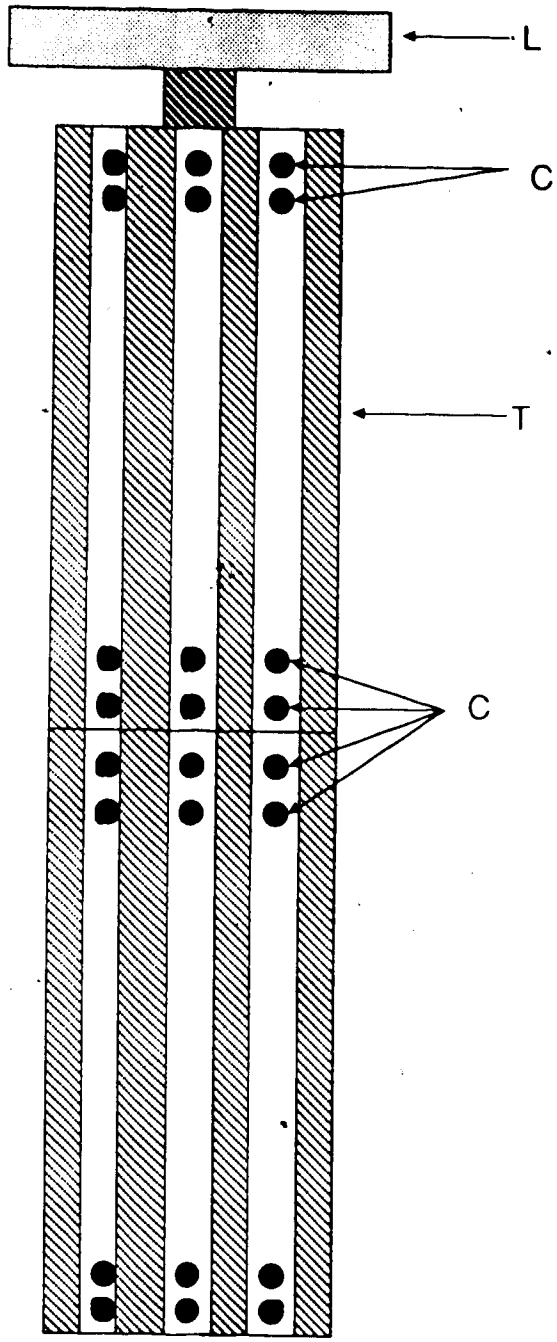

Fig.(2.2.1): The Sample Holder, Designed to Accommodate 12 Samples With Four Contacts Each.

2.3) Sample Preparations :

2.3.1) Potassium and Sodium Samples Preparation :

Samples were prepared from pure potassium (purity 99.9% supplied by MSA Research Corporation) or sodium (purity 99.95% supplied by CERAC Inc.). In order to overcome the problem of oxidation, a dry box with helium atmosphere was used in which all necessary tools were placed. A mixture of helium and 5% hydrogen was circulated through a furnace containing a catalyst to remove oxygen and then through a dryer to clean up the helium atmosphere. A naked-filament light bulb was illuminated for at least 30 minutes in the dry box to test this oxygen-free atmosphere. Also a piece of potassium or sodium was scratched and left for a similar period of time to see if there was any possible change in surface color. After all of these precautions, samples were extruded in a wire form using a hydraulic press with dies of different hole diameters. The diameters used for the present work were between 0.33 and 3 mm. The samples were melted to the copper contacts in the specimen holder after "tinning" the contacts with the same metal, potassium or sodium. The electrical continuity was then tested. The sample holder was sealed in a brass can by using an indium o-ring. A sheet of "Kapton" insulation was used around the inner surface of that can to prevent any accidental contact to the samples. The sample can was taken out of the dry box and leak-tested at room temperature then mounted in one of the cryostats for measurements.

2.3.2) **Indium Samples Preparation** :

Indium samples were extruded in the ambient atmosphere by using a hydraulic press with dies of different diameters similar to those used for the preparation of the potassium and sodium samples. All samples were made out of the same ingot of pure indium (purity 99.999 % supplied by A.D.Mackay Inc.). The treatment and mounting of the indium specimens beyond this point did not differ significantly from that of the potassium and sodium specimens.

2.4) Experimental Arrangement :

During the present work two different experimental arrangements were used; namely, an automatic data acquisition system and a current comparator bridge system. These two set ups are described in fair details in the following two sections.

2.4.1) Automatic Data Acquisition System :

This system has been developed by the author using an IBM personal computer as a controller, see Fig.(2.4.1). An interface card made by "TECMAR" Inc. employing the standard IEEE488 bus protocol was installed to enable two-way communications between the computer and different devices. A digital nano-voltmeter, Keithley model #181, was used to measure the voltage drop on the sample with a measured precesion of ±10 nano-volts. A constant current source, Lake Shore model #120, was used to supply sample currents which were stable and accurate within 0.1% of the current value. A simple circuit was constructed by the author to enable the computer to switch the sample current back and forth automatically in order to cancel out any possible thermal E.M.F. in the sample circuit; see appendix (1) for details. Another more complicated switching circuit, which was designed and constructed to meet the IEEE488 standard (see appendix (2)) was used to control different equipment by computer, e.g. a voltage ramp

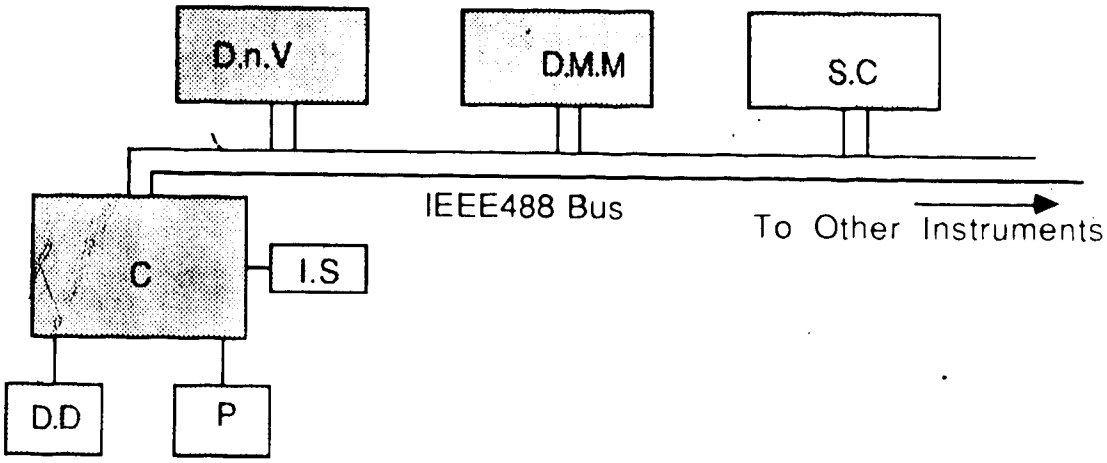

Fig.(2.4.1) : The computer system constructed and used during the present work.

C : IBM-PC Computer.

D.nV. : Digital nano-Voltmeter.

D.M.M.: Digital Multi Meter.

S.C. : Switching Circuit.

I.S. : Sample current Switch.

P : Printer.

D.D. : Disk Drive.

generator, heaters, ... etc. The thermometer resistance was measured by a digital multimeter, Keithley model #197, using four-terminal configuration with an resolution of $\pm 10^{-3}$ Ohm. The system was programmed to collect data every 0.2 K for $300 \geq T \geq 20$ K and every 0.1 K for $T<20$ K. The raw data was stored on a diskette for later analysis.The program algorithm is shown in Fig.(2.4.2) and the actual list is in appendix (3).

2.4.2) Current Comparator System :

In this system the sample resistance was measured manually by a current comparator bridge, Guildline model #9920. A photocell galvanometer amplifier, Guildline type 5214 / 9460, was used as a null detector with a Guildline type 9461 galvanometer. This arrangement gave a sensitivity of ± 3 nano-volts. The basic circuit[40] is shown in Fig.(2.4.3). The sample was connected as one arm to the bridge by four wires. The sample current was supplied by a built-in adjustable current source. When the bridge is balanced (i.e. G reads zero) the voltage drop across R_s is equal to that across R_x, where R_s is a standard resistance and R_x is the sample resistance.This means that :

$$I_s R_s = I_x R_x ,$$

i.e. $$(I_s / I_x) = (R_x / R_s). \qquad (2.4.1)$$

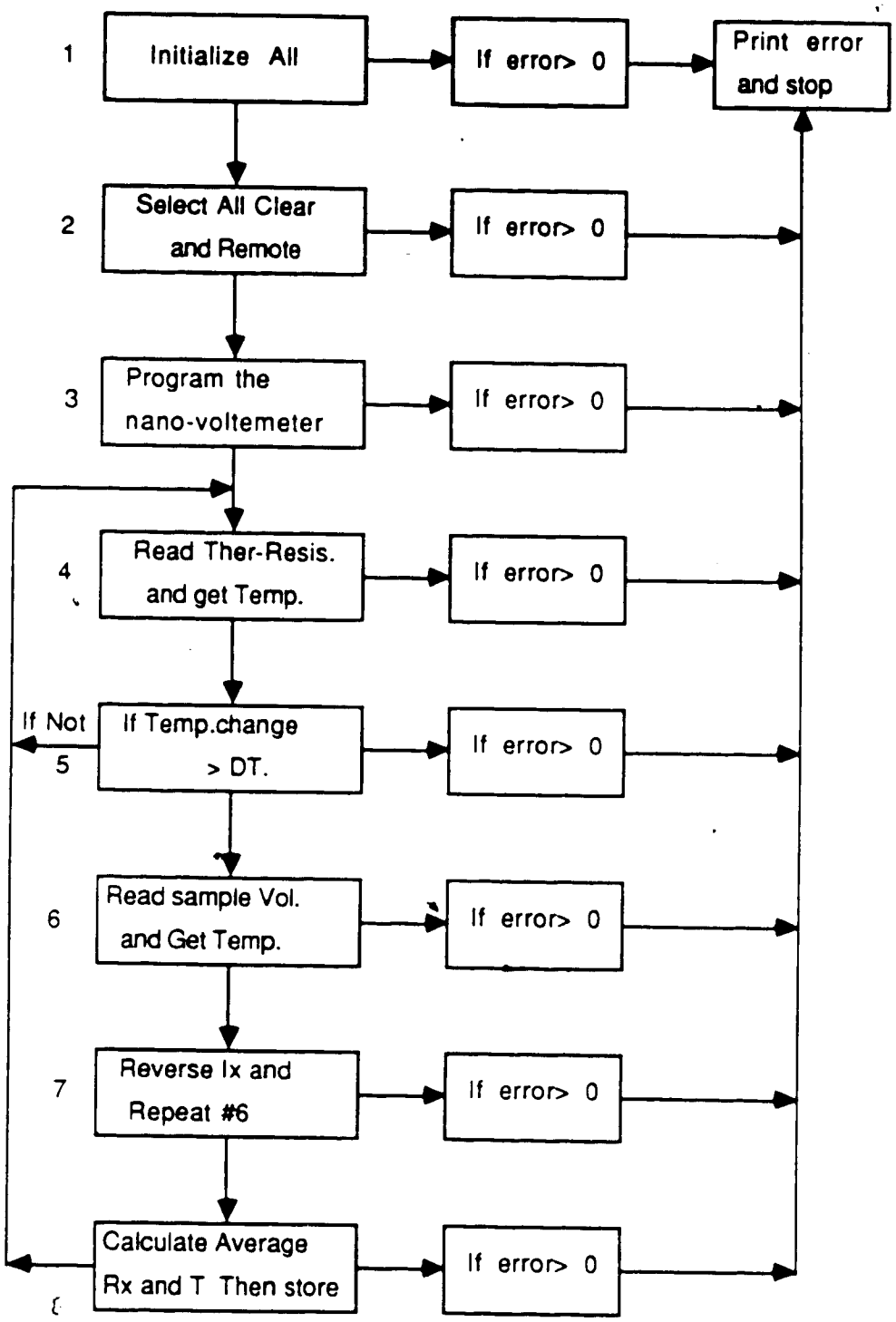

Fig.(2.4.2) : The Algorithm of The Computer Program Written and Used for Automatic Data Acquisition.

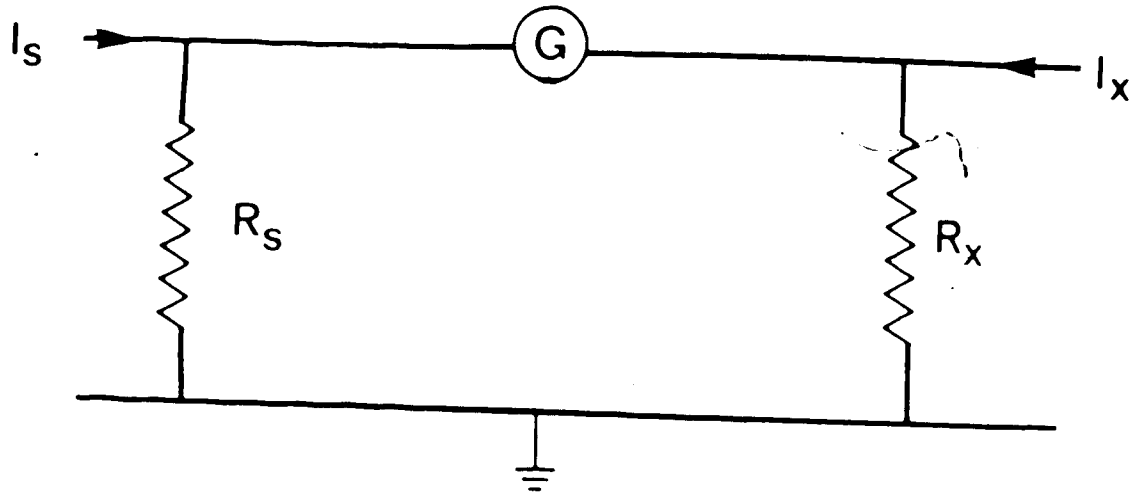

Fig.(2.4.3) : The Basic Circuit for The Current Comparator System.

The ratio of (I_s / I_x) was directly determined from the seven dials on the comparator. The sample resistance was determined by balancing the bridge while the sample current was switched back and forth several times to eliminate the effect of possible thermal E.M.F. The standard resistance used in this work was 0.1 ohm kept at ambient temperature in an oil bath to minimize any possible thermal fluctuations.

2.5) Temperature Control and Measurement :

For the cryostat described in Fig.(2.1.1), samples were brought to the refrigerant, nitrogen or helium, boiling point by introducing helium exchange gas in the outer can C2. Temperatures below those of the coolant bath were obtained by pumping on the liquid in the pumping chamber, P.C., with the outer vessel under vacuum ($\cong 10^{-6}$ torr). The pressure in P.C. was controlled and maintained at a steady value by pumping through a manostat. Temperatures above those of the refrigerant bath were obtained by evacuating the P.C. and passing an electric current through a carbon resistor (1000 ohm, 0.5 watt) mounted in a copper sleeve soldered to the top of the specimen chamber. An additional heater could be used if the power was not sufficient to achieve the desired temperature. This heater was an 8 watt 1500 ohm wire-wound resistor which was mounted on a copper rod soldered to the top of the specimen chamber. The temperature was measured by using an N.B.S. calibrated germanium thermometer for $2 \leq T \leq 20$ K and by an N.R.C. calibrated platinum resistance thermometer for $20 \leq T \leq 300$ K. Another platinum thermometer was calibrated against the N.R.C. calibrated one and used for some measurements during this work. The resolution of temperature measurements was ±20mK for the platinum thermometers and ±2mK for the germanium thermometer. Each thermometer was inserted in a well drilled in a small copper block which could be attached to the sample can. Silicon grease was used to improve thermal contact between the wells and thermometers.

As mentioned before, the four-terminal resistance of the platinum thermometers was measured directly by a digital multimeter, Keithley model #197, with an resolution of $\pm 10^{-3}$ ohm. The resistance of the germanium thermometer was measured by passing a 10μ A constant current through the thermometer and measuring the voltage drop across it with a digital micro-voltmeter. The thermometer resistance was converted to the corresponding temperature using a computer subroutine.The system was also programmed to switch thermometers at $T \cong 20$ K automatically.

For the simple cryostat shown in Fig.(2.1.2), the sample can was in direct contact with the refrigerant bath. This provided a very stable temperature over a sufficient period of time required for isothermal measurements of size effects on the sample resistance with and without magnetic fields. Temperatures below the coolant bath was achieved by reducing the pressure over that bath and temperatures values was measured by using the appropriate thermometer. The temperature was controlled and maintained at a steady value by pumping through a manostat that maintained the pressure at a pre-determined value.

2.6) A Typical Run :

After a set of twelve samples was prepared, the sample can was attached to the insert designed for the simple cryostat, cryostat II. The can was then fitted into the superconducting solenoid for the longitudinal magnetoresistance geometry. The samples were kept at room temperature for a period of time between 10 and 24 hours before measurements were carried out. The sample resistivity was then measured as a function of sample diameter at three different temperatures; namely room temperature, liquid nitrogen and liquid helium boiling points. At 4.2 K the magnetic field was switched on and the resistance of each sample was measured as a function of the applied magnetic field B. This field was controlled by varying the magnet current using an automatic voltage ramp generator. The field homogeneity was better that 1% across each sample. A computer program with an algorithm, similar to that shown in Fig.(2.4.2), was used to collect data automatically. The measurements for some samples were repeated using the current comparator system and good agreement was found between the two results within experimental errors(10^{-7} ohm). The samples were warmed up to room temperature where they were kept for about two weeks or so before the same measurements were repeated for different annealing conditions.

After about one month of annealing time at ambient temperature, the electrical resistivity of each sample was measured as a function of temperature.

A computer program, with the algorithm described in Fig.(2.4.2), was used for data acquisitions while temperature was allowed to vary slowly with an average rate of one degree/ 10 minutes. The data were collected during both cooling and heating and no thermal hysteresis were found within the experimental errors. The raw data for each sample were collected in a separate computer file for later analysis.

CHAPTER III

RESULTS AND DISCUSSION

3.1) General :

The total electrical resistivity of a metal can be generally written as[31] :-

$$\rho_{tot}(d,c,T) = \rho_0(c) + \rho_i(T,\infty) + \Delta(c,T,d), \qquad (3.1.1)$$

where c is the concentration of physical defects and chemical impurities,d is the sample diameter, $\rho_0(c)$ is the residual resistivity at absolute zero, $\rho_i(T,\infty)$ is the temperature- dependent bulk resistivity of an ideally pure sample and $\Delta(c,T,d)$ are deviations from "Matthiessen's Rule" (MR), mentioned before. There are different mechanisms that could produce deviations from MR. These mechanisms are discussed in detail in the comprehensive review article by Bass[31] and in a more recent one published by Cimberle et al[41]. The residual resistivity is due to scattering of the conduction electrons by static lattice defects such as impurities, vacancies, dislocations and strains in the metal lattice, while the ideal resistivity is caused by intrinsic scattering mechanisms of the bulk material such as electron-phonon and electron- electron scattering. So $\rho_i(T,\infty)$ can be written as[42]:

$$\rho_i(T,\infty) = \rho_{ee}(T) + \rho_{ep}(T), \qquad (3.1.2)$$

where $\rho_{ee}(T)$ is the electron-electron scattering term and $\rho_{ep}(T)$ is the term due to electron-phonon scattering. The electron-electron interaction part, $\rho_{ee}(T)$, can be written as :

$$\rho_{ee}(T) = A\ T^2, \tag{3.1.3}$$

where A is a coefficient giving the magnitude of ρ_{ee} and T is the absolute temperature. The electron-phonon interaction resistivity can be approximated by the Gruneisen-Bloch relation[43] :

$$\rho_{ep}(T) = [\ C/\ (M\ \theta_R)]\ (T/\ \theta_R)^5 \int_0^{\theta_R/T} Z^5\, dZ/\ [(e^Z-1)(1-e^{-Z})], \tag{3.1.4}$$

where C is a constant, M is the atomic weight; T is the temperature in Kelvin, θ_R is a characteristic temperature of the metal, $\theta_R \sim \theta_D$ the Debye temperature and $Z=\hbar\ \omega/\ KT$, ω is the phonon frequency. For temperatures lower than about $0.1\theta_R$ this relation reduces to :

$$\rho_{ep}(T) = 124.4\ (C/\ M)\ [\ T^5/\ \theta_R^6]. \tag{3.1.5}$$

On the other hand for $T \geq \theta_R$ it gives :

$$\rho_{ep}(T) = (C/\ 4M)\ [\ T/\ \theta_R^2]. \tag{3.1.6}$$

The Gruneisen-Bloch relation was derived for a free-electron-like metal with a spherical Fermi surface and Debye phonon spectrum, neglecting the effect of possible Umklapp processes. The published experimental results do not agree[42,44,45] in detail with equation (3.1.4), but in general it gives a good approximation at low and high temperatures.

3.2) Analysis of Results :

In the present work the size effect on the electrical resistivity has been measured for three different metals; namely potassium, sodium and indium. The resistivity data for each metal were calculated from resistance measurements by using the equation :

$$\rho(T,d)= F\,R(T,d), \qquad (3.2.1)$$

where F is a geometrical factor which depends on the shape of the specimen. For a straight uniform wire of length L between the potential contacts and of cross-sectional area A, F= A/ L. It is common to use the room temperature values for A and L to calculate F, but since F has the dimensions of length it is temperature-dependent. In order to correct for the variations of F with temperature, one has to multiply the right hand side of equation (3.2.1) by a factor related to the expansion coefficient[39,46], $\alpha(T)$, as :

$$\rho_{corrected}(T,d)= [1- \alpha(T)]\,F(293)\,R(T,d), \qquad (3.2.2)$$

where :

$$\alpha(T)= [\,L(293)- L(T)]/\,L(293). \qquad (3.2.3)$$

Expansion coefficients for different solids are tabulated by Corruccini and Gniewek[47]. This correction is usually small; for example $\alpha(T= 6\ K) = 0.014$ for sodium and $\alpha(T= 10\ K) = 0.007$ for indium.

The measurements error for ρ, $\delta\rho$, can be estimated as follows:

Since $\rho = (\,V/\,I\,)\,(\,A/\,L\,)$, (3.2.4)

where V is the measured voltage drop across the sample and I is the sample current. So one can write:

$$\delta\rho/\rho = (\delta V/ V) + (\delta I/ I) + (\delta A/ A) + (\delta L/ L). \qquad (3.2.5)$$

The measured value of ($\delta I/ I$) is 0.001 and for ($\delta A/ A$) is 0.002. The largest contribution to ($\delta\rho/\rho$) comes from ($\delta V/ V$), which has a measured value between 0.01 and 0.05, and ($\delta L/ L$), which has a measured value of ≤ 0.02. At low temperatures there is an additional source of error due to the sample annealing condition, which affects the residual resistivity (ρ_0). This error has a random nature and hard to estimate.

3.3) Presentation of The Results :

On the following pages the results are presented, graghically, for the electrical conductivity or R(300)/ R(T) at different temperature values as function of sample diameter and the ratio [R(4.2, H) - R(4.2, 0)] / R(4.2, 0) as function of the external applied magnetic field parallel to the wire axis. The actual data are tabulated in appendix(4). A number of samples were prepared at one time, as described in chapter II, and referd to as a set with a set number. For purposes of clarity, the temperature at which the data were collected and the sample set number as well as the annealing time at room temperature are listed for each data table. The results are organized in the following order :

1) H = 0 measurements :

A) For potassium.

B) For sodium.

C) For indium.

2) H ≠ 0 measurements :

A) For potassium.

B) For sodium.

C) For indium.

Fig(3.1.a) : The Electrical Conductivity Versus Diameter For Potassium at 4.2 K , Set # 1. The annealing time at room temperature is indicated on each curve.

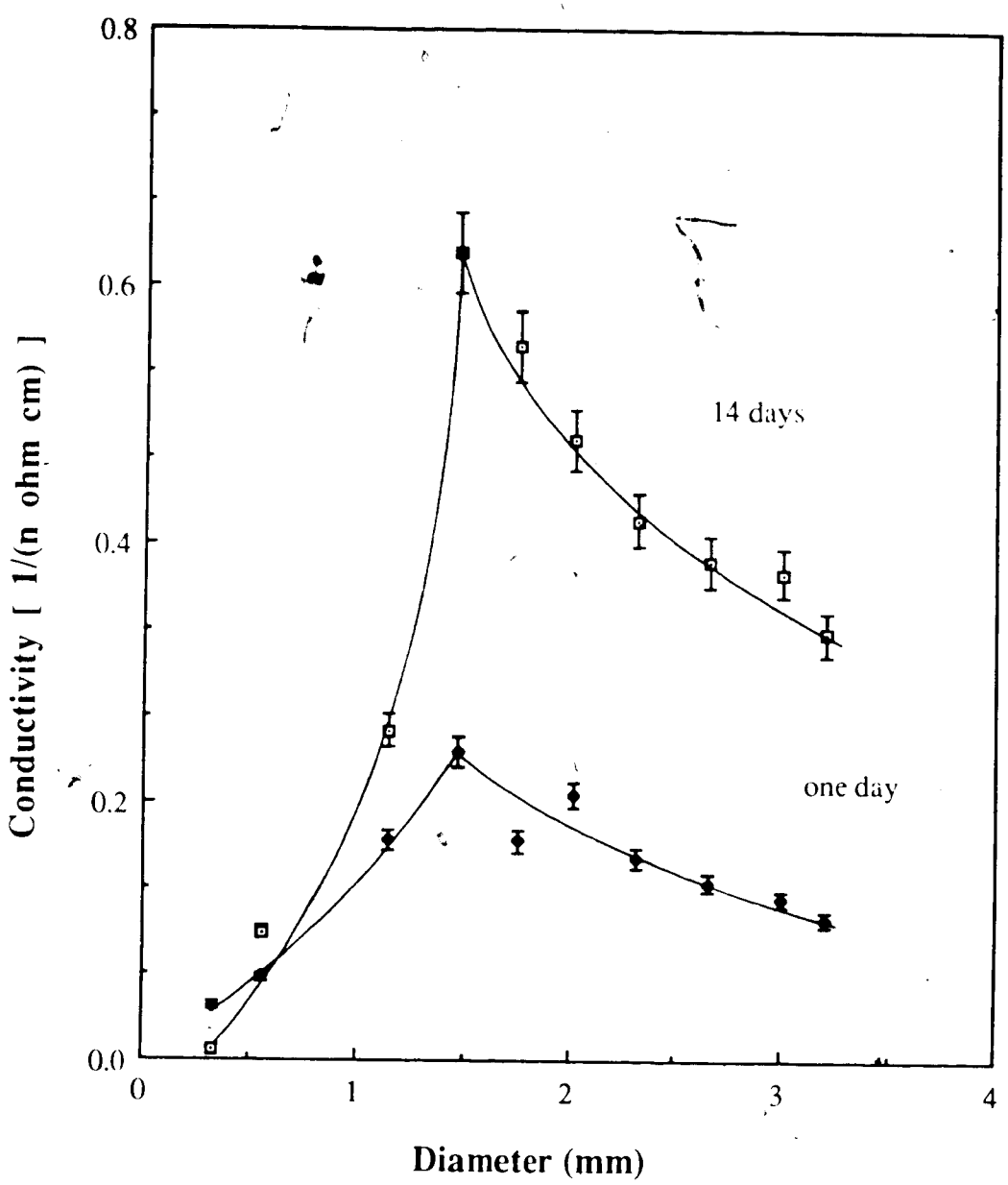
0.8
0.6
0.4
0.2
0.0
0
1
2
3
4
Conductivity [1/(n ohm cm)]
Diameter (mm)
14 days
one day

Fig(3.1.b) : RRR Versus Diameter For Potassium at [illegible] K, Set # 1. The annealing time at room temperature is indicated on each curve.

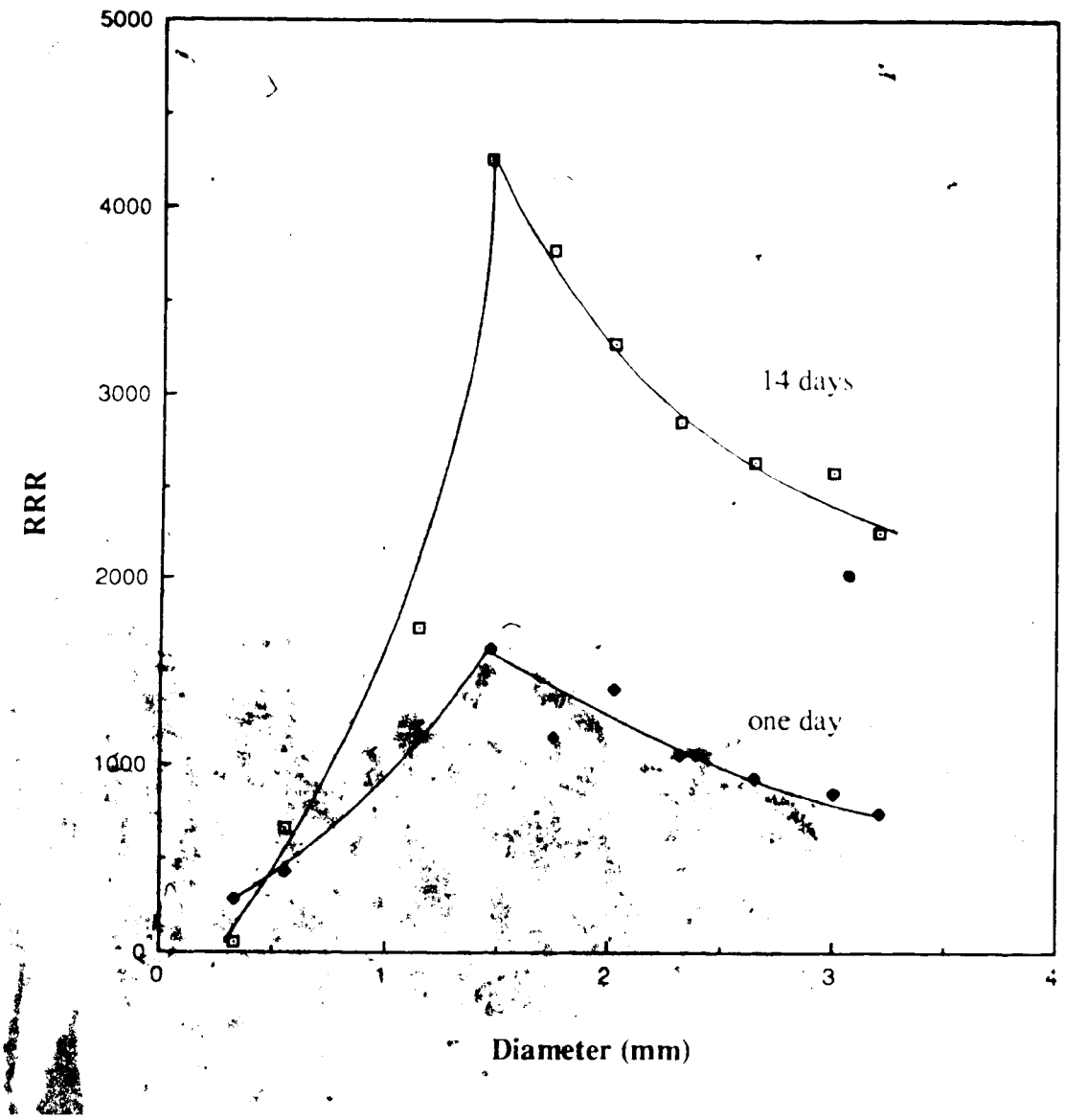
5000
4000
3000
2000
1000
0
RRR
0
1
2
3
4
Diameter (mm)
14 days
one day

Fig(3.2) : RRR Versus Diameter For Potassium at 4.2 K , Set # 2 (◻) and Set # 3 (× , o) . The annealing time at room temperature is indicated on each curve.

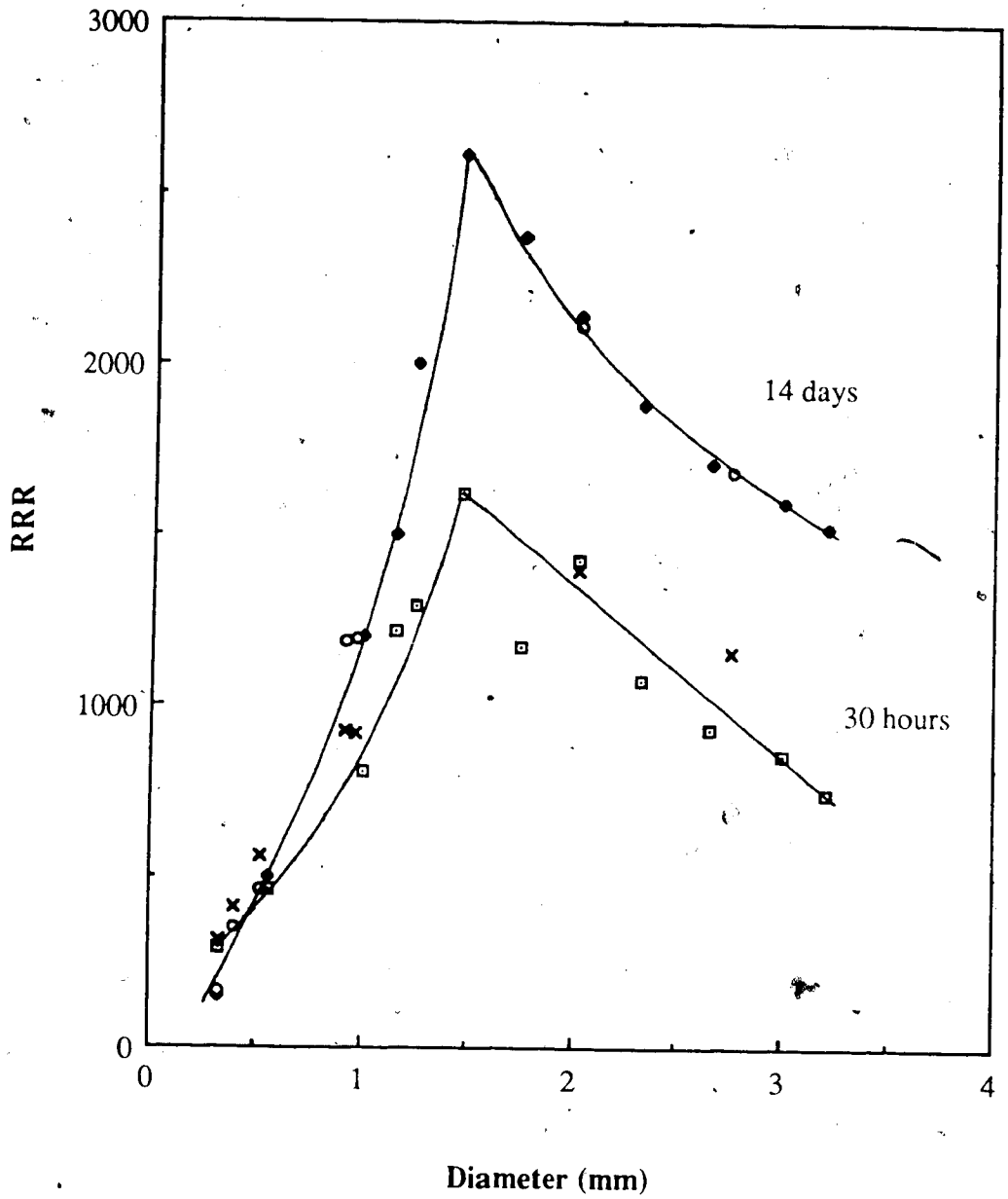
3000
2000
1000
0
RRR
0
1
2
3
4
Diameter (mm)
14 days
30 hours

Fig(3.3) : [R(300)/ R(T)] Versus Diameter For Potassium at T= 10 and 15 K, Set # 2 (⊡) and Set # 3 (x) . The annealing time at room temperature ≥ one month.

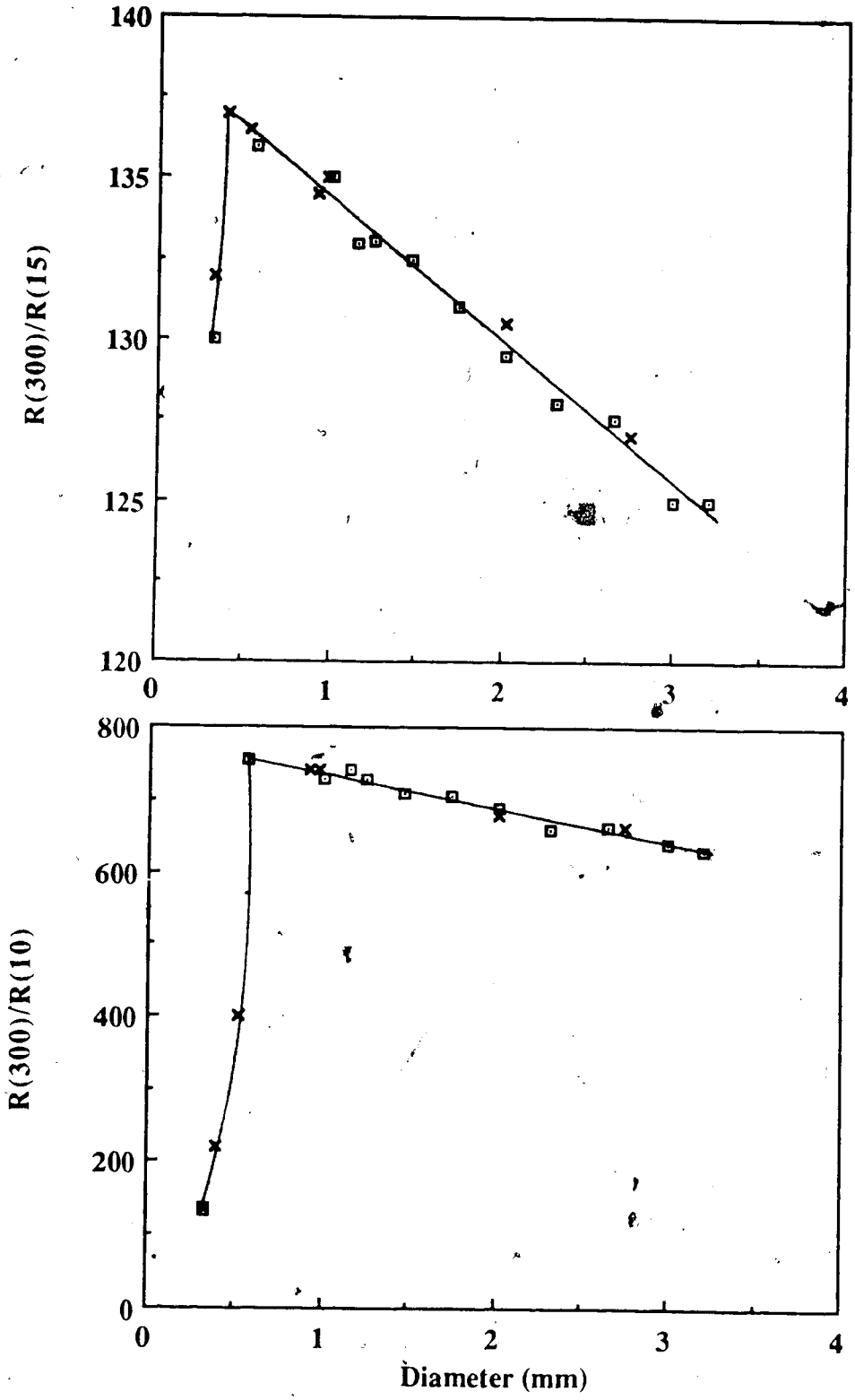
140
135
130
125
120
R(300)/R(15)
0
1
2
3
4
800
600
400
200
0
R(300)/R(10)
0
1
2
3
4
Diameter (mm)

Fig(3.4) : [R(300)/ R(T)] Versus Diameter For Potassium at T= 20 and 30 K, Set # 2 (⊡)and Set # 3 (x) . The annealing time at room temperature ≥ one month.

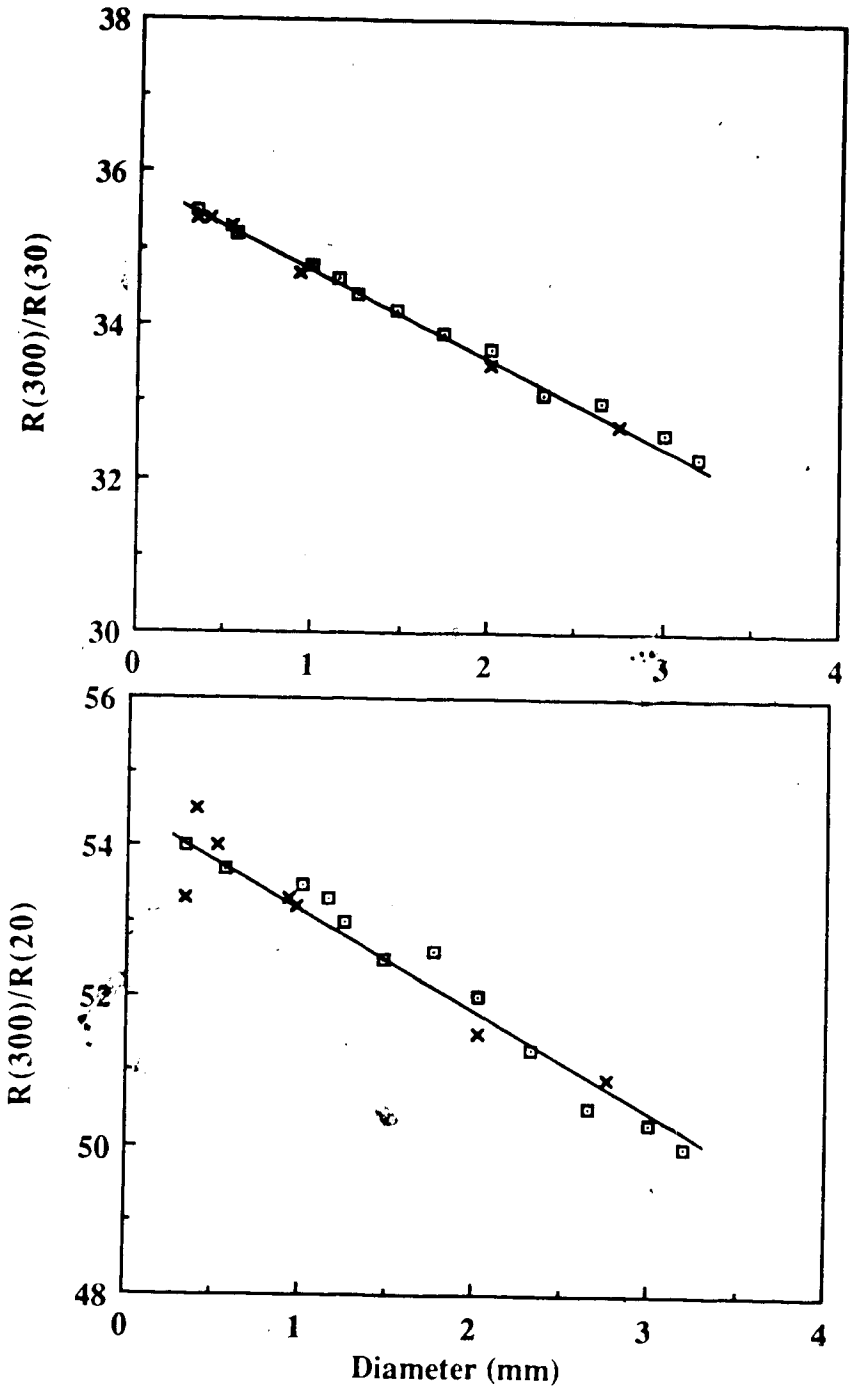
38
36
34
32
30
R(300)/R(30)
0
1
2
3
4
56
54
52
50
48
R(300)/R(20)
0
1
2
3
4
Diameter (mm)

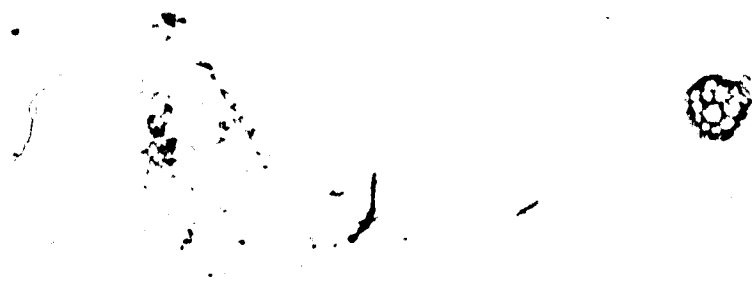

Fig(3.5) : [R(300)/ R(T)] Versus Diameter For Potassium at T= 40 and 50 K, Set # 2 (⊡)and Set # 3 (x) . The annealing time at room temperature ≥ one month.

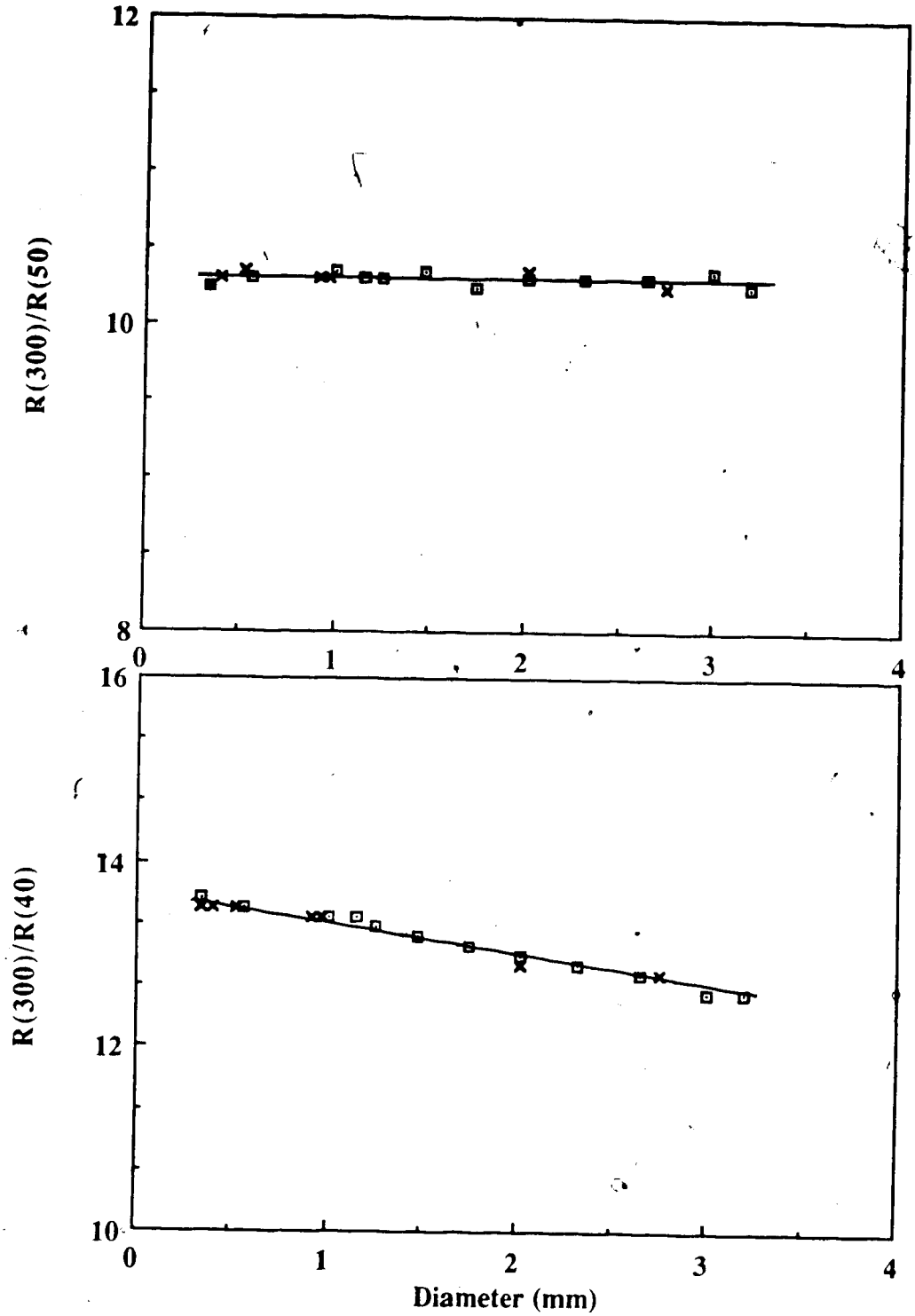
12
10
8
R(300)/R(50)
0
1
2
3
4
16
14
12
10
R(300)/R(40)
0
1
2
3
4
Diameter (mm)

Fig(3.6) : [R(300)/ R(T)] Versus Diameter For Potassium at T= 77 K, Set # 1, Set # 2 and Set # 3 .The annealing time at room temperature ≥ one month.

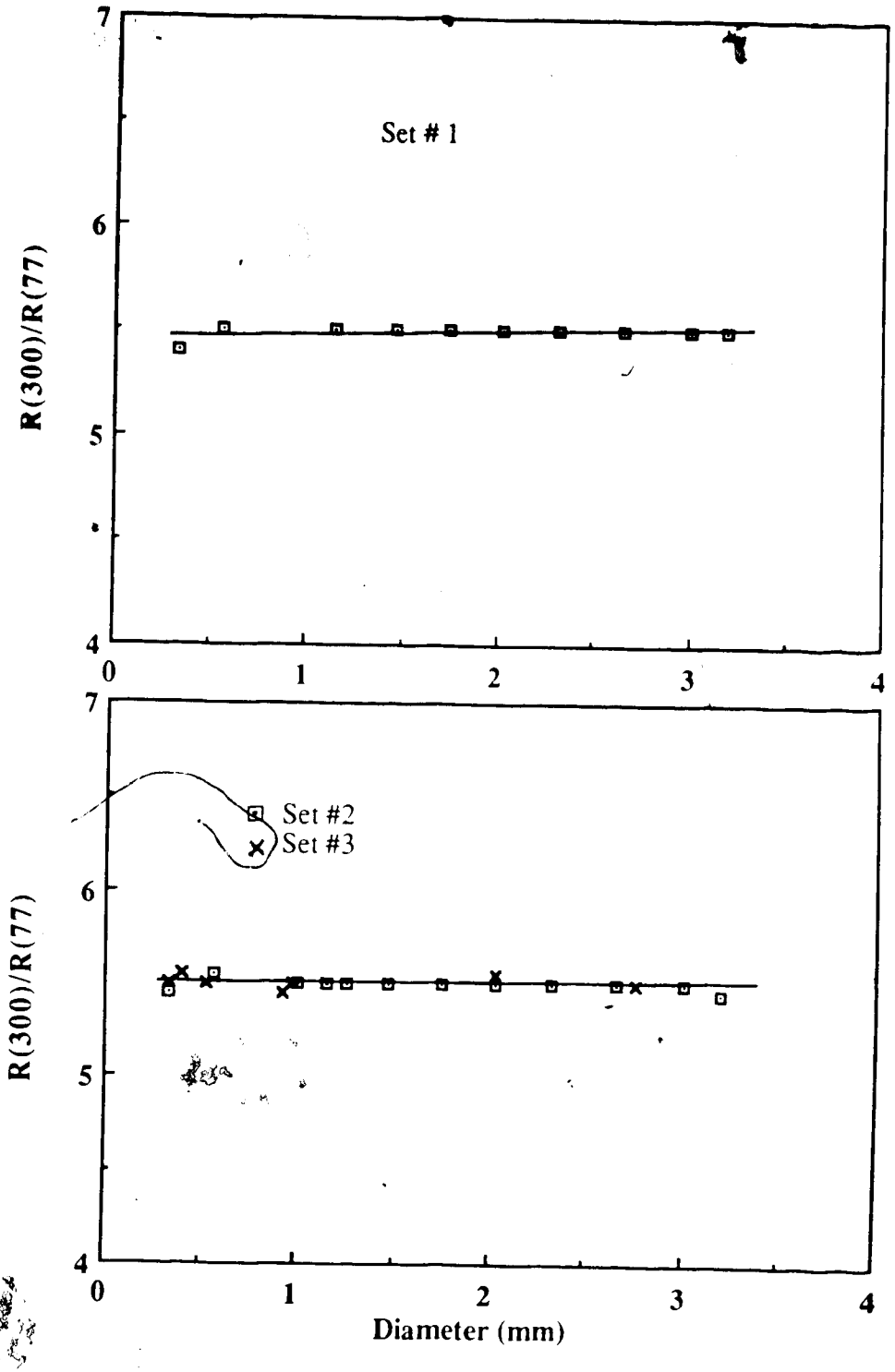
Set # 1
R(300)/R(77)
7
6
5
4
0
1
2
3
4
Set #2
Set #3
R(300)/R(77)
7
6
5
4
0
1
2
3
4
Diameter (mm)

Fig(3.7) : The Electrical Conductivity Versus Diameter For Sodium at 4.2 K , Set # 1 and Set # 2.

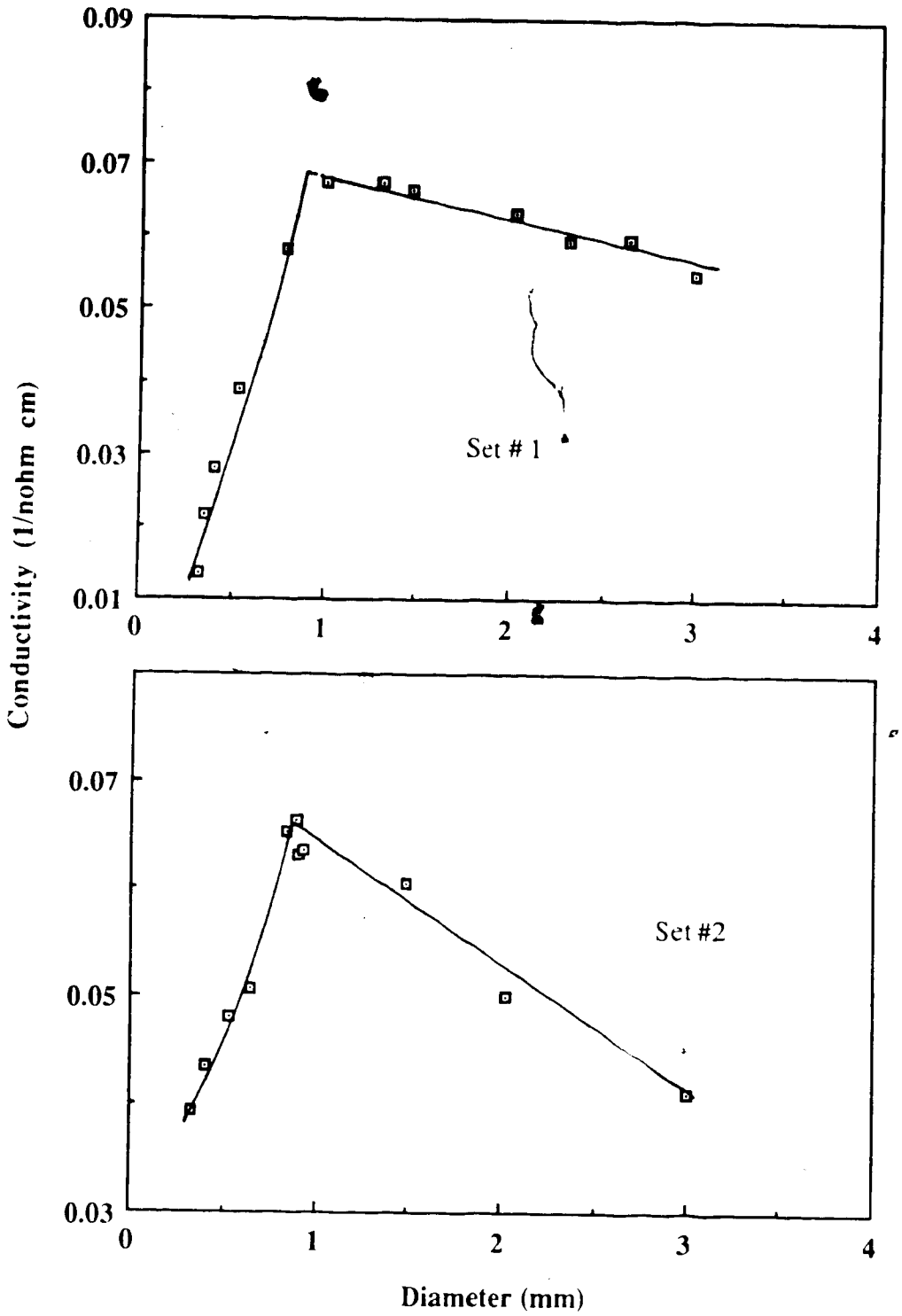
0.09
0.07
0.05
0.03
0.01
0
1
2
3
4
Set # 1
Conductivity (1/nohm cm)
0.07
0.05
0.03
0
1
2
3
4
Set #2
Diameter (mm)

Fig(3.8) : RRR Versus Diameter For Sodium at 4.2 K , Set # 1 and Set # 2.

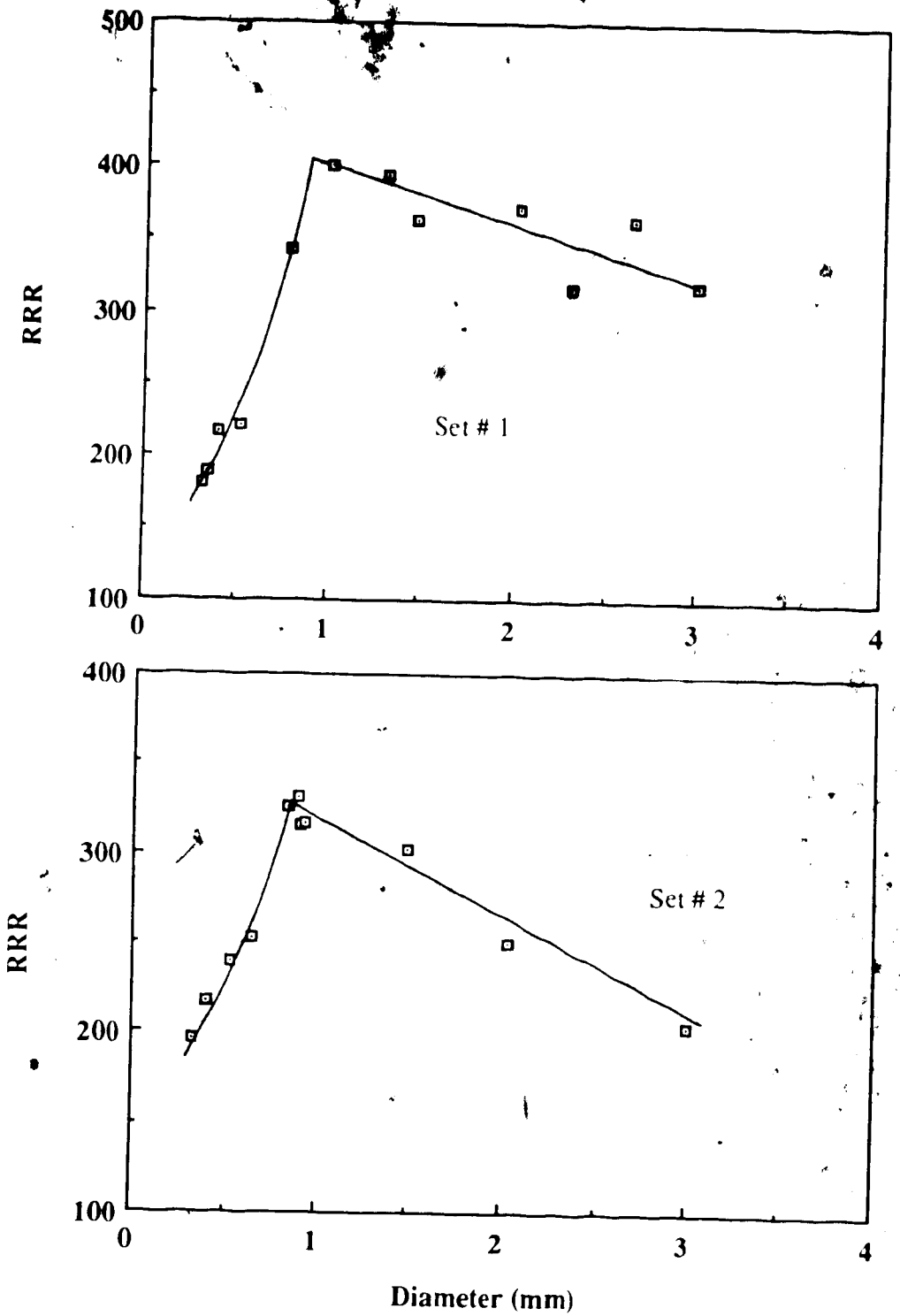
500
400
300
200
100
RRR
Set # 1
0
1
2
3
4
400
300
200
100
RRR
Set # 2
0
1
2
3
4
Diameter (mm)

Fig(3.9) : RRR Versus Diameter For Sodium at 4.2 K , Set # 3 (⊡ , ■) and Set # 4 (+, x).The annealing time at room temperature is indicated on each curve.

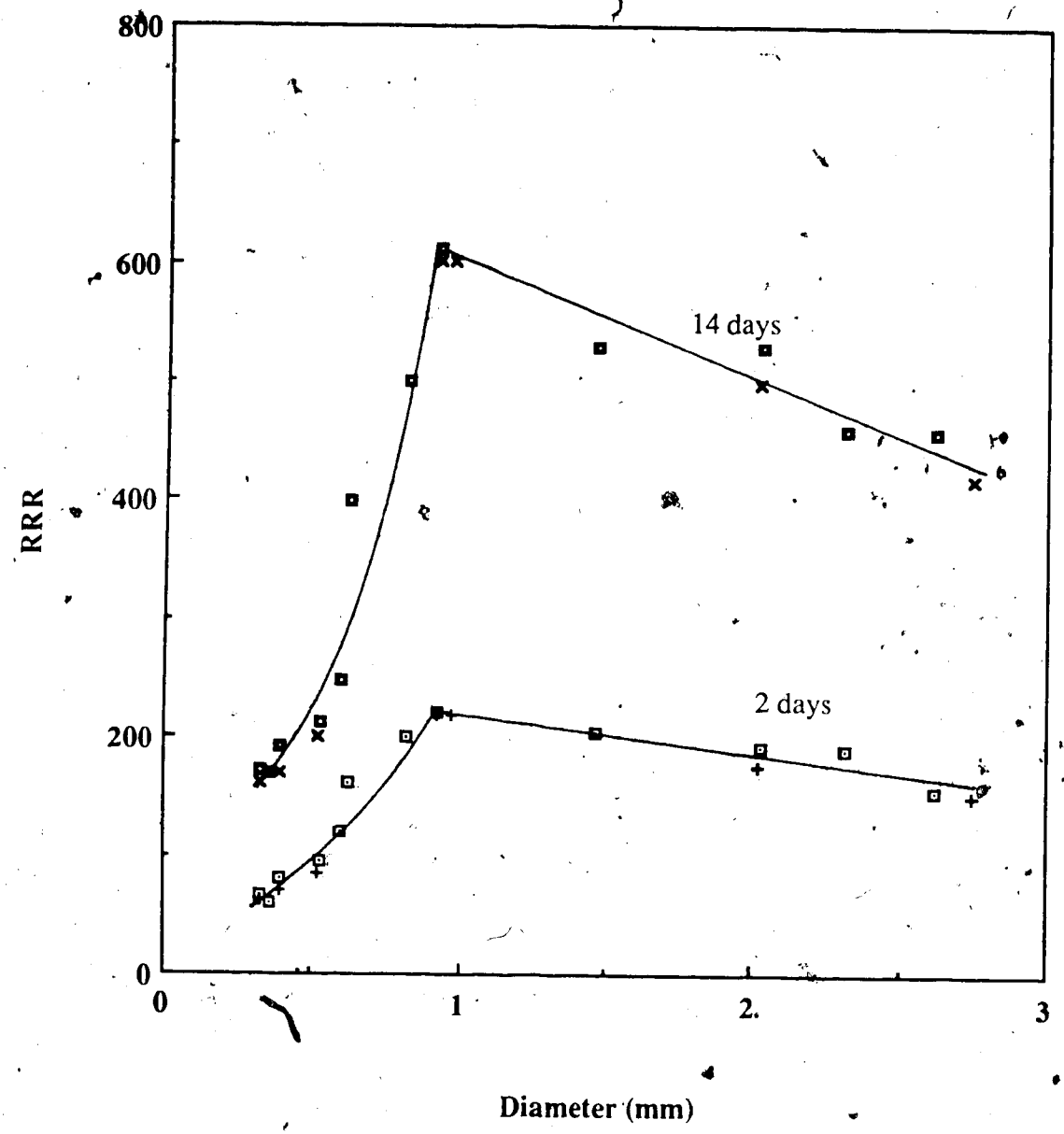
800
600
400
200
0
RRR
14 days
2 days
0
1
2
3
Diameter (mm)

Fig(3.10) : R(300)/R(T) Versus Diameter For Sodium at T=10 and T=15 k, Set # 3 (⊡) and Set # 4 (x).The annealing time at room temperature ≥ one month.

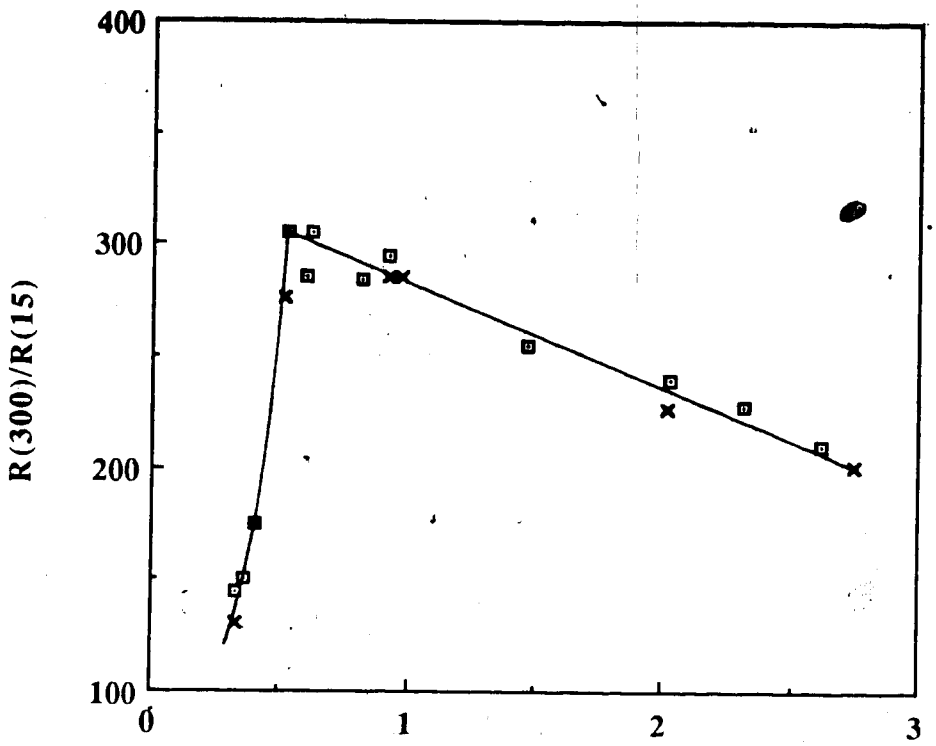
400
300
200
100
R(300)/R(15)
0
1
2
3

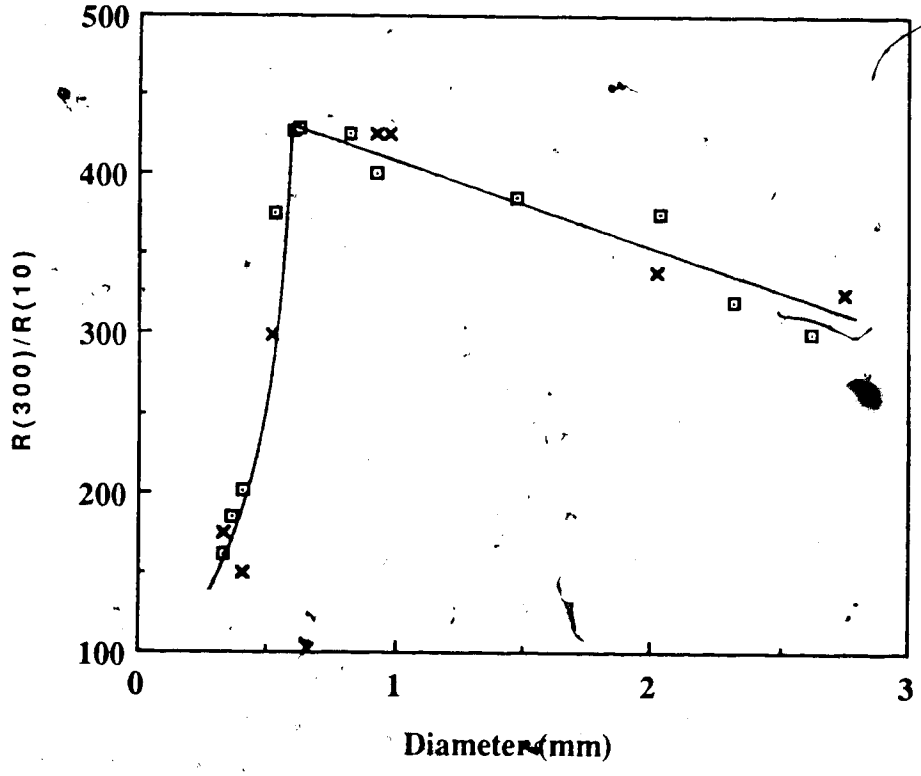
500
400
300
200
100
R(300)/R(10)
0
1
2
3
Diameter (mm)

Fig(3.11) : R(300)/ R(T) Versus Diameter For Sodium at T=20 and T=30 k, Set # 3 (⊡) and Set # 4 (x).The annealing time at room temperature ≥ one month.

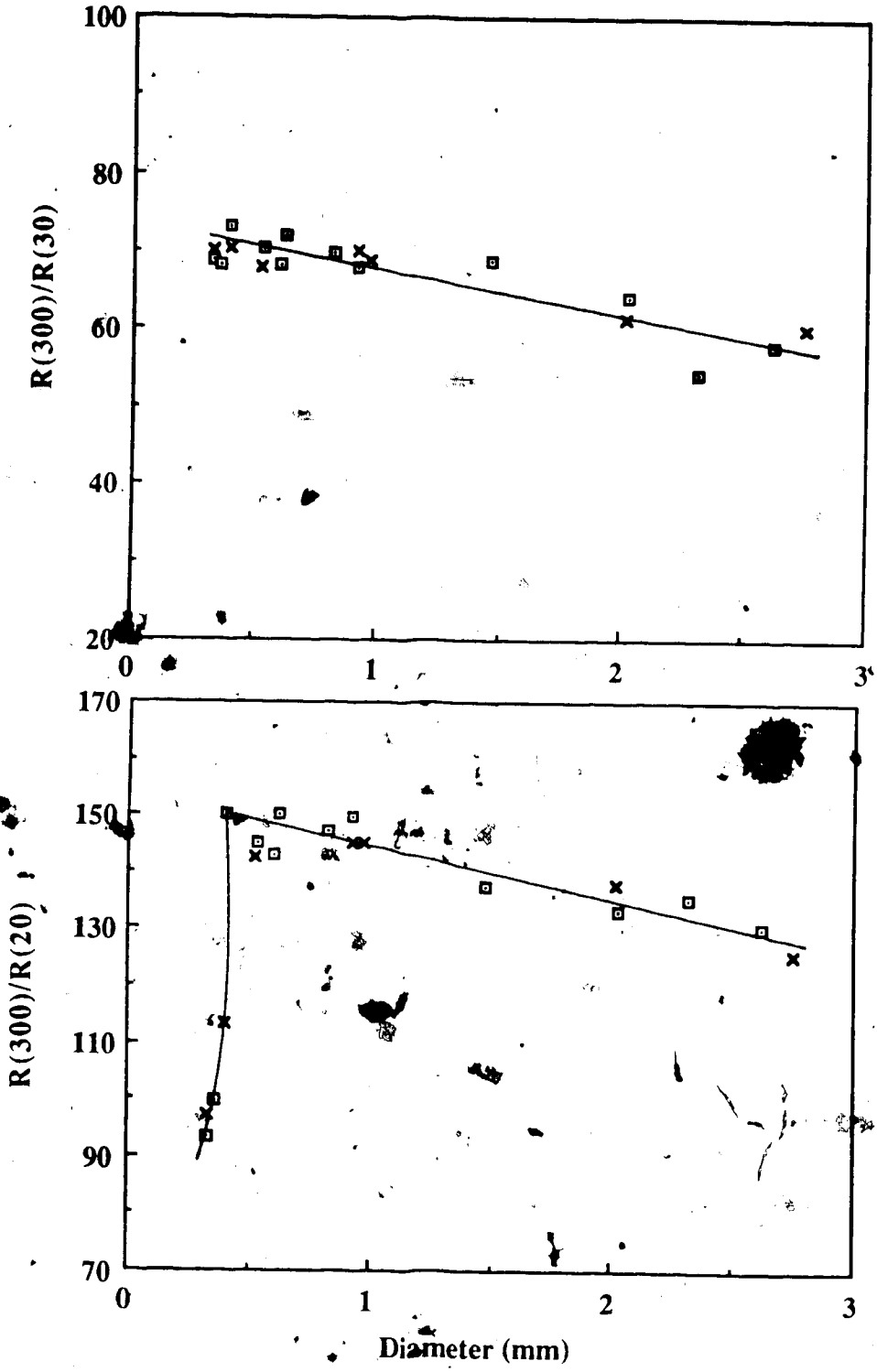
100
80
60
40
20
R(300)/R(30)
0
1
2
3
170
150
130
110
90
70
R(300)/R(20)
0
1
2
3
Diameter (mm)

Fig(3.12) : R(300)/ R(T) Versus Diameter For Sodium at T=40 and T=50 k, Set # 3 (⊡) and Set # 4 (x).The annealing time at room temperature ≥ one month.

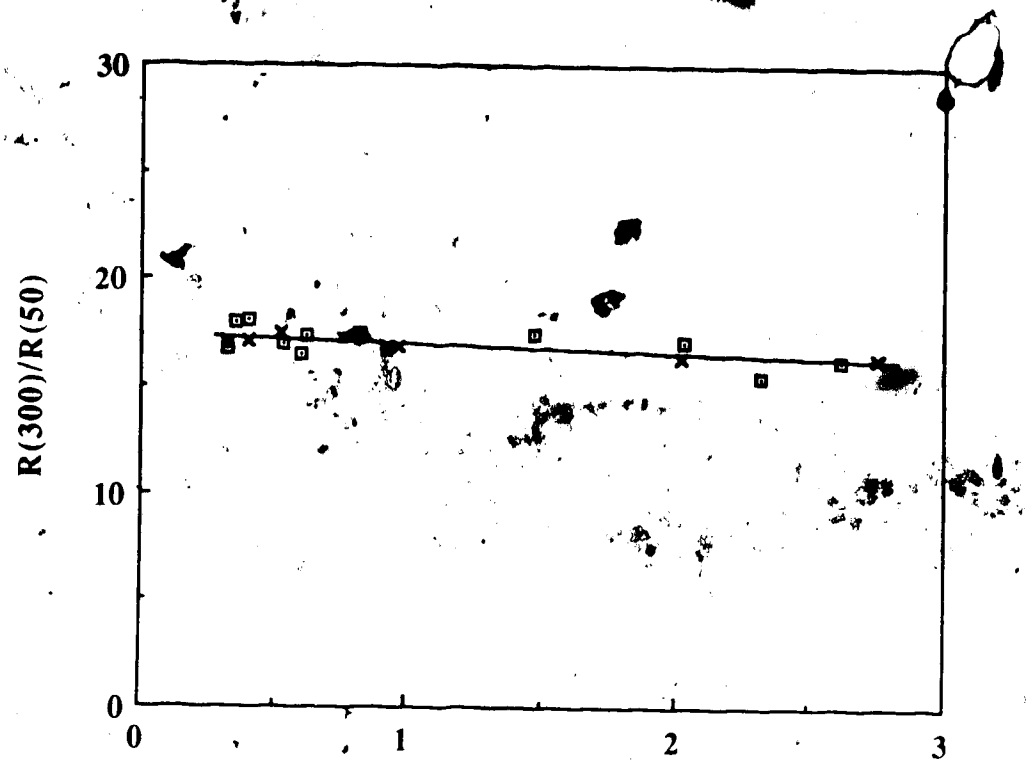
30
20
10
0
R(300)/R(50)
0
1
2
3

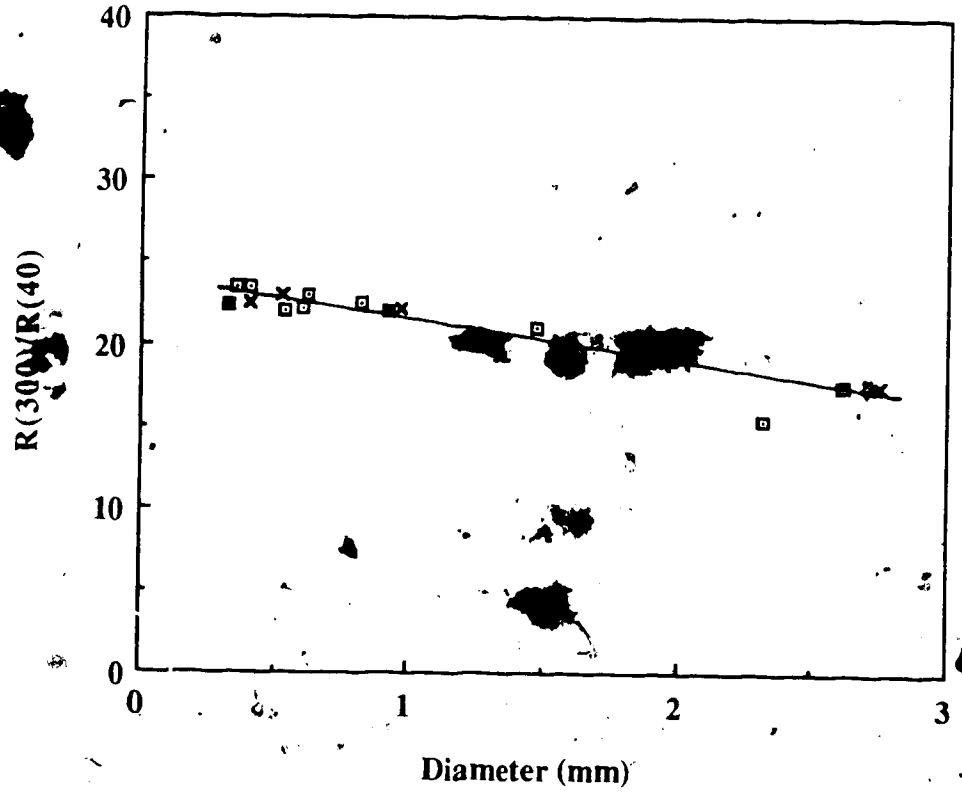
40
30
20
10
0
R(300)/R(40)
0
1
2
3
Diameter (mm)

Fig(3.13) : R(300)/ R(T) Versus Diameter For Sodium at T=60 and T=70 k, Set # 3 (⊡) and Set # 4 (x).The annealing time at room temperature ≥ one month.

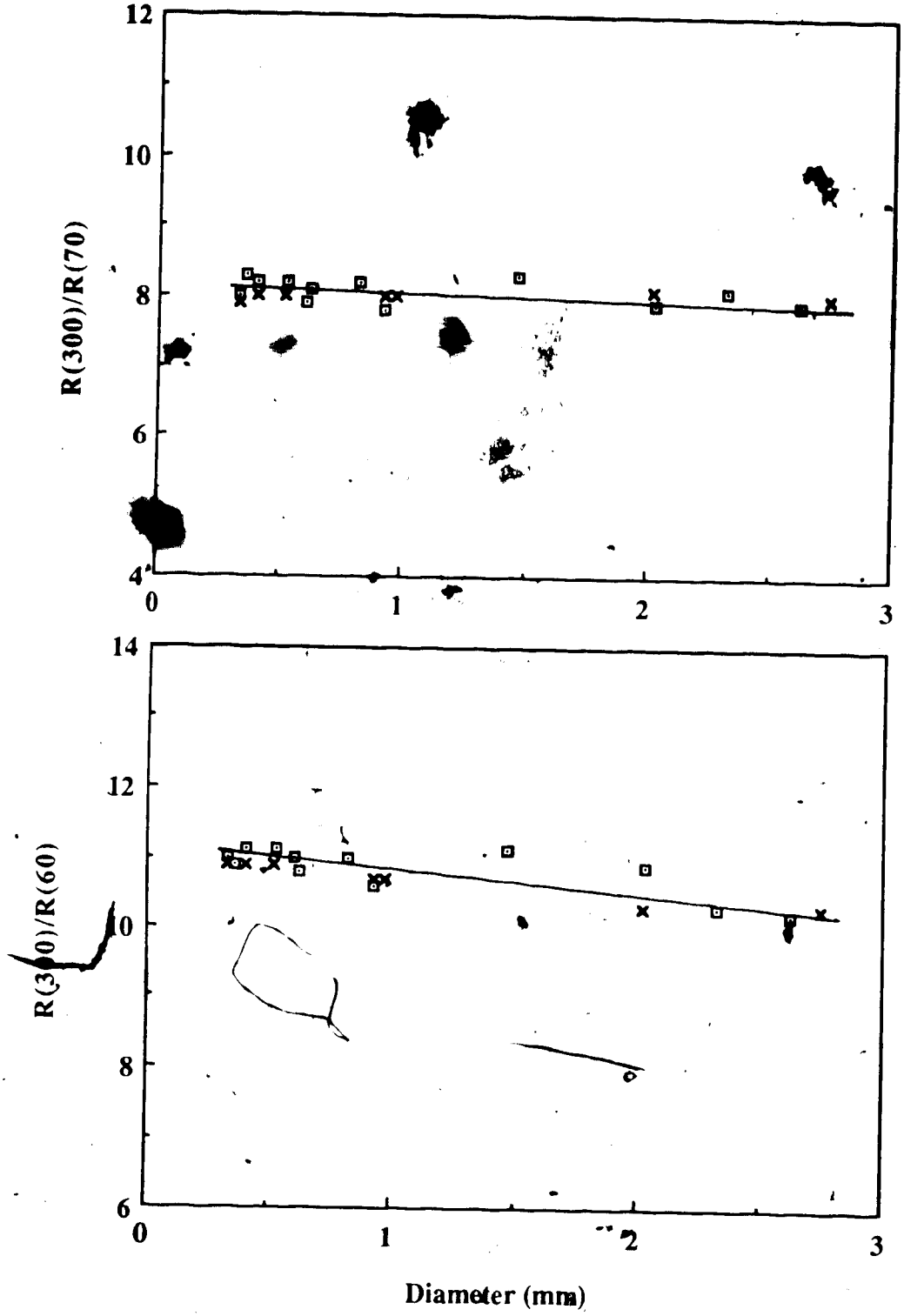
12
10
8
6
4
R(300)/R(70)
0
1
2
3
14
12
10
8
6
R(300)/R(60)
0
1
2
3
Diameter (mm)

Fig(3.14) : R(300)/ R(T) Versus Diameter For Sodium at T=77 and T=90 k, Set # 3 (⊡),and Set # 4 (x),The annealing time at room temperature ≥ one month.

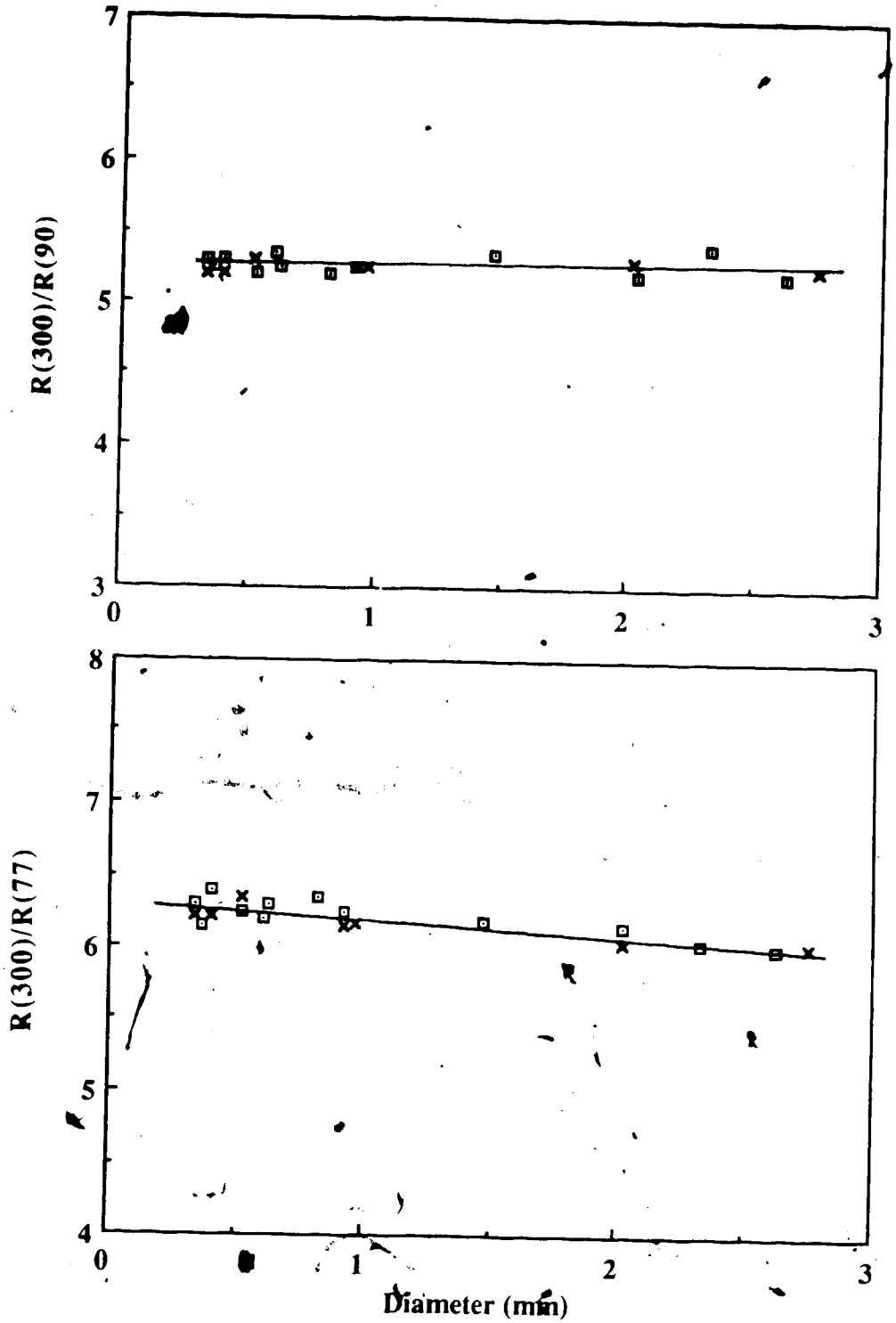
R(300)/R(90)
7
6
5
4
3
0
1
2
3
R(300)/R(77)
8
7
6
5
4
0
1
2
3
Diameter (mm)

Fig(3.15) : R(300)/ R(T) Versus Diameter For Sodium at T=77, Set # 2 .

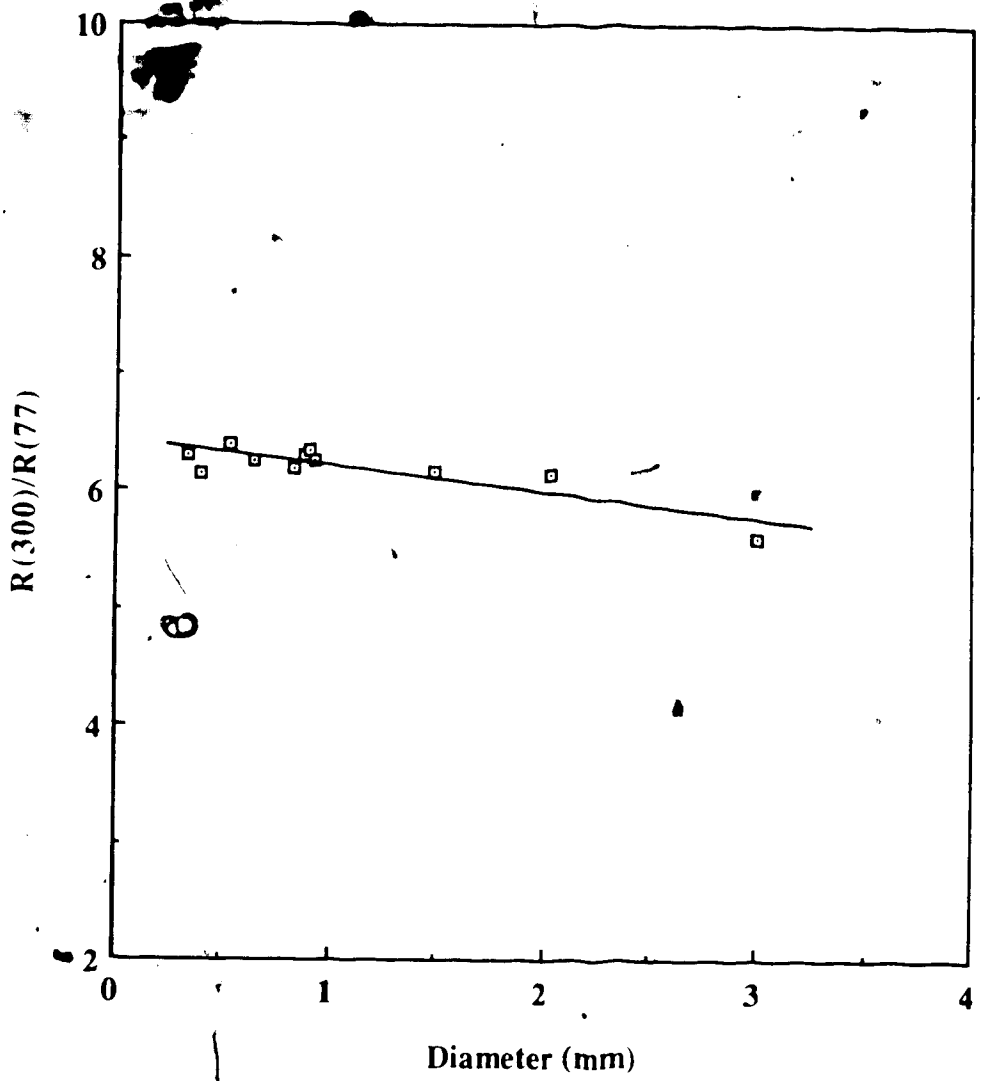
10
8
6
4
2
R(300)/R(77)
0
1
2
3
4
Diameter (mm)

Fig(3.16) : The Electrical Resistivity Versus Diameter For Indium at 4.2 K, (⊡, x) The Present Work and (o) Olsen's Results.

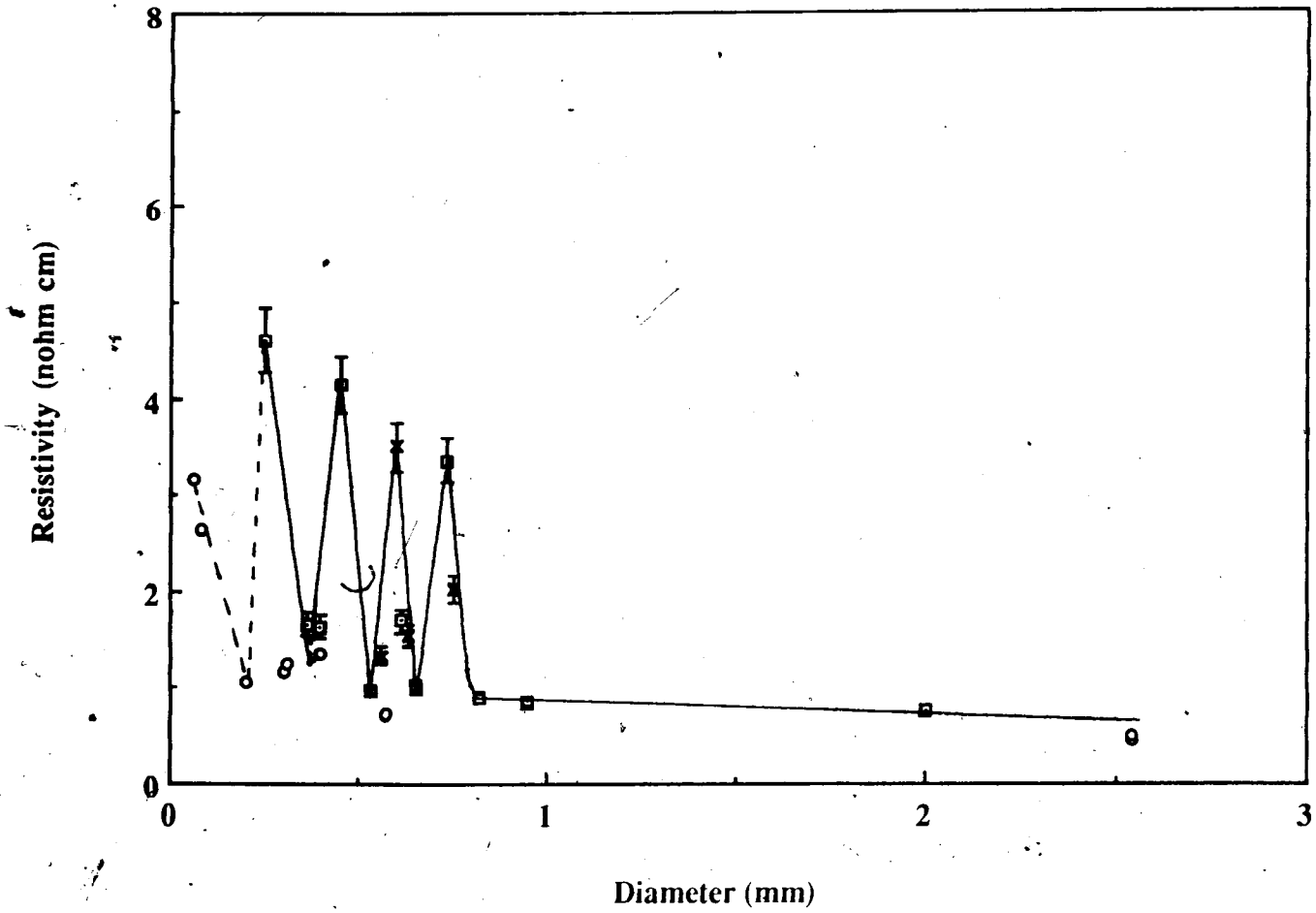
Resistivity (nohm cm)
Diameter (mm)
0
2
4
6
8
0
1
2
3

Fig(3.17) : $D\rho$ [$D\rho = \rho(d)-\rho(3\ mm)$] Versus $(d/2)^{-2/3}$, d is The Sample Diameter in mm, For Sodium at 4.2 K.

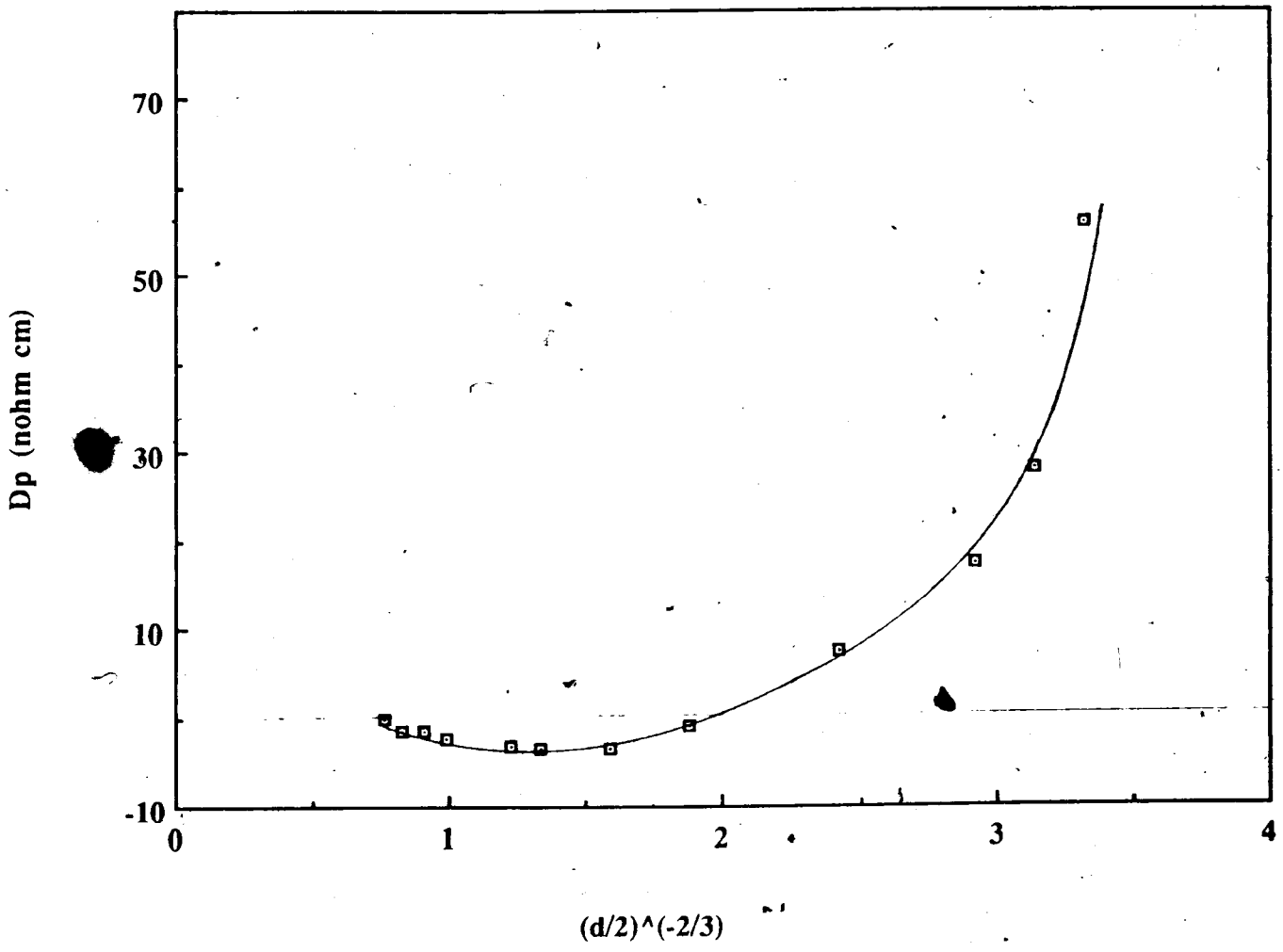
Dp (nohm cm)
70
50
30
10
-10
0
1
2
3
4
(d/2)^(-2/3)

Fig(3.18) : $\rho(d)$ Versus $(1/d)$, d is The Sample Diameter in mm , For Potassium at 4.2 K. Annealing time at room temperature is as indicated.

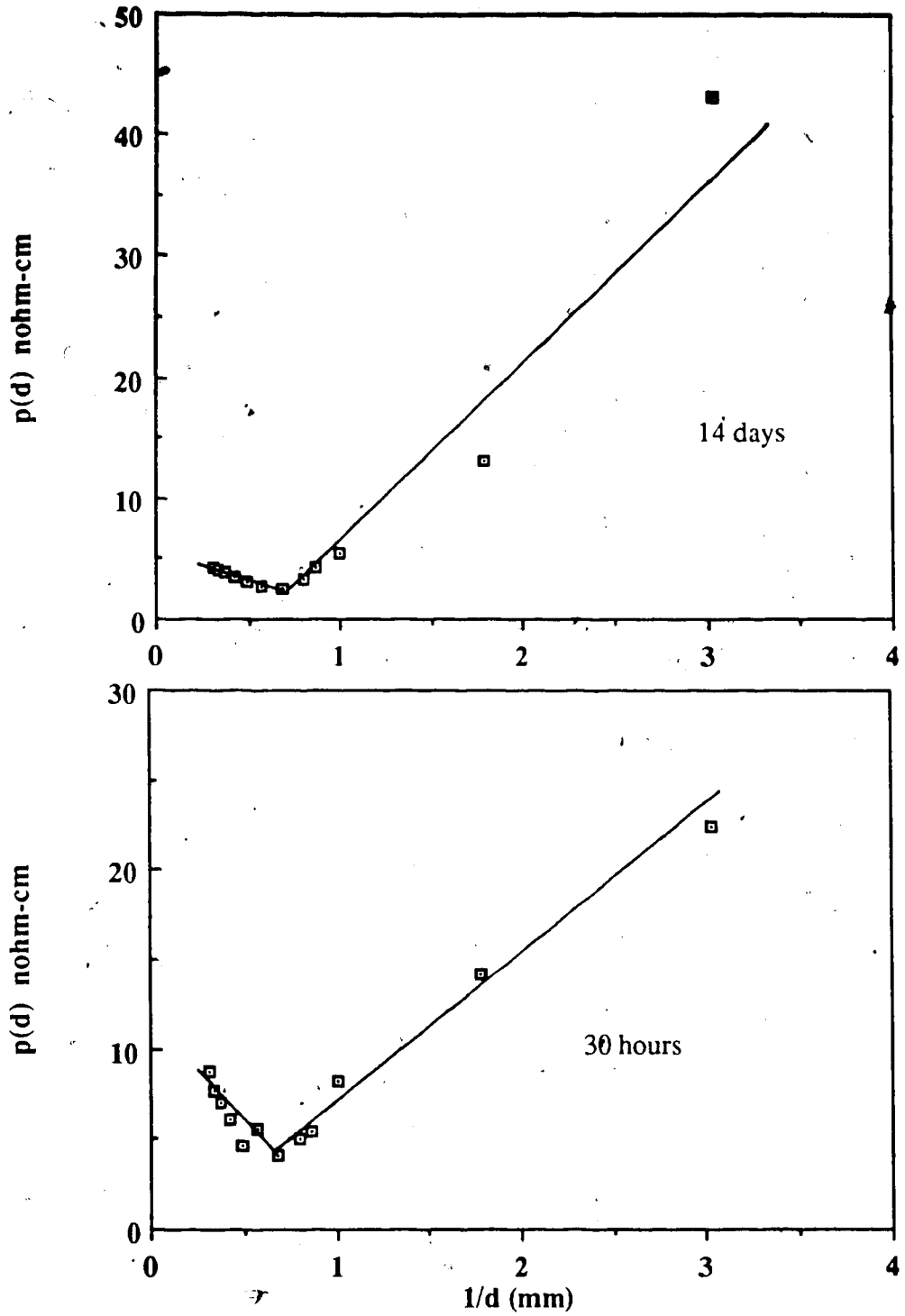
50
40
30
20
10
0
p(d) nohm-cm
14 days
0
1
2
3
4
30
20
10
0
p(d) nohm-cm
30 hours
0
1
2
3
4
1/d (mm)

Fig(3.19) : $\rho(d)$ Versus $(1/d)$, d is The Sample Diameter in mm , For Sodium at 4.2 K.

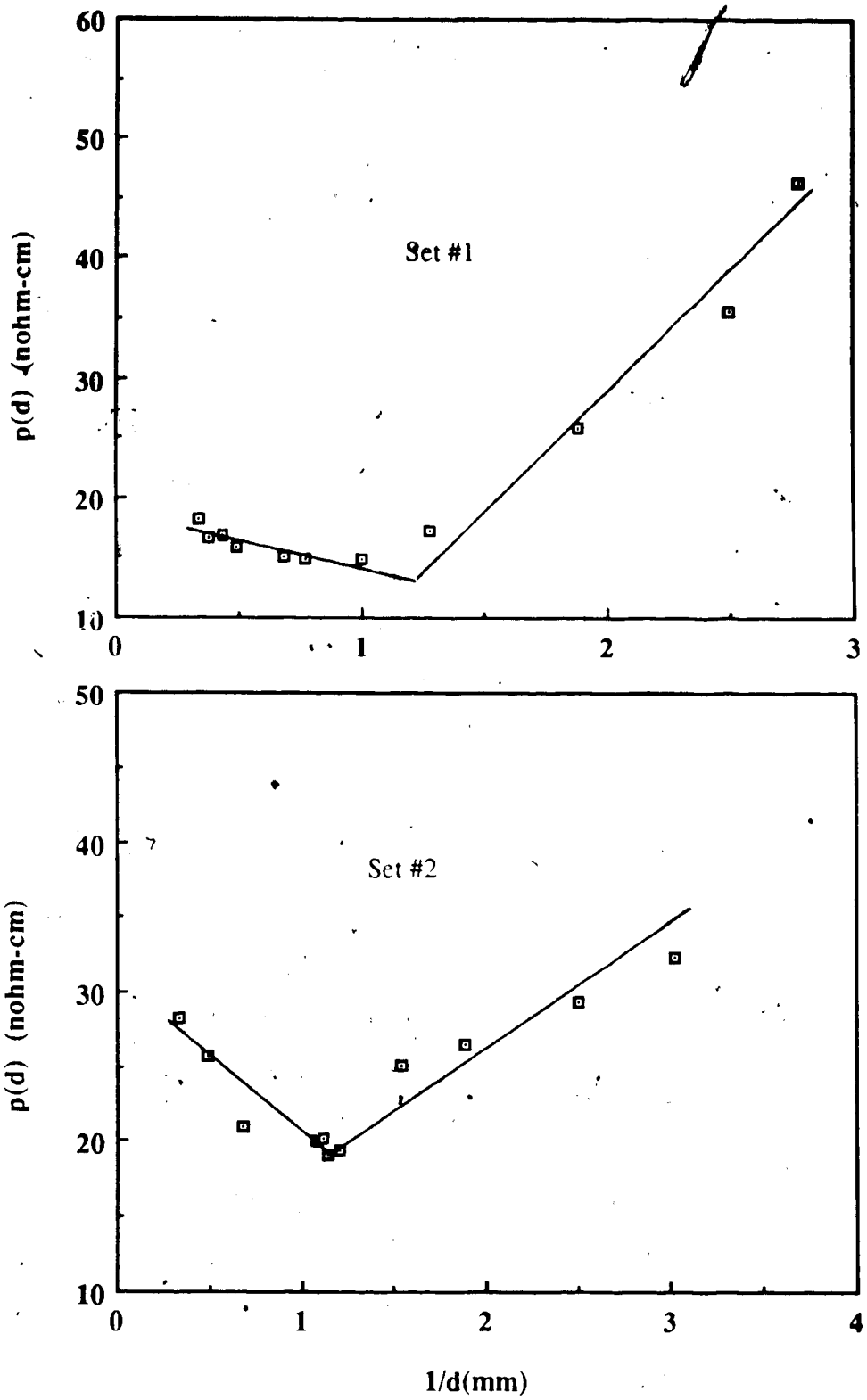
60
50
40
30
20
10
0
1
2
3
p(d) (nohm-cm)
Set #1
50
40
30
20
10
0
1
2
3
4
p(d) (nohm-cm)
Set #2
1/d(mm)

Fig(3.20) : ρ(d) Versus (1/ d), d is The Sample Diameter in mm , For Indium at 4.2 K, (⊡ , x) The Present Work and (o) Olsen's Results.

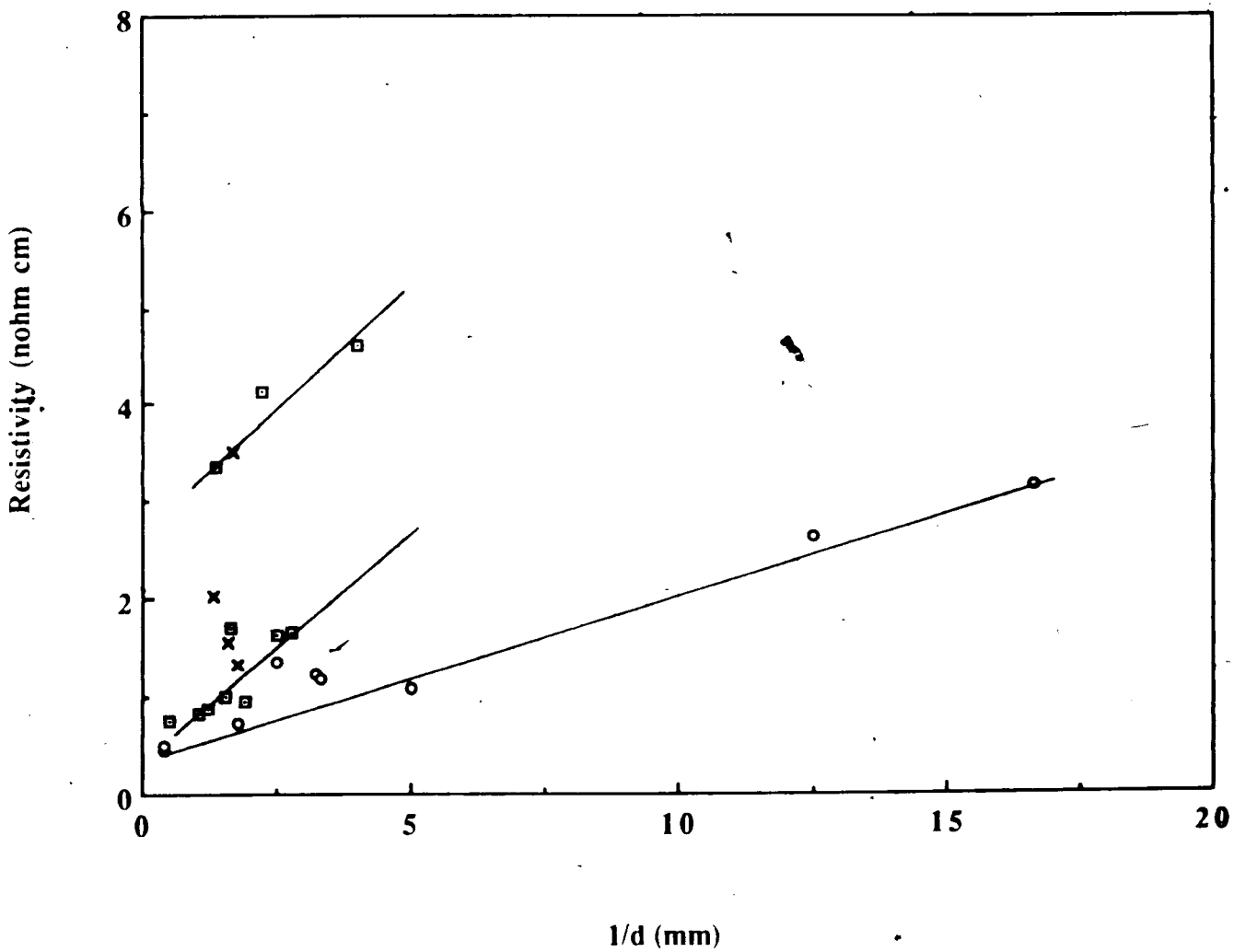
Resistivity (nohm cm)
8
6
4
2
0
0
5
10
15
20
1/d (mm)

Fig(3.21) : Magnetoresistance For Different Diameter Wires of Potassium at 4.2 K. The Diameter Values are as Indicated on Each Curve.

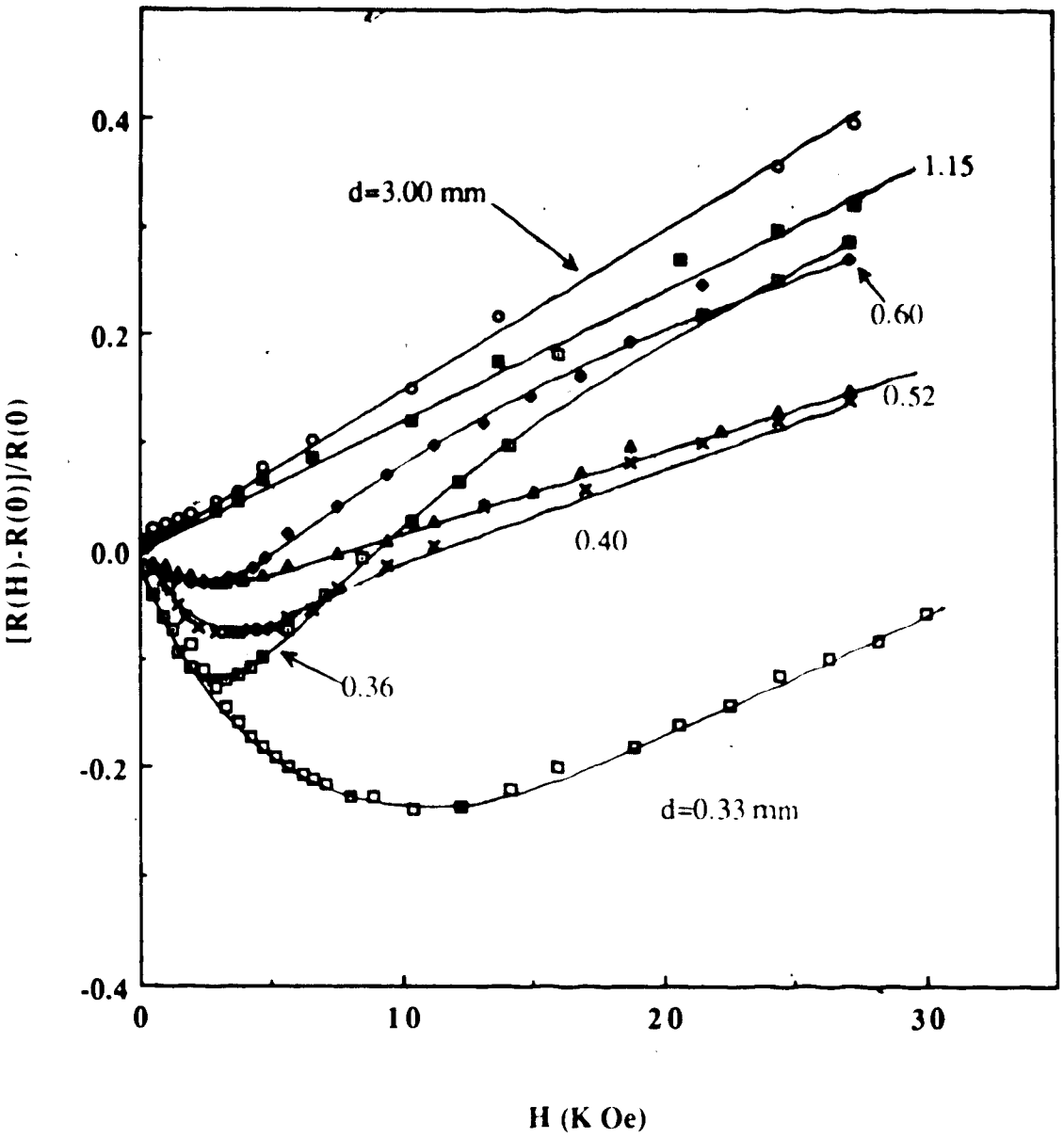
0.4
0.2
0.0
-0.2
-0.4
0
10
20
30
[R(H)-R(0)]/R(0)
H (K Oe)
d=3.00 mm
1.15
0.60
0.52
0.40
0.36
d=0.33 mm

Fig(3.22) : Low Field Magnetoresistance For Different Diameter Wires of Potassium at 4.2 K. The Diameter Values are as Indicated on Each Curve.

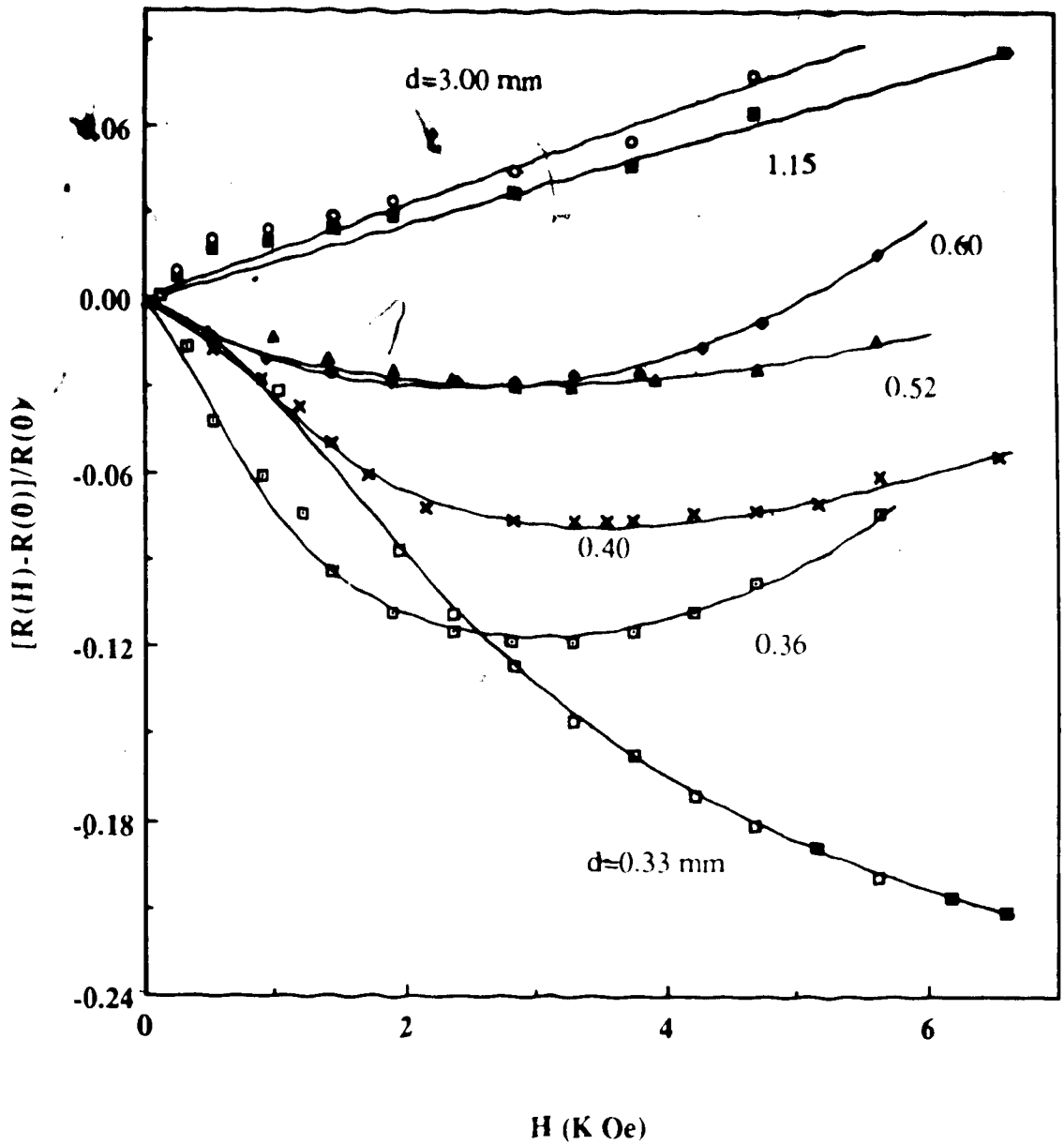
d=3.00 mm
1.15
0.60
0.52
0.40
0.36
d=0.33 mm
0.06
0.00
-0.06
-0.12
-0.18
-0.24
0
2
4
6
[R(H)-R(0)]/R(0)
H (K Oe)

Fig(3.23) : Effect of Annealing at Room Temperature on The Magnetoresistance of Potassium at 4.2 K.

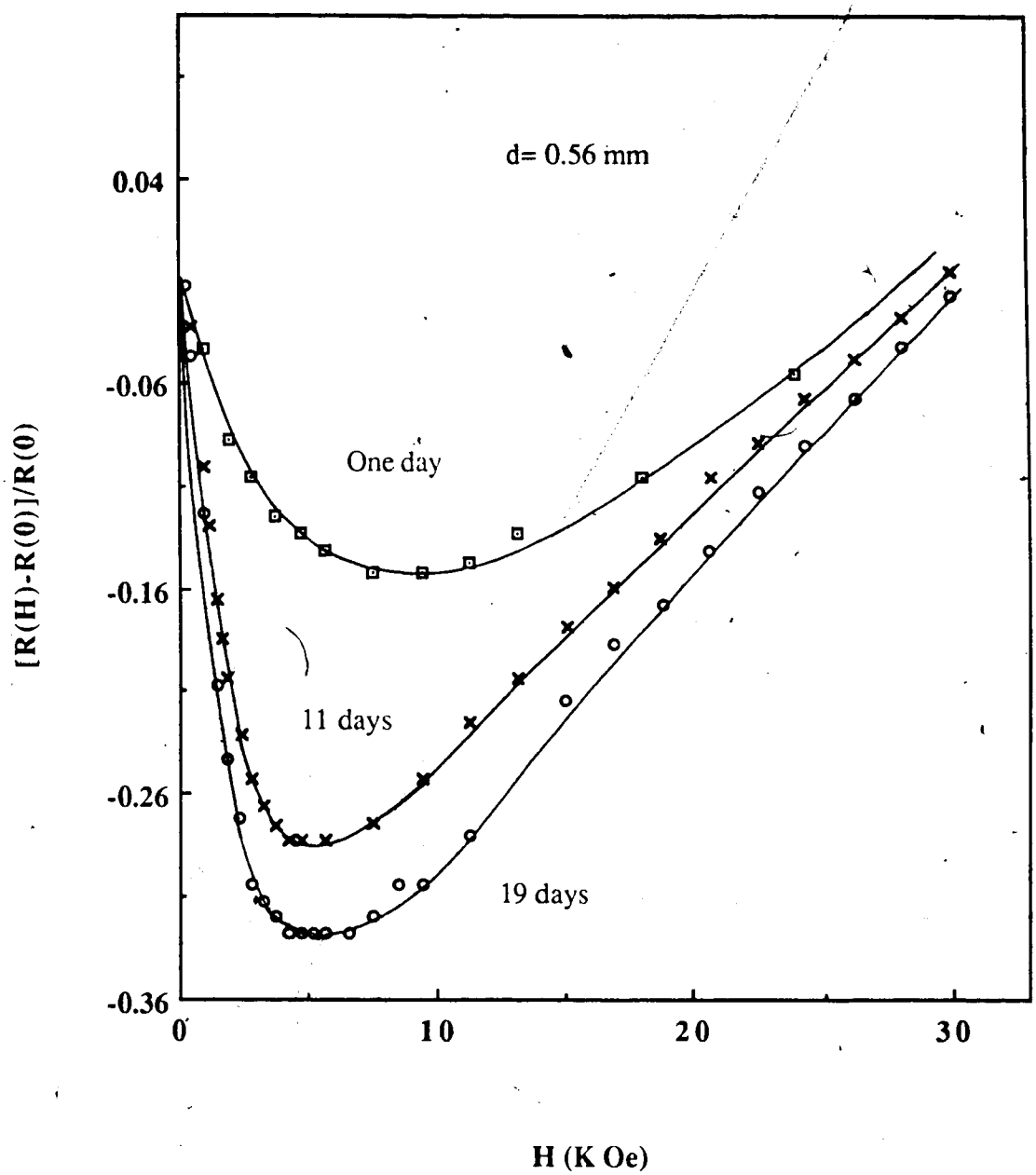
d= 0.56 mm
0.04
-0.06
-0.16
-0.26
-0.36
0
10
20
30
One day
11 days
19 days
[R(H)-R(0)]/R(0)
H (K Oe)

Fig(3.24) : Magnetoresistance of a Thin Potassium Wire Extruded Through a Die Made of a Machinable Ceramic.

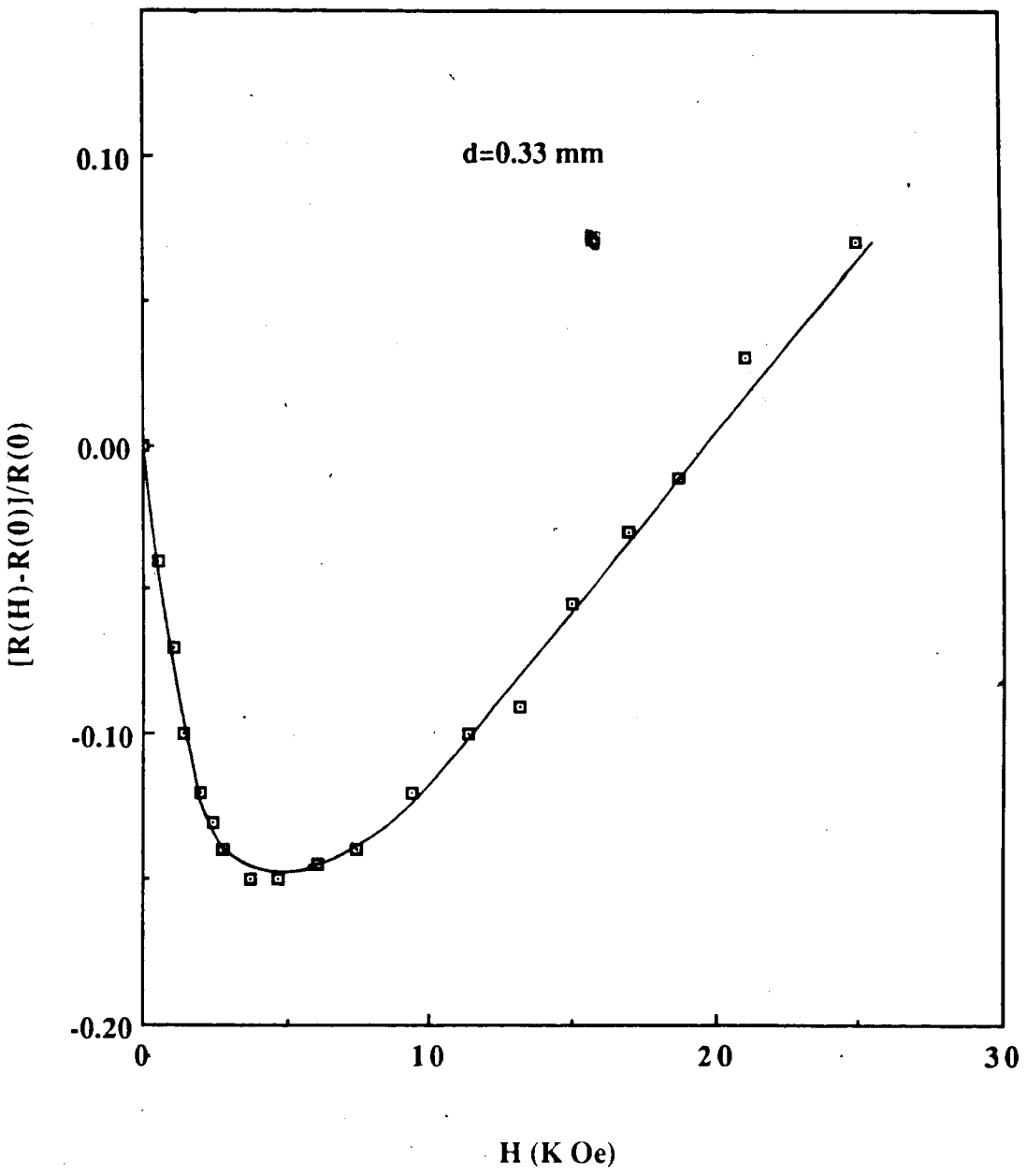
d=0.33 mm
0.10
0.00
-0.10
-0.20
[R(H)-R(0)]/R(0)
0
10
20
30
H (K Oe)

Fig(3.25) : Magnetoresistance For Different Diameter wires of Sodium at 4.2 K, Set # 1. The Diameter Values Are as Indicated.

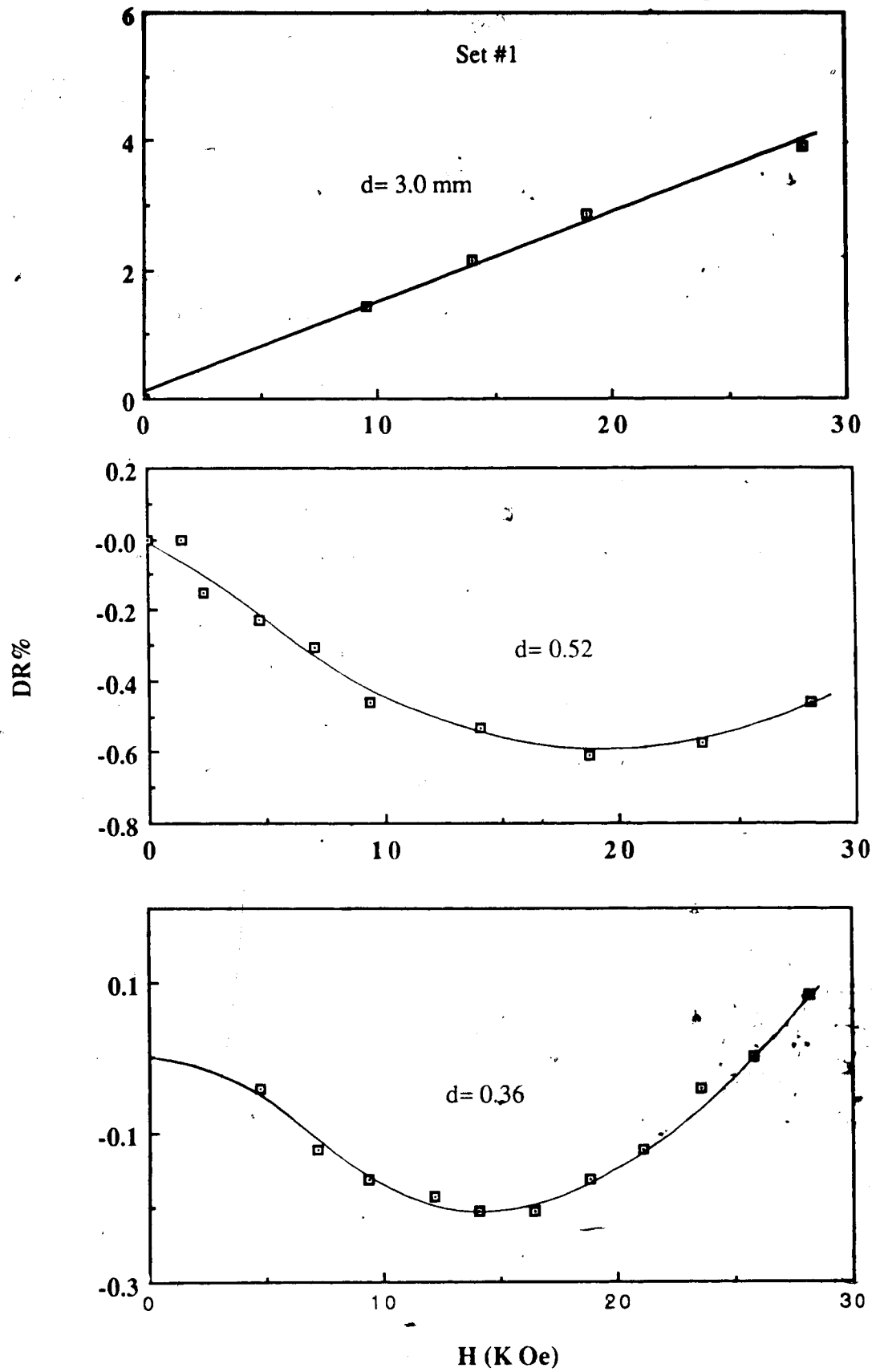
Set #1
d= 3.0 mm
d= 0.52
d= 0.36
DR%
H (K Oe)
6
4
2
0
0.2
-0.0
-0.2
-0.4
-0.6
-0.8
0.1
-0.1
-0.3
0
10
20
30

Fig(3.26) : Magnetoresistance For Different Diameter wires of Sodium at 4.2 K, Set # 2. The Diameter Values Are as Indicated.

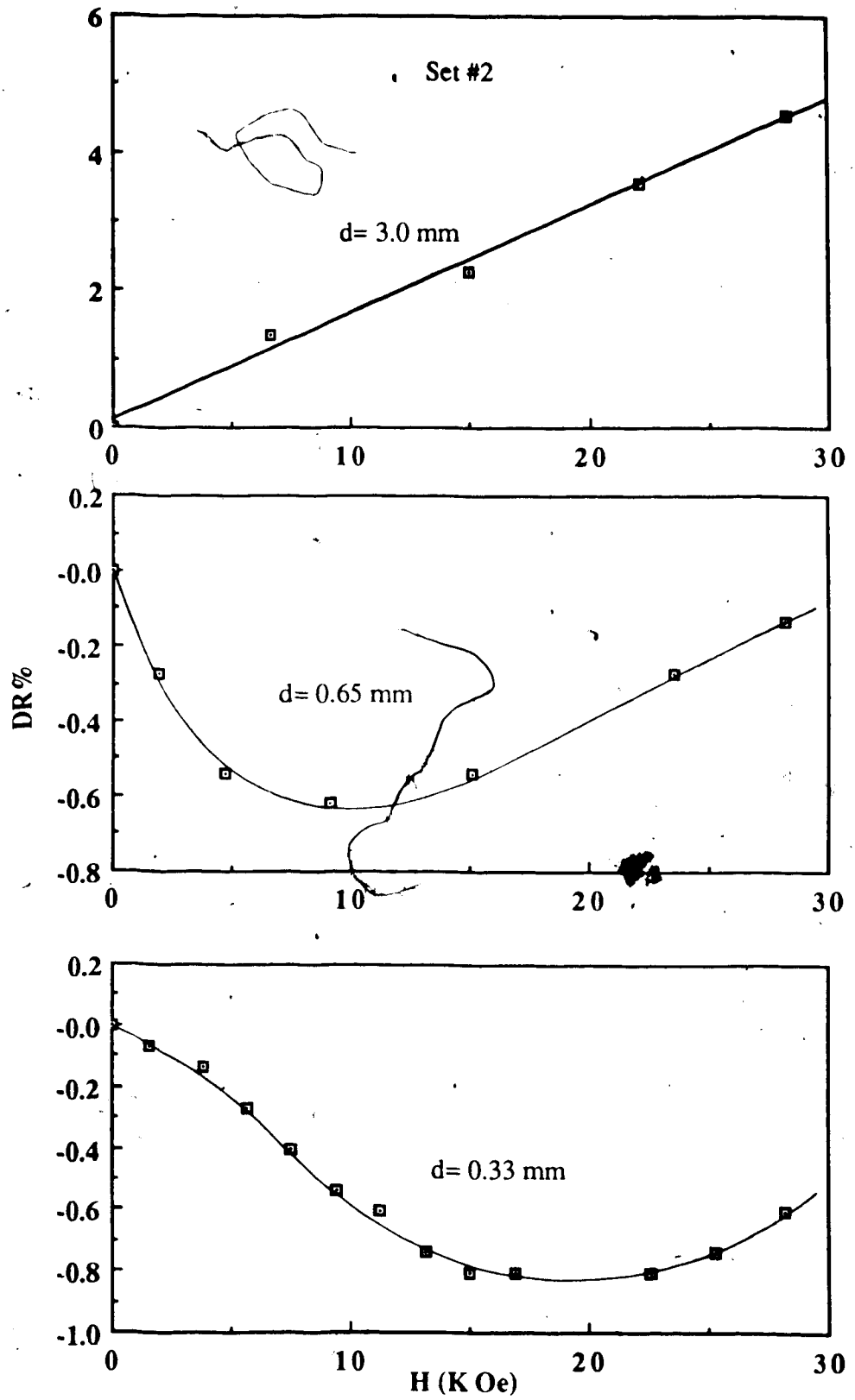
Set #2
d= 3.0 mm
d= 0.65 mm
d= 0.33 mm
DR%
H (K Oe)
6
4
2
0
0.2
-0.0
-0.2
-0.4
-0.6
-0.8
-1.0
0
10
20
30

Fig(3.27) : Magnetoresistance For an Indium wire, d=0.36 mm at 4.2 K.

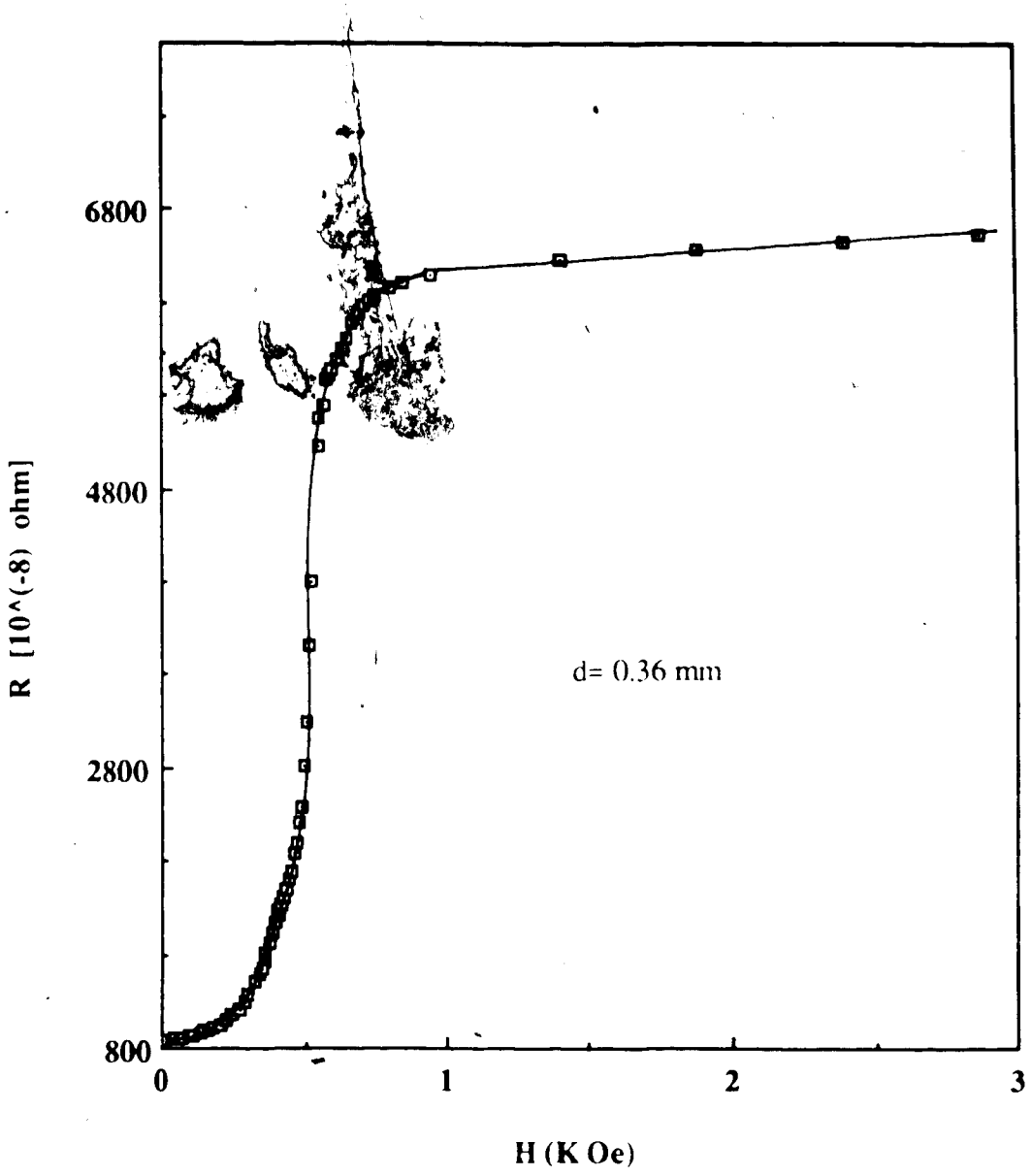
6800
4800
2800
800
R [10^(-8) ohm]
d= 0.36 mm
0
1
2
3
H (K Oe)

Fig(3.28) : Magnetoresistance For an Indium wire, d =0.75 mm at 4.2 K, An X-Y Plotter Output.

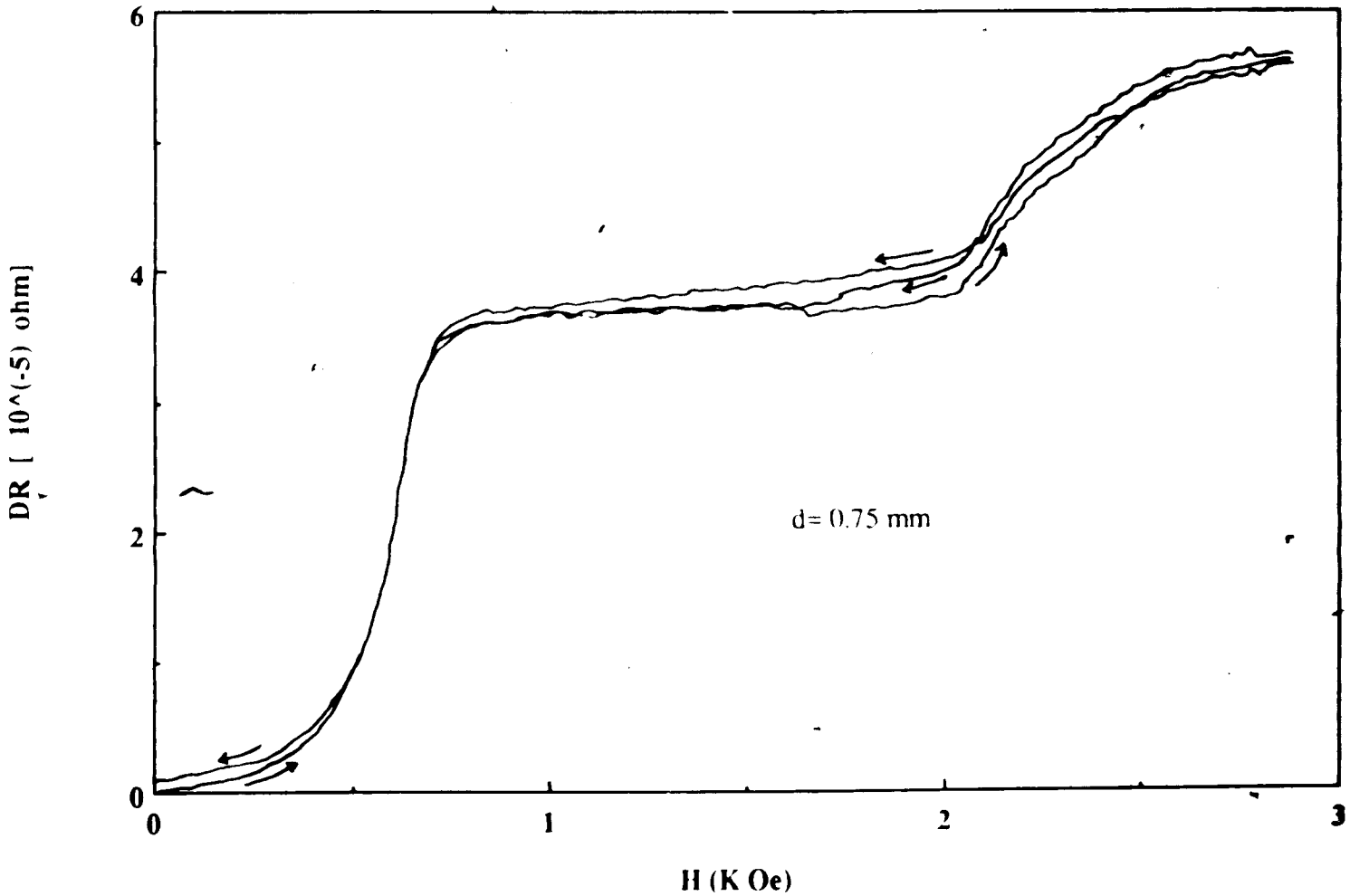
6
4
2
0
0
1
2
3
DR [10^(-5) ohm]
H (K Oe)
d= 0.75 mm

Fig(3.29) : (ρ/ρ_{∞}) Versus $(d/2R_H)$ For a Thin Potassium Wire,

d= 0.33 mm, at 4.2 K.

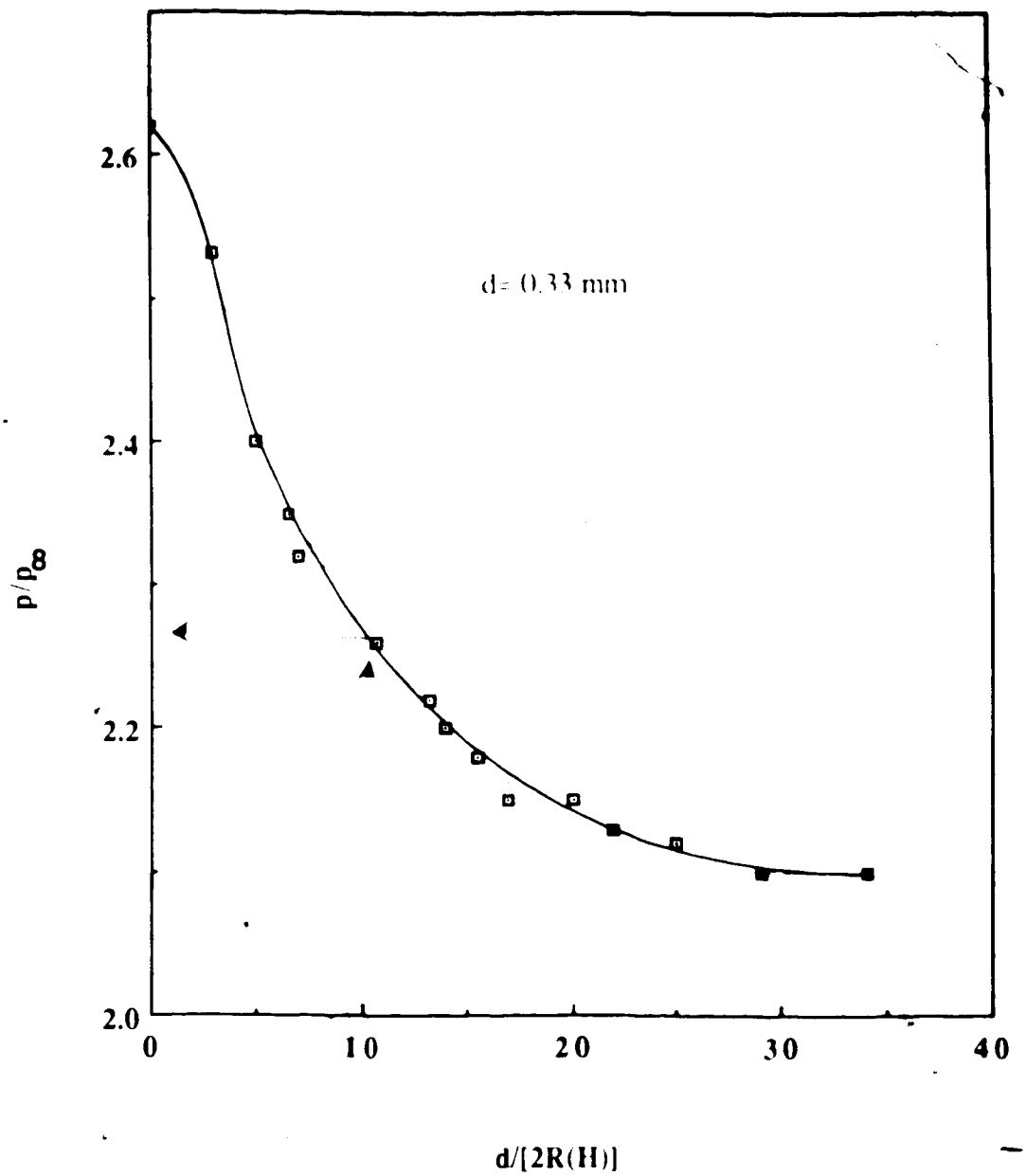

R(H) = [mv/eH] ~ 0.06/H for potassium

R(H) is in mm and H is in K Oe.

Fig(3.30) : (ρ/ρ_{∞}) Versus $(d/2R_H)$ For a Thin Sodium Wire,

d= 0.33 mm, at 4.2 K.

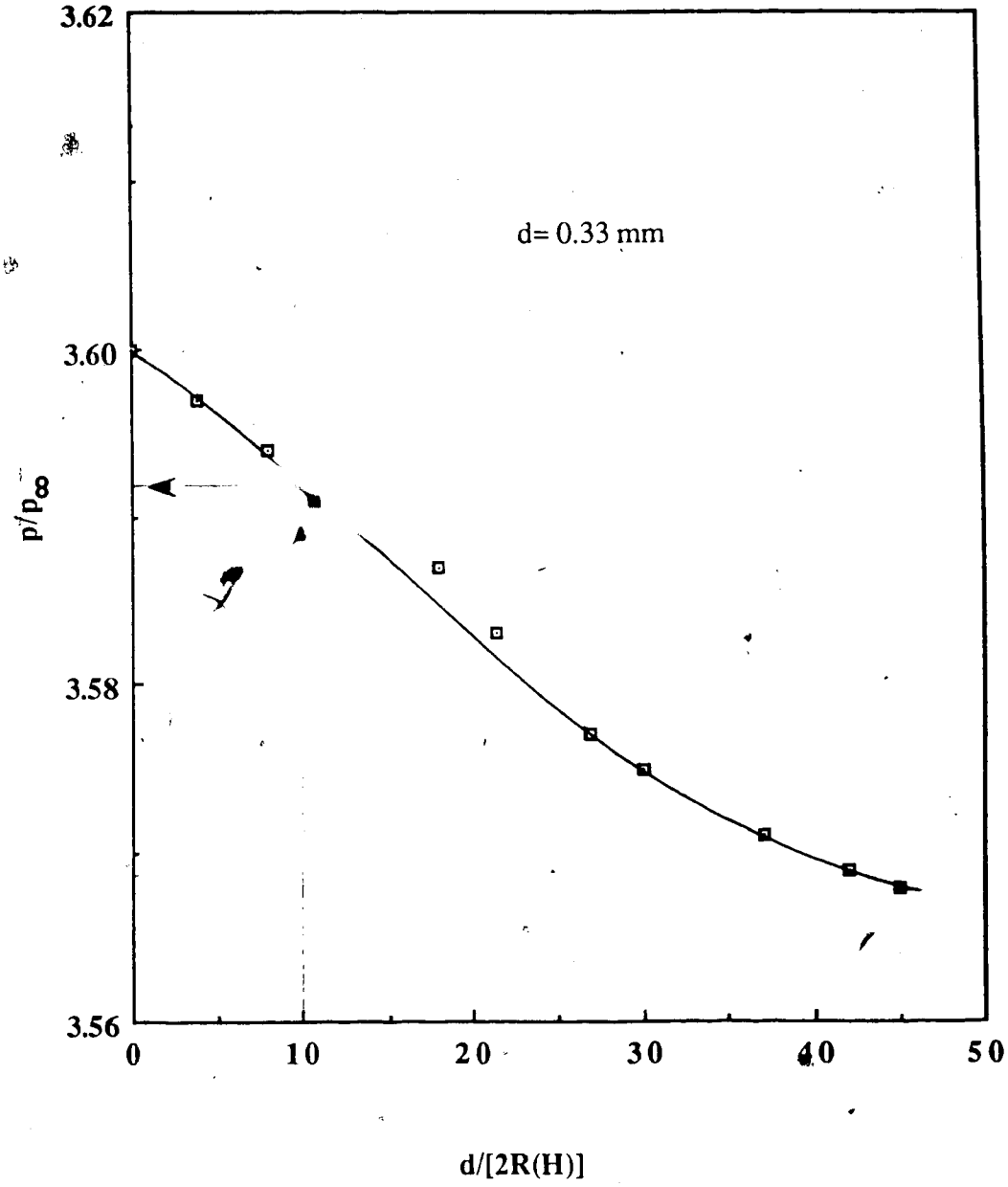

R(H)=[mv/eH] ~ 0.061/H for sodium

R(H) is in mm and H is in K Oe.

3.4) DISCUSSION OF THE RESULTS :

Fig.(3.1a) shows the electrical conductivity (σ) at T=4.1 K for potassium wire versus diameter (d) which shows a fast increase with "d" reaching a conductivity maximum at 1.47 mm after which σ decreases slowly as d increases further. During the time the specimens were held at room temperature, prior to cooling for these measurements, annealing occurred which reduced the residual resistivity ρ_0 ($\sigma_0=1/\rho_0$ increased). Two sets of measurements are shown in fig (3.1) carried out after different annealing times. Not only is ρ_0 smaller for the longer annealing time but also the observed size effect is stronger. This long term decrease in ρ_0 was observed before for one sample by Rowlands, Duvvury and Woods[4] and also by Van Kempen et al[48] in contrast to Gugan's[49] observations which showed that simple physical defects annealed in a few minutes even much below room temperature. In order to rule out any possible error in measuring the geometry factor, F, defined as ρ=FR, we have plotted the residual resistivity ratio , RRR, defined as R(300)/R(4.1) versus diameter in Fig.(3.1b) which shows essentially the same behavior as σ(4.1) versus d .The RRR is often used as an indication of sample purity but from fig(3.1b) and fig (3.2), one can see that RRR is also a function of the sample diameter and thermal history. The results of RR(T), defined as RR= R(300)/ R(T), versus the sample diameter for T= 10, 15,

20, 30, 40, 50, and 77 K are shown in figures (3.3) to (3.6). From these results one can see the following :

1) The conductivity maximum observed at helium temperature shifts towards smaller diameter values as the temperature is increased and disappears at T≥ 20 K.
2) The RR(T), or σ, became independent of the sample diameter for T≥ 50 K.
3) The over all effect became smaller as the temperature was increased.

Similar measurements have been carried out for sodium wires which gave very similar results. These results are summarized in figures (3.7) to (3.15) in which one can see that for T=4.2 K, the conductivity maximum occurred at d= 0.9 mm as opposed to d= 1.5 mm for potassium. That maximum disappeared at T= 30 K while the observed decrease of RR(T) with diameter for d≥ 0.9 mm persisted up to higher temperatures, but eventually vanished at T= 90 K. To our surprise, the observed effect for sodium was not washed out by the structure transformation at T= 40 K which was classified by Barrett[50] as a martensitic type. This transformation can lead to a hysteresis in the electrical resistivity as function of temperature in pure metals and alloys[51-53] . In order to minimize any possible effect due to such a transformation for sodium one has to collect all data in only one direction, either increasing or decreasing the sample temperature; for the present work data were collected while the specimens were being warmed.

The results for indium at T= 4.2 K are summarized in Fig.(3.16), which shows a completely different behavior than those for potassium and sodium. The electrical resistivity oscillated as a function of the sample diameter with equally-spaced peaks while the oscillation amplitude decreased with increasing diameter. The measurements were repeated after very long annealing times at room temperature but no change in the results was observed. This indicates that, for indium, any physical defects introduced due to sample extrusion were annealed out in a short time at ambient temperature. This property for metallic indium enabled us to obtain more data points, more than 12 points, by preparing more samples with the intermediate diameter values after analysis of the results for the first set. It also enabled us to compare our results with Olsen's[31] data, as indicated on Fig.(3.16). Olsen noticed the resistivity fluctuations for indium samples of different diam- -s at 4.2 K but he just tabulated his results without any further investigations. These results are listed in appendix(4),table (A4.49). In applying their calculations to the experimental results, Sambles et al[15] did not consider Olsen's data because of the data scattering is large. According to the present work one can see that this scattering is not due to just experimental error but rather due to some effect related to the sample size. This effect is easy to overlook because of the fact that the RRR is very often used as a measure of the sample purity, as mentioned before. Having that in mined, most of times an experimentalist may discard any sample with a poor residual resistivity ratio,

RRR. Also the absence of a theoretical prediction of such behavior may discourage one to belive any oscillation of ρ as function of d he might see.

Now, according to Sambles et al[15] theory, discussed in chapter I, one can write the size dependent electrical resistivity for a simple metal as:

$$\rho(d) = \rho_\infty + \alpha\,(\rho_\infty \lambda_\infty/d), \qquad (3.4.1)$$

where ρ_∞ and λ_∞ are the bulk resistivity and mean free path respectively and α=0.75 for diffuse scattering and $d>\lambda_\infty$. On the other hand for $d<\lambda_\infty$ and for fairly smooth surfaces $\rho(d)$ can be written as:

$$\rho(d) = \rho_\infty\,(1 + \alpha k^{-2/3}), \qquad (3.4.2)$$

where $k=d/\lambda_\infty$.This equation is similar to that predicted by Blatt and Satz[21] in 1960.

According to our results for potassium, ρ(3.2 mm)≈ 9.1 nΩ cm at 4.1 K after one day annealing at room temperature which corresponds to a resistive mean free path $\lambda_\infty = m v_f/\rho\, ne^2 \approx 0.024$ mm, where the values for m,v_f and n were taken from Ref.(54). After two weeks of annealing time ρ(3.2 mm)≈3.03 nΩ cm which corresponds to $\lambda_\infty \approx 0.074$ mm. This will put our results for both curves in fig(3.1a) in the limit of equation (3.4.1). Even if we use the data from ρ(1.47 mm), $\lambda_\infty \approx 0.053$ and 0.139 mm for the above two annealing conditions respectively, the results are still in the limit of equation (3.4.1). In order to show that equation (3.4.2) does not apply to the present results, we plotted $(\rho-\rho_\infty)$

versus $(d/2)^{-2/3}$ as shown in Fig.(3.17) which does not give the straight line predicted by the equation. According to equation (3.4.1), if we plot $\rho(d)$ versus 1/d we should get a straight line of positive slope, $\alpha\ \rho_\infty\lambda_\infty$, and y-intercept of ρ_∞. Fig(3.18) shows that relation which indicates that the theory might explain the observed results at 4.2 K for $d \leq 1.47$ mm but the measurement for $\rho(d \geq 1.47)$ are in total disagreement with the theory aside from the fact that it has a linear trend but with a negative slope. Similar relationships for the sodium results, shown in Fig.(3.19) , revealed that equation (3.4.1) may explain the observed size effect for $d \leq 0.9$ mm but not for $d > 0.9$ mm. In Fig.(3.20) we have plotted the resistivity of indium wires versus 1/d. They fall into three sets of data points, each of which can be fitted to a straight line. This straight line feature is in good agreement with equation (3.4.1) but now the question is: Why should there be more than one line for the same material ?. This question can not be answered by Sambles et al[15] theory which was designed for free electron systems with spherical fermi surfaces.

In a recent paper, Van Der Mass and Huguenin[55] have reported a similar study on a cadmium single crystal. The sample thickness, d, was reduced by chemical polishing from 1 to 0.04 mm. They found a minimum in $(\rho - \rho_\infty)$ as function of the residual resistivity, ρ_0 , when d~ the mean free path and offered no explanation for that feature. They concluded that their results are in qualitative agreements with the size effect theories by Sambles et al[15, 56].

To our knowledge there is no theory which predicts a decrease of the sample conductivity as diameter increases other than "weak localization" theories[57-59] designed for three dimensional disordered metallic systems. These theories require a sample resistivity $\sim 10^5$ higher than the resistivity of our samples and it hardly seems appropriate to apply them for our results at least at this stage where there is no theoretical calculations for a pure metal limit.

Recently, Rzchowski et al[60] have found an indication of a high mobility surface layer on copper and aluminum surfaces at low temperatures in their study of the microwave surface conductivity of these two metals. This work was stimulated by the earlier measurement done by Witteborn et al [61,62] and Lockhart et al [63] who were measuring the effect of gravity on a free-falling electron through vertical metallic tubes. They found evidence for a shielding electron layer on the surface of a copper tube they used at low temperatures. As a trial to explain our observations of the decrease of the electrical conductivity as the sample diameter increased, one may use Rzchowski et al results as follows:

Assume that there is a surface layer which has a higher conductivity than the bulk material of thickness $t << a$, where a is the wire radius. The apparent resistance of the sample will be the result o[illegible] inted resistances R_B and R_S, the bulk material and the surface layer resis[illegible]ely. In this case , one can write:

$$1/R_{App} = 1/R_B + 1/R_S$$

or:

$$G_{App} = G_B + G_S, \tag{3.4.3}$$

where G is the conductance; G= 1/ R. Now, since G= σA/ L, where A is the cross-sectional area and L is the distance between the potential leads, we may write (3.4.3) as:

$$G_{App} = \sigma_B\ [\pi(a-t)^2/ L] + \sigma_S\ [2\pi at/ L] \tag{3.4.4}$$

where a is the wire radius and t is the surface layer thickness. For t= 0, equation (3.4.4) will become:

$$G_{App} = G_{t=0} = \sigma_B\ [\pi\ a^2 / L] \tag{3.4.5}$$

From (3.4.4) and (3.4.5), we can write:

$$[\ G_{App}(T)/ G_{t=0}\ ] = [\ (a-t)^2 /a^2\ ] + (\sigma_S/ \sigma_B\ )\ (\ 2t\ /a\ ) \tag{3.4.5}$$

Neglecting terms of $(t/a)^2$, one can write (3.4.5) as :

$$\begin{aligned}[\ G_{App}(T)/ G_{t=0}\ ] &= 1 - [\ 2t\ /a\ ] + (\sigma_S/ \sigma_B\ )\ (\ 2t\ /a\ ) \\ &= 1 + [\ (\sigma_S/ \sigma_B\ ) - 1\ ]\ (\ 2t\ /a\ ) \\ &= 1 + 4\ [\ (\sigma_S/ \sigma_B\ ) - 1\ ]\ (\ t\ /d\ ) \end{aligned} \tag{3.4.5}$$

This will give a 1/ d dependence of [$G_{App}(T)/ G_{t=0}$], but this dependence will vanish if $\sigma_S = \sigma_B$ or $t \Rightarrow 0$.

From these arguments one can see that at a fixed temperature the apparent conductance of the sample is proportional to 1/ d. This dependence will be measurable till $4\ [\ (\sigma_S/ \sigma_B\ ) - 1\ ]\ (\ t\ /d\ ) << 1$ where $G_{App}(T) \sim G_{t=0}(T)$. Now, since by definition G= 1/ R, therefore :

$$[\, G_{App}(T)/ G_{t=0}(T)] = [\, R_{t=0}(T)/ R_{App}(T)\,]$$
$$= [\, R_{t=0}(T)/ R(300)\,]\, [\, R(300)/ R_{App}(T)\,]$$
$$= A(T)\, [\, R(300)/ R_{App}(T)\,],$$

where $A(T) = [\, R_{t=0}(T)/ R(300)\,]$ is a characteristic of the bulk material. This may explain the observed decrease of the ratio $[\, R(300)/ R_{App}(T)\,]$ as the sample diameter is increased for both potassium and sodium as shown in figures (3.1) to (3.15).

It might be interesting to note that $d_{max}\, T$ = constant, where d_{max} is the diameter value at which $[\, R(300)/ R_{App}(T)\,]$ is maximum at a given temperature T. This constant ~ 6 mm K for potassium and ~ 4 mm K for sodium. Also :

$$[\, d_{max\,(potassium)}/ d_{max\,(sodium)}]_T \sim 1.5$$
$$\sim [\, \theta_{D(sodium)} / \theta_{D\,(potassium)}]_{T\sim 0K}\,,$$

where θ_D is the Debye temperature.This may indicate that d_{max} is related to some characteristic length of the phonon systems in the two metals.

Longitudinal magnetoresistance results for potassium are summarized in fig(3.21) which shows a negative dR/dH for sample diameters less than 1.15 mm at low fields but for higher fields dR/dH changes sign and becomes almost constant. In fig(3.22) we have plotted the low field magnetoresistance which shows that the negative magnetoresistance becomes stronger as the sample diameter gets smaller this agrees qualitatively with Chambers[17] and Golledge et al[16] theory. We have studied the effect of annealing at room temperature on the low field magnetoresistance at 4 K. The results are summarized in fig (3.23) which indicate that the negative magnetoresistance effect becomes stronger as the annealing time increases for the same sample. This agrees with the previous result because of the following :

1. From figures (3.1) and (3.2), we have seen that the effective mean free path increases with annealing, since σ increases, so $K \equiv d/\lambda_\infty$ effectively decreases for fixed d.

2. From fig(3.22) we have seen that the negative dR/dH becomes larger for smaller diameter (i.e. for small K).

From (1) and (2), one would expect that the negative dR/dH would be larger for longer annealing time for a given sample as in fig (3.23).

In order to rule out the effect of any possible magnetic impurities due sample extrusion through stainless steel dies, we have prepared some samples by

extruding them through dies made of a machinable ceramic, as mentioned before, and repeated the same measurements. The results, shown in Fig.(3.24), are found to be the same which indicates that the observed negative dR/dH are due the sample size and not due to impurities, such as tiny amounts of iron.

The measurements of the longitudinal magnetoresistance for sodium showed very similar features as those for potassium; see figures (3.25) to (3.26). The only difference one may notice is that the values of dR/dH for sodium are about one order of magnitude smaller than those for potassium. This can be attributed to the difference in the bulk mean free paths[23] for the two metals as indicated by the difference in RRR discussed before. A similar negative dR/dH was seen by White and Woods[64] for 0.35 mm diameter sodium wire caste in a glass tube. Their result agrees very well with the observed results of this study.

For indium, the results are quite different as indicated in figures (3.27) and (3.28). The sample resistance shows a sudden rise for magnetic fields ~ 300 to 600 Oe giving a large percentage change, ~ 800%, then tends to saturate for higher fields. This large change in the sample resistance can be attributed to the bulk property of indium since it is known[65] that it becomes a compensated metal (i.e. $N_e = N_h$, where N_e and N_h are the electron and hole concentration respectively) for applied magnetic fields ~ 200 to 400 Oe[66]. This condition of $N_e = N_h$ gives rise to the so-called " Static Skin Effect " introduced by Azbel[67-70] who predicts

just that kind of behavior. Since the discussion of such a theory is beyond the theme of the present work, we may leave it as this point, where we have considered some more investigations and the détail discussion will be published later.

According to existent theories, as mentioned in chapter I, the longitudinal magnetoresistance for bulk simple metals should be zero[17,23,27], however linear magnetoresistance has been observed for bulk alkali metals for the last four decades[64, 71-74] and in the present work as illustrated in the above-mentioned figures for large diameter or high magnetic fields. On the other hand a negative dR/dH was predicted for samples with diameters of the same order of magnitude as the bulk mean free path. The theoretical calculation done by Chambers[18] for diffuse surface scattering and those done by Golledge et al[16] for more general cases are discussed in detail in chapter I of this thesis. Since the theory does not yield an analytical expression, a graphical comparison such as in Fig.(1.4.2) serves our purposes effectively. Since the theory was devised for a zero bulk magnetoresistance, one would expect best agreement with theory will be for those samples with large size effect in which case the bulk contribution will be least. According to the present study this occurs for well annealed samples of smaller diameters. In calculating the Larmor radius R_H one obtains for potassium:

$$R_H = m v_f / e H \approx 0.06/H ,$$

where R_H is in mm and H is in KOe. Therefore $d/2R_H = dH/0.12 = 2.8$ H for d=0.33 mm. Fig (3.29) shows an example of such graphs for a potassium sample of diameter 0.33 mm after subtracting a linear term for bulk contribution. The figure shows a qualitative agreement between experimental results and theory but quantitatively ρ/ρ_0 was supposed to reach a value of unity when $d/2R_H = 10$, where according to Fig.(3.29) $\rho/\rho_0 = 2.3$ at this value. When $d/2R_H = 30$, ρ/ρ_0 saturates at the value of 2.1. Fig.(3.30) shows a similar graph for sodium wire with d= 0.33 mm which indicates that the theory can explain the observed results only qualitatively. The ratio $\rho/\rho_0 = 3.59$ at $d/2R_H = 10$ and saturated at the value of 3.57 when $d/2R_H = 45$. This agrees very well with the conclusion by Chambers[17], who measured the longitudinal magnetoresistance for a thin sodium wire and could not find quantitative agreement between his measurements and his theory. He attributed that to the simple model he used in the theory which deals with the conduction electrons as non-interacting classical particles and neglects the possible effects due to non-zero interaction between these electrons and to their quantum mechanical nature.

3.5) Summary and Conclusion :

From the present study one may make the following concluding remarks:

1. For pure potassium and sodium $\rho(4.1, H=0)$ is much affected by the sample size as well as the annealing condition.

2. The RRR, which is often used as a measure of sample purity is also affected by the sample dimensions as well as the thermal history.

3. The behavior of $\rho(4.1)$ as a function of the diameter can be explained at least qualitatively by Sambles et al theory[15] for $d \leq 1.47$ mm (potassium) and $d \leq 0.90$ mm (sodium) but not for larger diameters. For indium the theory does not explain why the resistivity should oscillate with the sample diameter although a straight line can be drawn through the maxima or the minima on a graph of $\rho(d) >< 1/d$. The theory predicts a straight line for $\rho(d)$ as function of $1/d$.

4. The results of $\rho(d)$ for large diameters and high temperatures may be interpreted in terms of a high conductivity surface layer at temperatures well below room temperature, as discussed in section (3.4).

5. The negative longitudinal magnetoresistance for potassium and sodium at low fields can be explained qualitatively by Chambers[17] and Golledge et al[16] theory but at high fields or large diameters, where non-zero bulk magnetoresistance is observed, the results remain unexplained by the theory.

6. The positive longitudinal magnetoresistance for bulk indium is so large that it may screen the negative term predicted by Chambers[17] and Golledge et al[16] theory due to the sample size effect.

Finally, we hope that the present study has brought us one step further towards a better understanding of the transport properties of simple metals, which might be essential to understand the more complicated systems.